From the Department of Internal Medicine II of the Department of Medicine of the Justus-Liebig-University Giessen

Director: Prof. Dr. Werner Seeger

Bone marrow derived mesenchymal stem cells in the treatment of influenza virus-induced acute lung injury

Inaugural Dissertation

submitted to the Faculty of Medicine in partial fulfillment of the requirements for the Doctor in Philosophy (PhD)

by

Lina Jankauskaite

Born in Kaunas, Lithuania

Giessen, 2017

1. Supervisor and Committee Member: Prof. Dr. med. Susanne Herold, PhD

2. Supervisor and Committee Member: Prof. Dr. H.-J. Thiel

Committee Member (Chair):

Committee Member:

Date of Doctoral Defense: 17 08 2017

Table of Contents

1. INTRODUCTION 6

1.1 Influenza viruses 6

1.1.1 Structure and nomenclature 6

1.1.2 Epidemiology 7

1.1.3 Influenza cycle within the infected cell and virus tropism 8

1.1.4 Host immune response to Influenza A virus 9

1.2 IV infection: clinical presentation and treatment strategies 12

1.2.1 Clinical manifestation of uncomplicated IV infection 12

1.2.2 IAV induced pneumonia and acute lung injury (ALI) 12

a) ALI/ARDS definition 13

b) Pathology and pathogenesis 14

c) Resolution and repair 15

1.2.3 IV infection treatment strategies and challenges 16

1.2.4 Therapeutic strategies in IV-induced ARDS 16

1.2.5 Cell therapies 17

1.3 Mesenchymal stem cells (MSC) 18

1.3.1 Definition and identification 18

1.3.2 Therapeutic potential of MSC 19

a) MSC display a low immunogenicity profile 20

b) MSC are inflammation sensors and stimulate inflammation resolution 20

c) Main mechanisms involved in MSC therapeutic potential: paracrine action via soluble factors 21

d) MSC in ALI/ARDS models 22

e) MSC paracrine support via extracellular vesicles (EVs) 24

2. Aims of this work 27

3. Materials and methods 28

3.1 Mice strains 28
3.2 IAV strain 28
3.3 Primary cells and cell lines 28
3.3.1 Cell lines 28
3.3.2 Primary Murine Alveolar Epithelial Cells (AECs) 29
3.3.3 Primary Murine Bone Marrow Mesenchymal Stem cells (BM-MSC) 30
3.4 BM-MSC Characterization and differentiation 31
3.5 BM-MSC derived exosomes 32
3.5.1 Isolation 32
3.5.2 Exosome characterization 33
3.6 *In vivo* experiments and sample processing 33
3.6.1 Intra-tracheal IAV infection and cell application 33
3.6.2 Collection of Bronchoalveolar Lavage Fluid (BALF) 34
3.6.3 Preparation of Lung Cell Homogenate (LH) 34
3.6.4 Lung permeability assay 34
3.6.5 Histological assessment of the lung 35
3.7 *In vitro* IAV infection and cell culture assays 36
3.7.1 AEC culture and infection 36
3.7.2 AEC co-culture with BM-MSC, 3T3 cells or BM-MSC-derived conditioned medium (CM) 36
3.7.3 BM-MSC priming 37
3.8 Analysis of gene expression 37
3.8.1 RNA isolation and cDNA synthesis 37
3.8.2 Quantitative Real-Time Polymerase Chain Reaction (qRT-PCR) 38
3.8.3 Microarray experiments 38
3.9 Flow cytometry and cell sorting 39
3.10 Statistics 41

4. Results 42

4.1 BM-MSC isolation and characterization 42

4.2 BM-MSC exert a protective role on infected AEC *in vitro* by stimulating alveolar proliferation and anti-viral programs 44

4.3 The protective role of BM-MSC on infected AEC is mediated by paracrine factors 48

4.4 Intra-tracheal BM-MSC application improves survival and decreases ALI severity in mice challenged with influenza 51

4.5 BM-MSC application *in vivo* enhances proliferation of epithelial cells and protects the AEC pool against influenza induced apoptosis 54

4.6 Type I Interferon pathway is engaged to mediate the BM-MSC anti-viral potential *in vivo* 57

4.7 BM-MSC anti-viral potential can be amplified through poly I:C stimulation *in vitro* 58

5. Discussion 60

6. Summary 65

7. Zusammenfassung 67

8. References 69

9. Supplement 94

9.1 List of Figures 94

9.2 Materials: chemicals, antibodies, kits 96

9.3 Abbreviations 101

9.4 Curriculum Vitae 108

9.5 Acknowledgements 112

9.6 Declaration 113

1. INTRODUCTION

1.1 Influenza viruses

Influenza viruses (IV) are among the most important respiratory pathogens in human population [1] and constitute a significant threat to global health with 3 to 5 million of severe IV infections and about 250 000 to 500 000 lethal cases per year [2, 3]. Considering the high IV prevalence and its capacity to cross the interspecies barrier together with easy adaptation to a new host [4], they are one of the greatest public health concerns worldwide.

1.1.1 Structure and nomenclature

IV are negative sense single-stranded segmented RNA viruses with a lipid-containing envelope (Figure 1-1). Three genetically and antigenically distinct IV subtypes, A, B and C belong, together with thogoto- and isaviruses, to the *Orthomyxoviridae* family. In this thesis the focus is on influenza A viruses (IAV) which are responsible for annual epidemics as well as pandemic outbreaks [5]. IAV can be subtyped based on antigenic properties of their surface glycoproteins hemagglutinin (HA) and neuraminidase (NA) [6] (Figure 1-1). Currently, strains from 18HA subtypes and 11NA subtypes have been identified [7, 8].

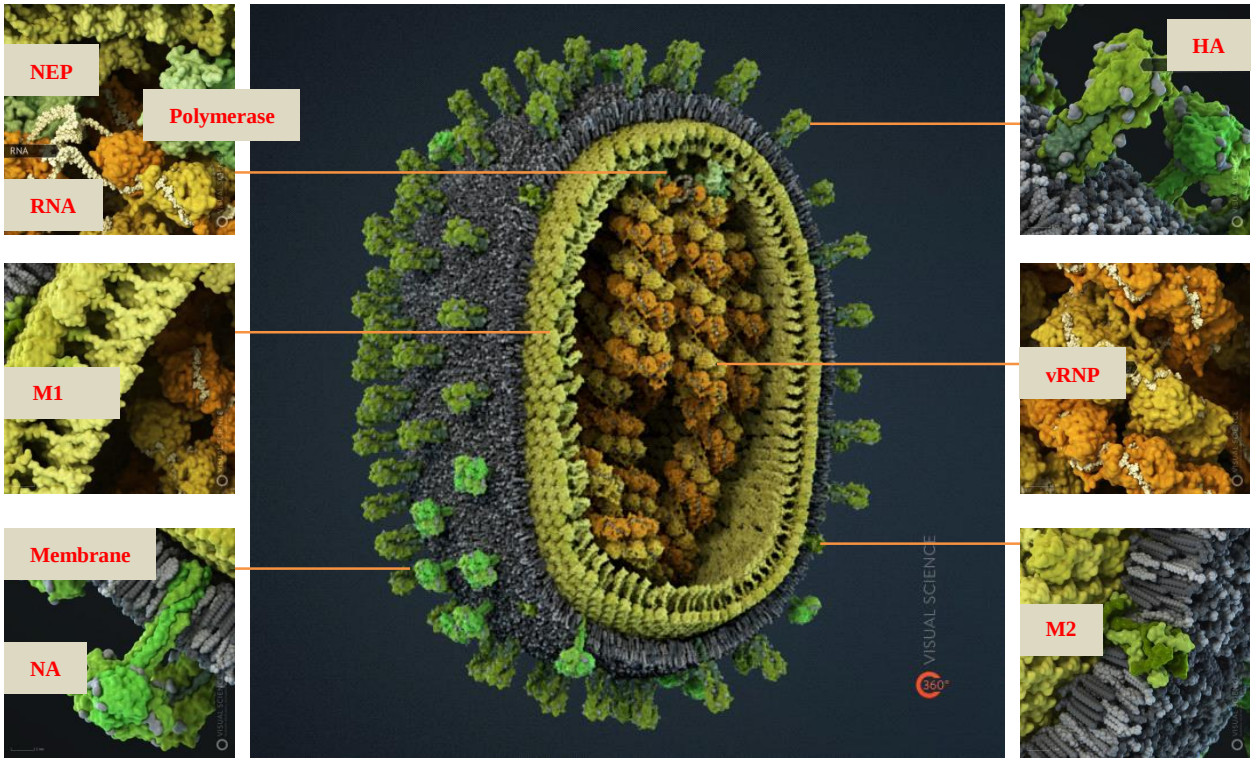

Figure 1-1. Schematic picture representing Influenza virus structure. HA, hemagglutinin; vRNP, viral ribonucleoprotein; M2, transmembrane protein M2; M1, matrix protein; NEP, nuclear export protein; NA, neuraminidase. Addapted from http://visual-science.com.

All known subtypes of IAV can infect birds, except subtypes H17N10 and H18N11 (found in bats). Only two IAV subtypes (H1N1 and H3N2) are, together with influenza B viruses, seasonally circulating among humans, whereas highly pathogenic avian IV (e.g. H5N1 or H7N9) infect humans occasionally with high lethality, and bear a putative pandemic threat. The IAV genome contains 8 segmented RNA encoding at least 11-12 proteins. Three gene segments encode the polymerase polypeptides PB1, PB2 and PA and two smaller proteins, mitochondria-associated protein (PB1-F2) and N40 [9].

Surface glycoprotein HA is playing an important role in host tropism as it binds to host cell receptors containing N-acetyl sialic acid (SA) moieties. Human IAV mainly recognize receptors with terminal α-2,6-SA moieties, found on bronchial epithelial cells of the upper respiratory tract (URT), whereas avian strains predominantly prefer α-2,3-SA abundantly expressed on epithelial cells in the intestinal tract of birds and lower respiratory tract (LRT) of humans. NA is crucial for proper budding and release of progeny virions. Viral RNA is encapsidated by a viral nucleoprotein (NP) and bound to a heterotrimer PB1, PB2 and PA forming the viral polymerase, that together compose viral ribonucleoprotein (vRNP) complex. The matrix 1 (M1) protein forms a shell underlying the lipid bilayer membrane of the virion. M1 interacts with cytoplasmic domains of the surface glycoproteins and vRNP complexes. The lipid bilayer envelope contains transmembrane M2 protein as well as HA and NA. M1 is a structural protein important for the nuclear export of viral RNA and viral budding, whereas M2 functions as an ion channel. The IV genome encodes for two additional proteins important for viral replication: the nonstructural 1 (NS1) protein is an interferon signaling antagonist and regulates cell apoptosis, and NEP (nuclear export protein) that facilitates nuclear export of the vRNP complexes.

1.1.2 Epidemiology

IV cause widespread illness yearly, named seasonal influenza, during fall and winter in the northern hemisphere. Most influenza epidemics are caused by a predominant serotype, but different viruses may appear sequentially or simultaneously. IVs are evolutionary dynamic viruses with high mutation rates [10] directed by adaptation to host cell factors and change in

antigenicity to escape from the immune response of the host. HA and NA viral proteins show the highest genetic variability, which allows IV to evade pre-existing immunity. Genetic reassortment with other IV strains, so called *antigenic shift*, is responsible for IV pandemics [11]. In contrast, *antigenic drift* describes accumulation of mutations throughout the genome and results in seasonally recurrent infection waves, as these mutations render IV non-susceptible to detection by pre-existing anti-HA or anti-NA antibodies. Most IAV pandemics cause higher morbidity and mortality rates than seasonal epidemics during the inter-pandemic periods. Recording history, different antigenic subtypes of influenza A – H1N1, H2N2 and H3N2 – created a pandemic wave in the 20th century in 1918, 1957 and 1968 respectively, causing high mortality rates [12]. In March 2009, an outbreak of a novel reassorted H1N1 virus started in Mexico [13-16] and rapidly expanded across the globe. As human and avian IV bind to different SA receptors as well as avian IV show limited replication in humans, avian influenza viruses were initially thought to be incapable of causing human infection. However, in the past decade, extensive numbers of sporadic cases and local outbreaks of avian IAV infections as H5N1[17, 18], H7N7 [19, 20], H7N3 [21] and H7N2, H7N9, H9N2 [22, 23] in humans have occurred, some of them with high lethality, raising pandemic concern.

1.1.3 Influenza cycle within the infected cell and virus tropism

In the initial phase of IAV replication, the viral HA binds to host cell receptors containing α-2,6-linked or α-2,3-linked SA moieties [6] (Figure 1-2). The virion enters the cell by cathepsin-1 mediated endocytosis and an HA-dependent fusion of endosomal and viral membrane takes place. Acidification of endocytic vesicle opens M2 ion channel, resulting in dissociation of the RNP complexes that contain the viral genome. The viral RNA is imported to the nucleus via importin-α1 and dependently of NP protein, where the transcription and replication of the viral genome occurs. The host cellular machinery produces new viral proteins, as well as negative and positive-oriented viral RNA copies. Negative-oriented viral RNA copies accumulate at lipid raft domains, meanwhile positive-oriented serve either as template or as mRNA. After RNP assembly and budding, the new virions are released outside of the cell. Release from the host cell is mediated by NA, which cleaves SA-containing receptors for virion release from the membrane.

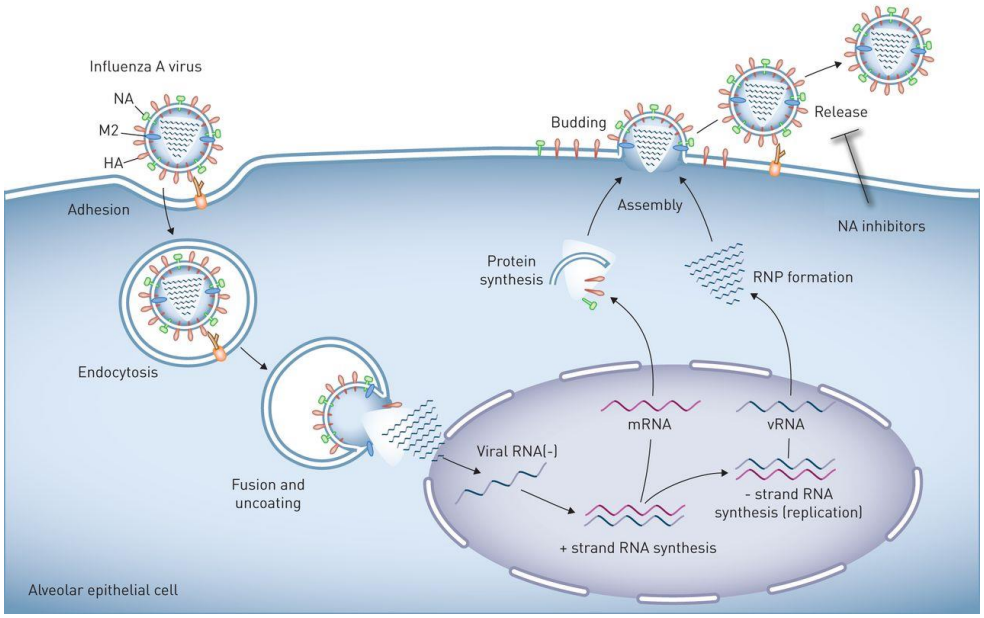

Figure 1-2. IAV replication cycle in infected host cells [24]. The virion is endocytosed after interaction between HA and sialic acids. After viral and endosomal membrane fusion, released vRNA is transported into the nucleus where the transcription to mRNA and new vRNA occurs. Viral protein translation takes place in cytoplasm and endoplasmic reticulum. New virions assemble and bud from the apical host cell membrane and are released via action of NA.

1.1.4 Host immune response to Influenza A virus

The host´s immune system is strongly activated during IAV infection. Epithelial cells of respiratory tract are able to mount an antiviral response upon viral detection by pattern recognition receptors (PRRs) such as Toll-like receptors (TLR), the retinoic acid-inducible gene I (RIG-I) protein [25], protein kinase R (PKR) and nucleotide oligomerization domain (NOD)-like receptor family (Figure 1-3). The TLR involved in recognizing IAV infection are expressed in the endosomes to sense double stranded RNA (dsRNA) occurring in virus-infected cells (TLR3), or single stranded viral RNA (ssRNA) that occurs during viral replication in endosomal compartments (TLR7/8) [26-29]. Cytoplasmic RIG-I receptors recognize 5'-triphosphates bearing viral RNA [30]. The NOD-like receptor family member pyrin domain-containing 3 (NLRP3), an inflammasome receptor, recognizes viral RNA within the cytosol of infected cells. The signalling cascade of TLRs, except for TLR3, starts with activation of myeloid differentiation primary response gene 88 (MyD88). Subsequently, MyD88 activates tumor necrosis factor (TNF) receptor associated factor 6 (TRAF6), either directly or via Interleukin-1 receptor (IL-1R)-associated kinase (IRAK 1). This leads to

activation of mitogen-activated kinases (MAPKs) and nuclear factor kappa-light-chain-enhancer of activated B cells (NF-κB). TLR3 cascade is initially activated via TRIF (TIR domain containing adapter inducing interferon β) eventually mobilising NF-κB and IRF3 (interferon regulatory factor 3) [31, 32]. RIG-I is crucial for viral detection and type I IFN production in infected epithelial cells, dendritic cells (DCs) and alveolar macrophages (AM) [33]. Its activation results in conformational changes exposing caspase activation and recruitment domains (CARDS) to ubiquitination by tripartite motif 25 (TRIM25) – an IFN-inducible E3 ubiquitin ligase. In the following, RIG-I associates with mitochondrial antiviral signaling protein (MAVS) and induces IRF3 and NF-κB activation [32, 33]. TLR3/7/8 and RIG-I trigger high levels of type I IFN production, to induce an anti-viral state, however, this occurs at the cost of a frequently exaggerated immune response and recruitment of high numbers of damage-inducing inflammatory cells [29, 34, 35].

The interferons (IFNs) are a group of secreted antiviral cytokines. This family of cytokines is now recognized as the first line of defense against viral infection. Three classes of IFN have been identified (I to III) and they are classified according to the receptor complex they are signaling through. IFNα/β will be further referred as type I IFNs and is in the focus of this study. The binding of type I IFNs to the heterodimeric IFNα receptor (IFNAR) initiates a signaling cascade, inducing more than 300 IFN-stimulated genes (ISGs) such as – MX, 2'5'-oligoadenylate synthetase (OAS), viperin, and many others, that serve as effectors to limit viral replication [29, 32, 34, 35] in infected and neighbouring cells by initiating an intracellular anti-viral programme. Type I IFN secretion is induced by IAV in alveolar macrophages (AM), DCs and infected lung alveolar epithelial cells (AECs) [29, 36, 37]. Generally, type I IFN have been attributed beneficial role in IAV induced acute lung injury (ALI) by decreasing viral load [38], when protecting cells from viral attack in the early course of the infection. Recently, however, many reports demonstrated detrimental IFN effects, especially when high IFN levels persist after viral clearance, e.g. by triggering TNF-related apoptosis-induced ligand (TRAIL) production causing apoptotic lung injury during IAV infection [39]. In addition, IAV infection of epithelial cells induces expression of many pro-inflammatory cytokines and chemokines such as – IL-1β, IL-6, IL-8, TNFα, CC chemokine ligand (CCL) 2, CCL3 and CCL10 and results in phagocyte activation and macrophage and neutrophil recruitment to sites of inflammation [29, 31, 32].

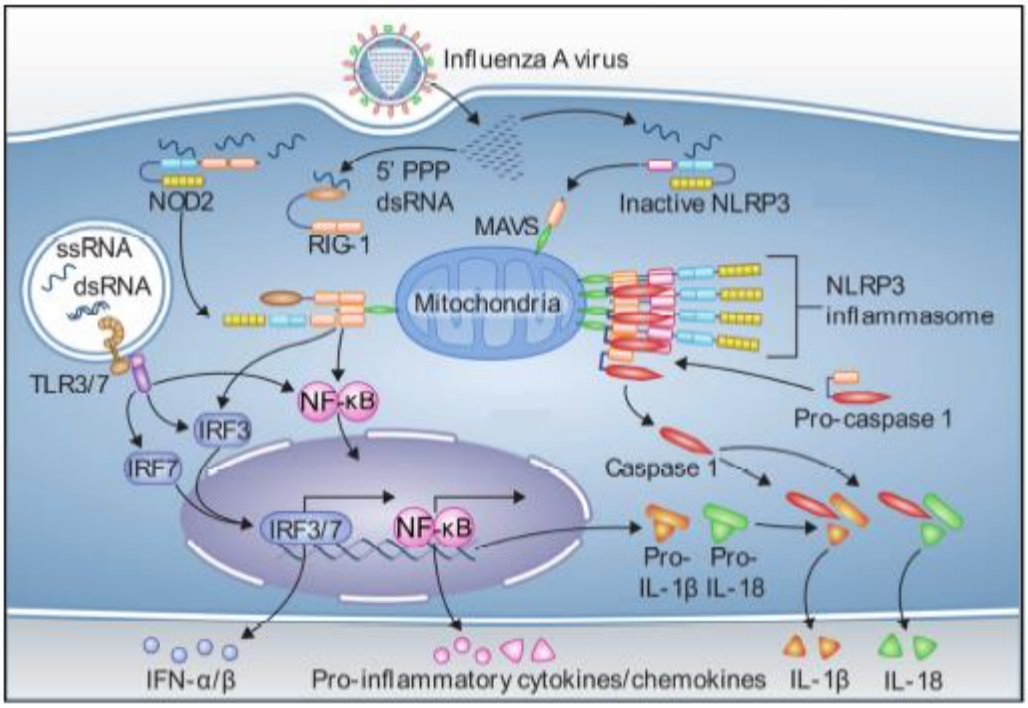

Figure 1-3 Host immune responses to IAV infection [25]. Toll like receptor (TLR) 3/7 is activated via intracellular viral RNA. This signalling pathway via IRF3, IRF7 and NFκB induces transcription of type I interferon and pro-inflammatory molecules. 5'PPP dsRNA activates RIG-I. IRF3 and NFκB are activated via MAVS and NOD-2, and also the NLPR3 inflammasome responds to IAV infection. These processes result in release of type I IFN, but also in release of many other pro-inflammatory cytokines and chemokines.

Recruited myeloid immune cells (bone-marrow-derived macrophages and DC as well as neutrophils) release various pro-inflammatory mediators (IL-6, TNFα, NOS2 (nitric oxide synthase 2)) at the site of infection contributing to severe pathology induced by IAV [40-42]. DCs play an important role bridging the innate and adaptive immune system. Once the lung is infected with IAV, DCs acquire viral antigens both by direct infection with IAV or via phagocytosis of virus particles or apoptotic epithelial cells that they present to naive T and B lymphocytes for generation of adaptive immune responses and memory cells [43].

However, IAV has developed various strategies to escape the innate immune response. In particular, the NS1 protein specifically antagonises the antiviral innate immune response. NS1 displays multiple functions, including inhibition of RIG-I pathway and interferon induced proteins such as PKR and OAS by competing with them for RNA binding [43, 44]. Also, the polymerase complexes have been attributed a role in evasion from IFN responses [32, 43-45]. In addition, IAV induces expression of SOCS (suppressor of cytokine signaling) proteins which inhibit IFNα/β receptor signalling on the level of Janus kinase (JAK)/ signal transducer and activator of transcription (STAT) activation [43].

1.2 IV infection: clinical presentation and treatment strategies

1.2.1 Clinical manifestation of uncomplicated IV infection

Usually, large amounts of influenza viruses are presented in respiratory secretions of infected individuals resulting in a direct transmission via coughing and/or sneezing or a contact with contaminated items. The incubation period ranges from 1 to 4 days, with an average of about 48h. Typical influenza disease in adults is characterized by sudden onset of high fever, chills, myalgia, headache and fatigue. Subsequent upper respiratory tract symptoms include pharyngitis, nasal congestion, rhinitis, non-productive cough and conjunctivitis. Children may have prominent nausea, vomiting or abdominal pain and infants may present with a sepsis-like syndrome. These signs and symptoms are due to both, the damage at the site of virus replication and the systemic response to IAV.

1.2.2 IAV induced pneumonia and acute lung injury (ALI)

The most common complication of IAV infection is viral spread to the distal lung, causing diffuse alveolar damage resulting in severe consequences for the gas exchange function of the respiratory tract. Children under 5 years of age especially younger than 2 years old, elderly patients, obese or patients with comorbidities are more prone to develop complications from IAV infection and display increased mortality rate [46]. In case of highly pathogenic IV infections, as the 1918 pandemic or the 2009 pandemic H1N1 IAV, previously healthy patients younger than 60 years of age are more frequently affected [15, 47-51]. Of note, the larger risk to develop severe IV infection was observed among pregnant women [47, 52, 53]. However, also during seasonal epidemics, previously healthy individuals develop rapidly progressing primary viral pneumonia leading to acute respiratory distress syndrome (ARDS) and in very severe cases with multiple organ failure resulting in death [54]. Additionally, secondary bacterial pneumonia with *S. aureus, H. influenzae* and predominantly with *S. pneumoniae* was associated with increased mortality [55].

Alveolar epithelial damage is due to direct cytolytic effect of IAV and indirect damaging effect of an overwhelming and exaggerated host response [1, 5]. Diffuse alveolar damage

(DAD) caused by IAV, further histopathological changes in the lung and clinical features of IAV-induced acute lung injury (ALI) are similar to those caused by many other pathogens causing severe pneumonia.

a) ALI/ARDS definition

According to the recent Berlin consensus definition, acute respiratory distress syndrome (ARDS) is defined as a severe hypoxaemia refractory to supplement oxygen therapy occurring within 72h due to an acute inflammatory lung injury. Bacterial or viral pneumonia is the most prevalent cause of ARDS [56, 57]. The acute onset of inflammation in the lower compartment of the lung is followed by an increased vascular permeability due to a rapid disruption of the microvascular barrier, resulting in accumulation of protein- and inflammatory cell-rich edema fluid in the alveoli [58, 59]. ARDS is categorised as mild, moderate and severe with typically present bilateral opacities on chest radiograph (Figure 1-4), pulmonary artery wedge pressure ≤18 mmHg with lack of left atrial hypertension and PaO2/FiO2 ratio ≤300mmHg.

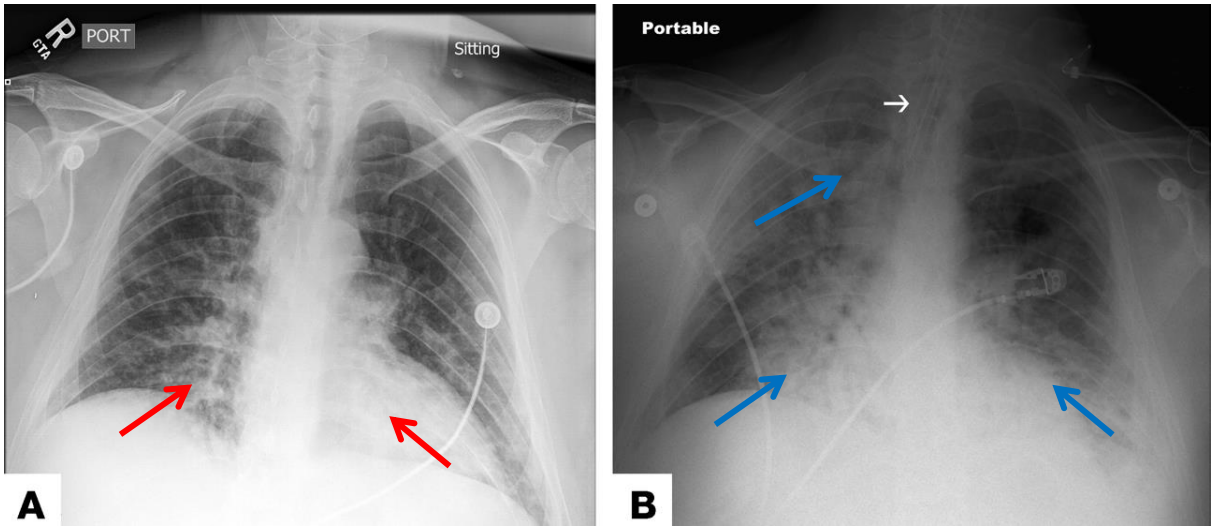

Figure 1-4. (*A*) Chest X-ray images illustrating early ALI, demonstrating patchy infiltrates in the right lower lung field and also in the left lower lung field (red arrow). (*B*) Chest X-ray in the time course of ALI progression towards ARDS, which required intubation (white arrow) and mechanical ventilation. The blue arrows represent progression of bilateral radiographic infiltrates and dense consolidation in the right upper, right lower, and left lower lung fields. Adapted from [58].

b) Pathology and pathogenesis

Histophatologically, three phases are recognized during the evolution of ALI/ARDS [57, 58, 60]. The initial or early phase, so called exudative phase, is characterized by diffuse alveolar damage and endothelial injury. It leads to accumulation of protein enriched and highly cellular edema. Edema fluid is rich in proteins such as fibrin and causes hyaline membrane formation. A variety of mediators boost alveolar endothelial and epithelial permeability, amplified by the inflammatory cells and their cytokines (Figure 1-5). The subacute or a proliferative phase of ALI can occur from day 5 onwards. It is characterized by persistent hypoxaemia, increased dead space ventilation, and reduced lung compliance. During this phase some of the edema is being reabsorbed and proliferation of alveolar epithelial type II cells (AEC II) and repair signs emerge. This is accompanied by interstitial fibrosis, and disruption of capillary function. In some patients these changes can resolve and clinical improvement can be observed. In more severe cases ARDS persists beyond 14 days and it leads to a chronic or fibrotic phase. This stage results from outspread pulmonary fibrosis and loss of the normal lung structure.

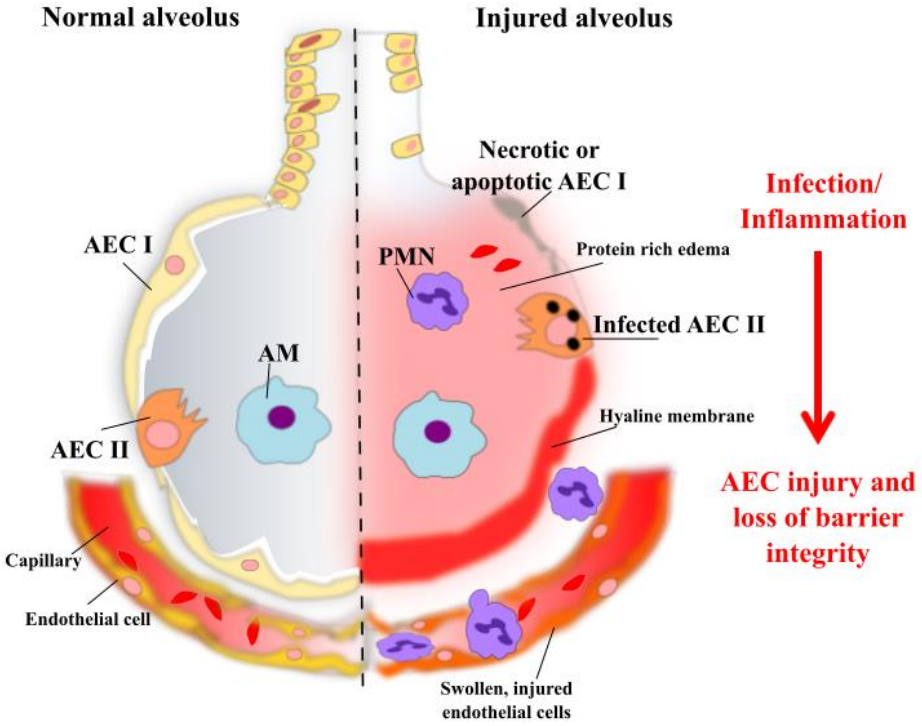

Figure 1-5. The schematic picture represents normal alveolus (left) and injured alveolus (right) during ALI/ARDS. The left picture shows an intact epithelial-endothelial barrier with healthy alveolar epithelium (AEC II, alveolar epithelial type II cells; AEC I, alveolar epithelial type I cells; AM, alveolar macrophage). The right picture demonstrates endothelial-epithelial barrier disruption, injury of AEC and alveolar edema, and

hyaline membrane formation. Intra-alveolar edema fluid is enriched with various proteins and inflammatory cells producing different cytokines. Adapted from [57].

The pathogenesis of ALI/ARDS is associated with dysregulated inflammation, inappropriate accumulation and activation of leucocytes and platelets, uncontrolled activation of coagulation pathways and lung alveolar epithelial-endothelial barrier disruption [58, 61]. Ultrastructural injury to alveolar type I cells (AEC I) was identified in patients who had died of ARDS [62]. IV induces lung epithelial apoptosis via NS1, PB1-F2 or M2, and a lot of signalling pathways, for example mitogen-activated protein kinases (MAPK), are involved in apoptosis initiation [45, 63]. Macrophages are excessively recruited from the circulation and injurious and pro-apoptotic cytokines are expressed and released from the cells. This contributes to extended apoptotic damage including non-infected neighbouring AECs [63, 64]. Additionally, neutrophils are critical players in the lung injury. They accumulate in the lung microvasculature where they get activated and degranulated resulting in release of several toxic mediators, such as proteases, reactive oxygen species (ROS), pro-inflammatory cytokines or pro-coagulant molecules. This results in increased endothelial permeability and loss of normal endothelial barrier function, resulting in impaired gas exchange [57]. Increased permeability of lung microvascular barrier is associated with alveolar haemorrhage and occurrence of erythrocytes in the alveolar space.

c) Resolution and repair

The most important task for survival and recovery from ALI/ARDS is to restore the normal physiological function of alveolus. The shift away from pro-inflammatory signaling and efficient clearance of inflammatory cells is a crucial point of recovery. It was thought that resolution of inflammatory injury occurs primarily due to the passive decline of various pro-inflammatory mediators [65]. Recent investigations demonstrated a complex class of specialized pro-resolving mediators (SPM) such as lipoxins, resolvins, protectins and maresins to be actively generated during resolution phase [66, 67]. They have been shown to carry both, anti-inflammatory and pro-resolving bioactivities. This leads to tissue damage limitation, shortening of resolution time and promotion of healing. Moreover, apoptotic neutrophils and other cells are removed by macrophages via efferocytosis. Additionally, resident and AM contribute actively to resolution of pulmonary inflammation as they, for example, initiate lung tissue repair [68]. Following clearance of the airspace from cells, excessive fluid and debris, the damaged alveolar epithelium must be repaired and the

epithelial-endothelial barrier function be returned to a basic functional state. Growth factors appear to play a major role in repair and resolution of lung injury. Different growth factors, such as keratinocyte growth factor (KGF), hepatocyte growth factor (HGF) or epidermal growth factor (EGF) promote repair of damaged alveolar epithelium [69-74]. Moreover, vascular endothelial growth factor (VEGF), primarily produced by epithelial cells, promotes endothelial repair in ALI [61, 75-77]. Endogenous lung stem/progenitor cells showed to self-renew, proliferate and replace damaged cells by differentiation [65, 78-80], thus promoting epithelial barrier repair, eventually guided by newly emerging lung vasculature [65]. At the same time as lung epithelial integrity is restored, effective edema fluid transport over the epithelium is started, together with restored surfactant secretion.

1.2.3 IV infection treatment strategies and challenges

Currently approved antivirals are Amantadine and Rimantidine, sterical M2 ion inhibitors, as well as Oseltamivir, Zanamivir, Peramivir or Laninamivir, which bind to the enzymatic active site of NA. However, Amantadine and Rimantidine are not recommended for currently circulating IV due to high prevalence of resistance [81, 82]. Moreover, recently, H1N1 IAV strains resistant to Oseltamivir have been reported [83-86]. Additionally, the approved medication is not tested in children less than 2 years of age. Also, the reports of especially virulent IAV causing rapid progression of respiratory infection leading to fatalities [54, 87] showed that the specific anti-viral therapies might not be enough effective for the treatment of complicated IAV pneumonia.

1.2.4 Therapeutic strategies in IV-induced ARDS

The significant progress in understanding the pathophysiology of ALI/ARDS has, unfortunately, not resulted in any specific treatment of this devastating disease except symptomatic intensive care treatments resulting in declined mortality rates from 60-80% to 30-50% [88, 89] since the ALI/ARDS was initially described in 1967.

A large number of different pharmacological therapies have been evaluated in Phase II and Phase III clinical trials for ALI/ARDS therapy but never resulted in a proof of efficacy of any specific treatment strategy, whereas some symptomatic treatments are now standard of care. Protective mechanical ventilation strategies proved advantages in survival [90-92].

Restrictive intravenous fluid therapy, nitric oxide (NO) inhalations [90], other pulmonary targeted pharmacological therapies, as surfactant instillations [60] and rescue strategies such as prone positioning [93, 94] or extracorporeal membrane oxygenation (ECMO) [95, 96] are highly recommended to improve patient's condition in pediatric and/or adult ARDS. Local or systemic use of glucocorticoids remains controversial [57, 97, 98], thus not recommended to date. Additionally to supportive care, antiviral treatment with NA inhibitors should be started as soon as possible [99, 100].

Unfortunately, despite considerable advances in clinical supporting measurements to treat ALI/ARDS, none of the previous mentioned pharmacological therapy methods has proven to be highly effective. Furthermore, growing prevalence of drug-resistant IAV strains request a necessity to consider and develop new therapeutic approaches.

1.2.5 Cell therapies

In terms of promising new therapies, cell therapy methods have been explored as a novel treatment approach in ALI/ARDS. This strategy encompasses methods where cells, whether endogenous or exogenous, are applied to ameliorate disease progression or in a case when regeneration or repair is necessary.

Stem cells are defined as undifferentiated precursor cells with self-renewal potential and ability to differentiate into cells of multiple lineages. They can be classified to pluri- or multi-potent and adult tissue-derived or embryonic. As embryonic pluripotent stem cells (ESC) have potential to form neoplasms due to their ability to proliferate indefinitely without differentiation [101, 102] and display immunological incompatibility between donors and recipients [103], their application as therapeutics is debatable. Endothelial progenitors (EPCs) are an interesting candidates as endothelial damage is a key pathophysiological feature of ALI/ARDS [65], but their use is limited, e.g. by the difficulties in their isolation [104].

Endogenous lung stem cells of mesenchymal or epithelial lineage have been considered for a therapeutic application, as they represent an ideal type of stem cells to regenerate injured lung [78, 105, 106], however, robust markers for their identification and protocols for expansion are still lacking [107, 108]. Similarly, the use of hematopoietic stem cells (HSCs), foetal stem cells or induced pluripotent stem cells (iPSCs) need more investigations regarding their clinical reliability for ALI/ARDS [104]. Due to the easy accessibility and low

immunogenicity, (bone marrow-derived) mesenchymal stem cells (MSCs) have come into focus as putative source of cell therapies to treat a variety of different acute and chronic diseases. They can be produced under GCP (good clinical practice) conditions to large quantities, and have been tested for efficacy in many clinical trials in recent years.

1.3 Mesenchymal stem cells (MSC)

1.3.1 Definition and identification

Mesenchymal stem or stromal cells (MSCs) are adult multipotent endogenous non-hematopoietic precursor cells with capabilities of high proliferation and self-renewal. MSCs were first described in the adherent fraction of bone marrow stroma in 1976 [109, 110], but have also been found in multiple anatomical locations, as skeletal muscle, umbilical cord, adipose and other tissues [111-130]. Despite a very low prevalence of around 0.001 to 0.1% of the total bone marrow nuclear cell pool [131-133], bone marrow derived MSC (BM-MSC) is a relatively easy accessible cell fraction. As shown in Figure 1-6, BM-MSC reside in a subendothelial position of the outer surface of sinusoids, a characteristic type of blood vessels in the bone marrow [134-136].

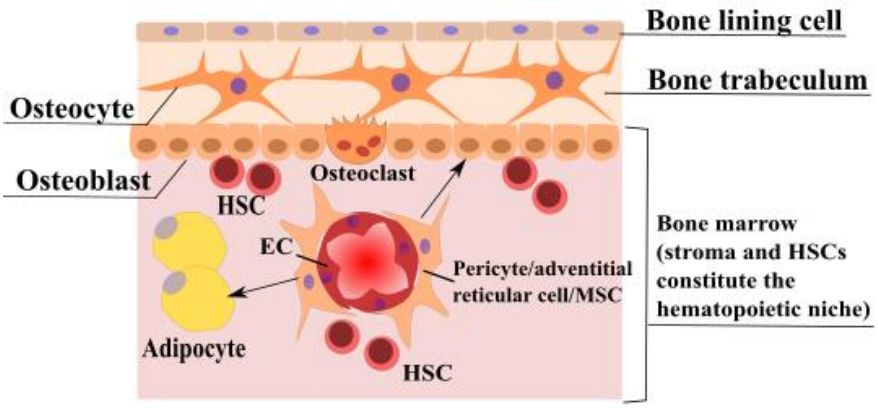

Figure 1-6. Schematic picture representing location of MSCs in the bone marrow subendothelial region adapted from Bianco et al [136]. HSC, hematopoietic stem cell; EC, endothelial cell; MSC, mesenchymal stem/stromal cell.

Recently, MSC have been reported to differentiate into a variety of cell types both *in vivo* and under proper culture conditions *in vitro* [137-148] (Figure 1-7).

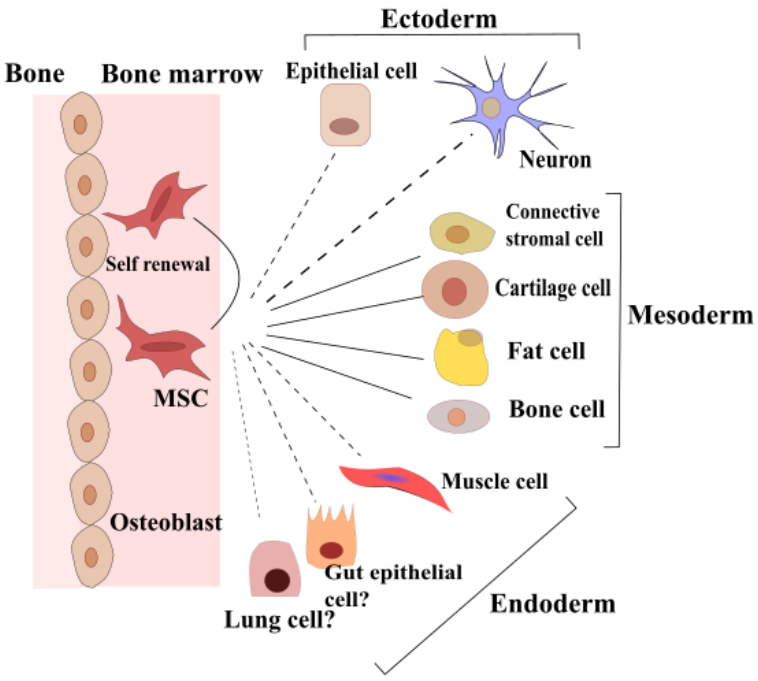

Figure 1-7. Differentiation and self-renewal potential of BM-MSC, adapted from Uccelli et al [137].

A consensus paper of International Society of Cellular Therapy defines the minimal criteria necessary to identify MSC [149] and standardize the procedures to be used. According to this statement, isolated MSCs must be *spindle-like cells* and *adherent to plastic* under standard culture conditions. Secondly, their phenotype must be confirmed via expression of *specific markers* as CD105 (endoglin), CD73 (known as ecto 5' nucleotidase) and CD90 (Thy-1). MSC must lack expression of CD45 (typical leukocyte marker), CD34 (primitive hematopoietic progenitor and endothelial cell marker), CD14 or CD11b (both expressed on differentiated myeloid cells), CD79α or CD19 (both B lymphocyte markers) and HLA-class II. Finally, these cells should be able to *differentiate into adipocytes, osteoblasts and chondroblasts* under specific culture-differentiating conditions. These guidelines can be applied to MSC isolated from human and murine tissues.

1.3.2 Therapeutic potential of MSC

The interest in MSC as a very attractive therapeutic approach for ALI/ARDS stems mostly from their potential to modulate host immune response to injury and infection and to contribute to following repair processes.

a) MSC display a low immunogenicity profile

Tolerance induction in the periphery is critical to prevent autoimmunity and maintain immune homeostasis. MSC demonstrate a low immunogenicity pattern due to constitutive low expression of histocompatibility complex (MHC) I and II proteins and lack of T cell co-stimulatory molecules (CD80 and CD86) [150-157]. Given that, MSC are safe for allogeneic transplantation [158, 159]. However, recent observations suggested that the mechanisms of action of MSC as "cellular tolerogens" can be far more complex [160] and that MSC might be less immunoprivileged as first proposed [161, 162].

b) MSC are inflammation sensors and stimulate inflammation resolution

MSC are sensors of inflammation able to acquire anti-inflammatory or pro-inflammatory phenotypes, however, the underlying mechanisms are undefined. The beneficial anti-inflammatory action of administered MSC largely relies on specific production of secretory proteins, likely depending on the type of injury and on the microenvironment. MSC can be primed by different stimuli and it has been suggested that they can be polarized into distinct phenotypes, improving host defense in the context of infection ("MSC1"), or driving tolerance, injury resolution and tissue repair ("MSC2") (Figure 1-8) [163-165].

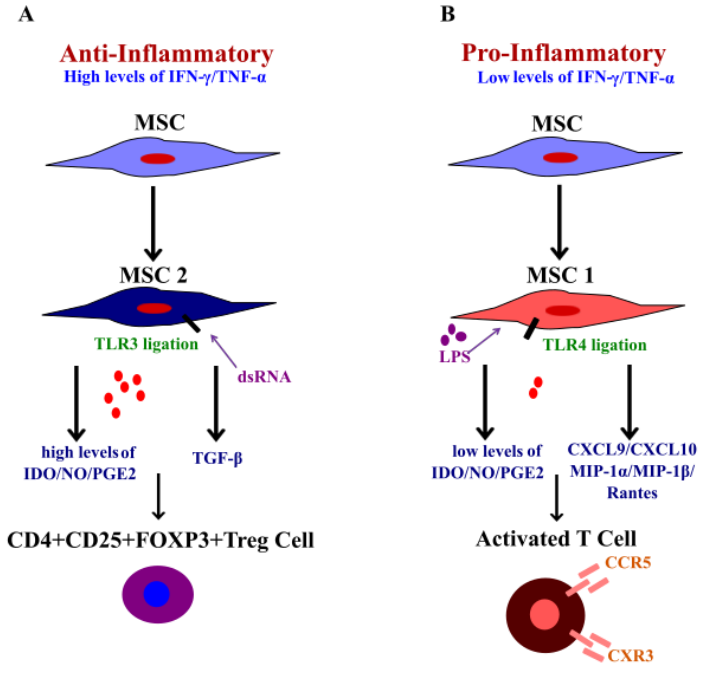

Figure 1-8. Polarization of MSC into pro-inflammatory and anti-inflammatory phenotypes. (*A*) Specific factors (high levels of IFNγ or TNFα) or direct stimulation of toll like receptor 3 (TLR3) drive MSC to adopt an immunosuppressive and tolerogenic phenotype (MSC2). (*B*) The switch towards a pro-inflammatory MSC phenotype (MSC1) is triggered by low levels of IFNγ or TNFα. This can be driven by activation of TLR4 as well and drive presence of activated T cells relevant for anti-pathogen host defense. Adapted from [163].

The switch towards MSC1 or MSC2 depends on levels of soluble factors as IFNγ or TNFα, and can also be stimulated via Toll like receptors (TLR) 3 or 4 activation [163, 166-169]. The balance between these pathways is crucial for promoting host defense without inducing excessive tissue damage and promoting repair. Moreover, recent investigations show that MSC conditioning via TLR3 can amplify their trophic factor production and enhance their anti-inflammatory potential [167, 169-171].

c) Main mechanisms involved in MSC therapeutic potential: paracrine action via soluble factors

A growing number of studies revealed different MSC and host tissue interaction pathways, e.g., mitochondrial transfer [172, 173], direct interactions with the host immune system cells [157, 161, 174-178]. However, the most robust evidence supported MSC mechanism of action is attributed to their paracrine effect via soluble factors. The proteomic analysis of the human MSC secretome revealed their capacity to produce a wide range of proteins with trophic (anti-apoptotic, stimulation of mitosis, proliferation and differentiation, angiogenic), immunomodulatory, anti-scarring and chemoattractant activities (Figure 1-9) [179, 180].

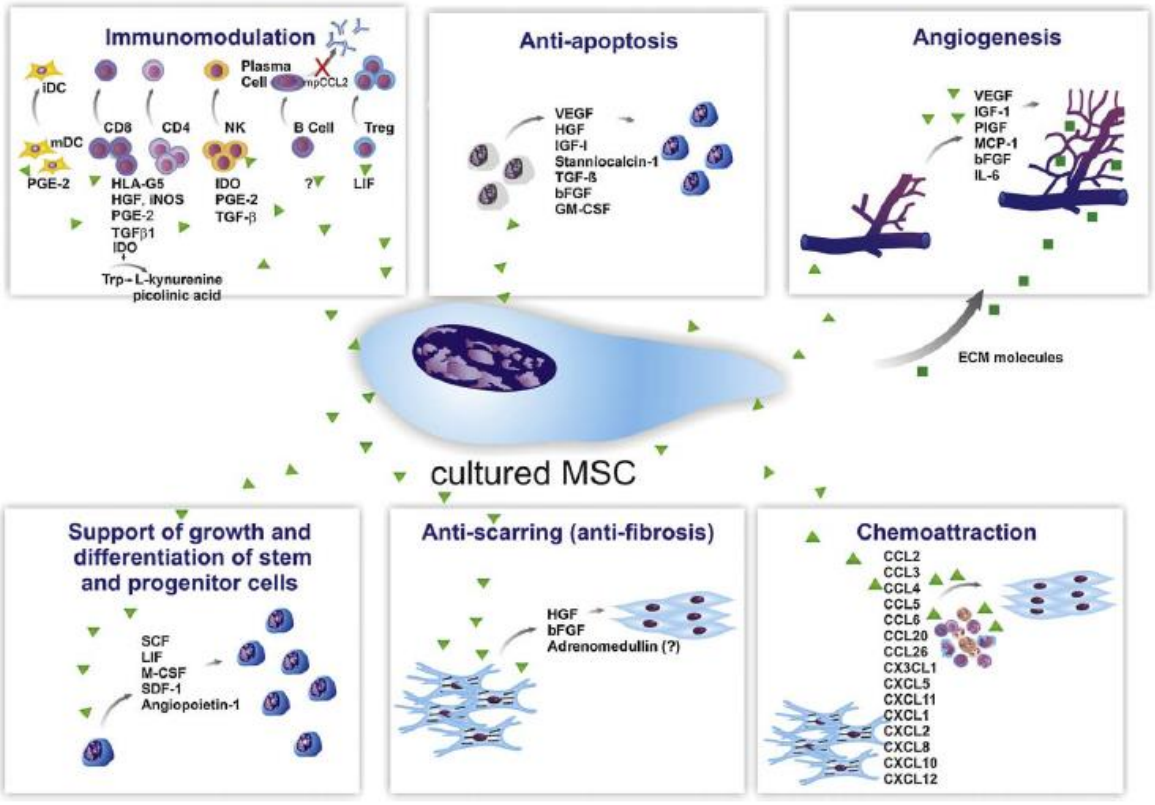

Figure 1-9. Paracrine effects of cultured MSCs. They secrete a broad range of bioactive molecules and now it is attributed to a therapeutic effect of these cells. The main mechanisms by which MSC achieve their therapeutic potential can be divided into six main categories: immunomodulation, anti-apoptotic, angiogenesis, growth and differentiation support of local stem/progenitor cells, snit-scarring and chemoattraction. Secretion of PGE-2 (prostaglandin E2), HLA-G5 (human leukocyte antigen G 5), iNOS (inducible nitric oxide synthase), HGF (hepatocyte growth factor), IDO (indoleamine 2,3-dioxygenase), TGF-β (tumor growth factor b), LIF (leukemia inhibitory factor) and IL-10 (interleukin 10) contributes to MSC immunomodulatory effect. MSC limit apoptosis principally by secreting VEGF (vascular endothelial growth factor), HGF, IGF-1 (insulin-like growth factor 1), Sta-1 (stanniocalcin-1), TGF-β and GM-CSF (granulocyte macrophage colony-stimulating factor). Moreover, local angiogenesis promoting effect is achieved by secreting extracellular matrix molecules, such as VEGF, IGF-1, PIGF (placental growth factor), MCP-1 (monocyte chemoattractant protein 1), bFGF (basic fibroblast growth factor) and Il-6. Additionally, mitosis and tissue progenitor/stem cells are stimulated via production of SCF (stem cell factor), LIF, M-CSF (macrophage colony-stimulating factor), SDF-1(stromal-derived factor 1) and angiopoietin-1. Finally, a group at least of 15 chemokines are constitutively expressed by cultured MSC. Adapted from [181].

As an example, therapeutically applied MSC secrete VEGF, HGF and insulin-like growth factor 1 (IGF-1) or stanniocalcin-1 (Sta-1), reducing tissue apoptosis levels in kidney and myocardial injury models [182-186] and also acting as anti-fibrotic molecules [187]. MSC-derived KGF and VEGF, released under defined injury-related conditions, were shown to contribute to tissue regeneration and repair process [188-191] and consequently linked to their anti-apoptotic potential [132, 192, 193]. Moreover, MSC secretory products are capable to directly induce growth, propagation and differentiation of local stem and progenitor cells and contribute to repair and regeneration of various tissues [194, 195].

d) MSC in ALI/ARDS models

Several studies have shown that BM-MSC may have therapeutic application in various clinical disorders, including sepsis, myocardial infarction, acute renal failure and others [158, 160, 192, 196-211]. Steadily increasing numbers of investigations demonstrate efficacy of application in a growing spectrum of lung injury *in vivo* models [164, 172, 193, 209, 211-239]. Although, the mechanisms of MSC´s beneficial action in these models is not fully understood, many studies indicate that MSC secreted soluble factors are involved and important in ameliorating acute and chronic lung injury. Initially, bleomycin-mediated ALI was used to address BM-MSC´s therapeutic potential. Despite low engraftment levels in the lung, systemic administration of BM-MSC showed to protect lung tissue from bleomycin induced lung damage and contributed to lung repair [230, 232]. The anti-fibrotic and anti-

inflammatory effects were found to be mediated by interleukin 1 receptor antagonist (IL1RN) [193].

To examine MSC effect in pathogen-induced ALI, MSC were applied in *Escherichia coli* endotoxin or live bacteria induced ALI. Intrapulmonary BM-MSC application increased mice survival, improved lung injury and showed downregulated pro-inflammatory responses to endotoxin via lowering levels of TNFα and MIP-2, and increasing levels of IL-10, which has lung-protective effect [212]. Subsequently, the same group demonstrated that, following the *E. coli* endotoxin-induced ALI, treatment with human MSC or MSC-derived conditioned medium (CM) reduced lung edema, and improved lung endothelial barrier function. Impaired alveolar fluid clearance (AFC) and disrupted epithelial-endothelial barrier function is very common in patients with ALI/ARDS. The level of AFC impairment is a significant prognostic value to determine patient morbidity and mortality [59, 240]. Increased endothelial-epithelial barrier permeability and insufficient AFC leads to accumulation of protein rich edema fluid in the alveoli. KGF secreted by BM-MSC was attributed a beneficial effect to reduce edema formation [215]. Together with angiopoietin-1 (Ang1) it was shown to contribute to edema resolution and reduce bronchoalveolar lavage protein levels [164, 191, 241]. In addition, several other experimental studies confirmed that MSC application decreased endothelial permeability and had a protective effect against inflammatory disruption of barrier function [209, 210, 242, 243]. Further endotoxin-mediated ALI studies confirmed therapeutic effect of BM-MSC by showing reduced pulmonary inflammation, injury and edema [213], improved vascular permeability [244], suppressed systemic response to endotoxin via decreased levels of TNF-α and IL-1β [231, 244] and simultaneously increased levels of IL-10 [244] after systemic infusion of BM-MSC. Additionally, Ang-1 transfected MSC reduced severity of LPS induced ALI [164, 214]. Moreover, MSC treatment improved survival, enhanced bacterial clearance, upregulated antimicrobial protein lipocalin 2 levels [234] and decreased bacterial growth [191, 209] in live bacteria injured lung. Furthermore, MSC produced and secreted antimicrobial peptide, human cathelicidin hCAP-18/LL-37 in pneumonia caused by Gram-negative bacteria (*E.coli* and *P.aeruginosa*). Jointly, this antibacterial effect and immuno-modulatory properties of MSC were proved in several bacterial sepsis models demonstrating reprogramming of endogenous macrophages resulting in increased IL-10 production [211].

BM-MSC therapeutic mechanism in ALI/ARDS is summarized and presented in the picture below (Figure 1-10).

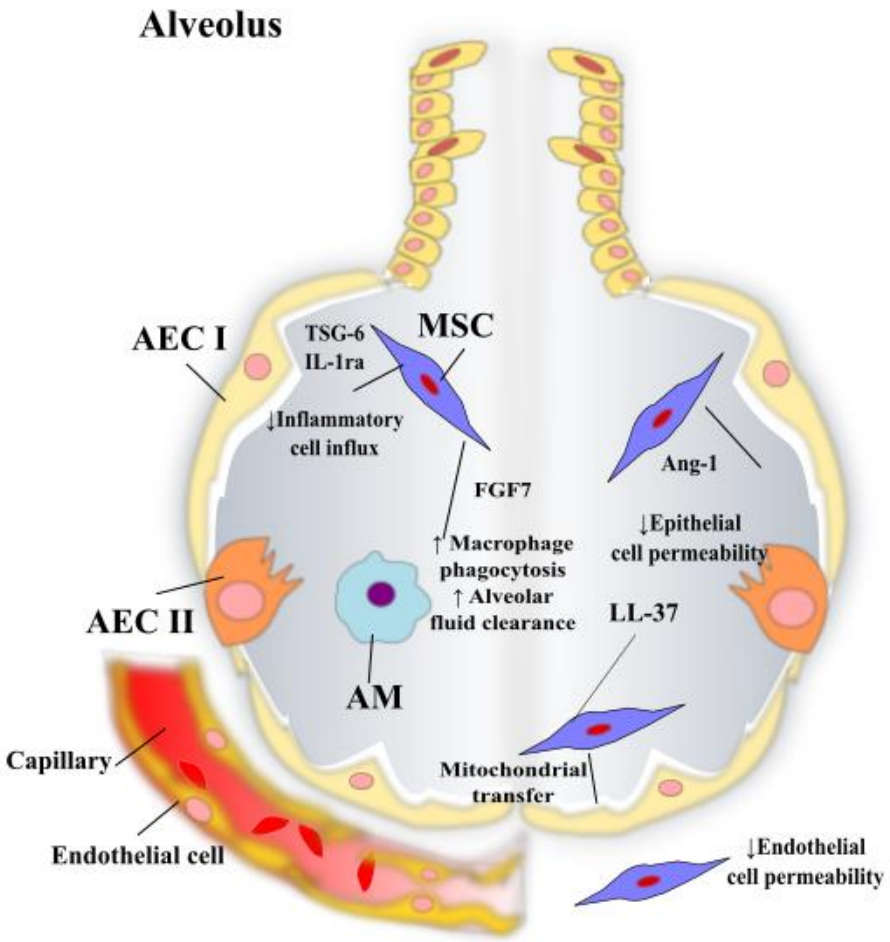

Figure 1-10. The beneficial actions of intravenously or intra-tracheally installed MSC in ARDS. The modulatory effects include: exertion of anti-inflammatory effects on host tissue, reduction of the permeability of the alveolar epithelial-endothelial membrane, improvement of alveolar fluid clearance, improved macrophage, monocyte and neutrophil phagocytic activity, exertion of anti-apoptotic effect on host cells, antimicrobial effect. MSC might modulate tissue repair through direct mitochondrial transfer or via exosomes. ARDS, acute respiratory distress syndrome; MSC, mesenchymal stem cell; AEC I, alveolar epithelial cell type I; AEC II, alveolar epithelial cell type II; AM, alveolar macrophage; FGF7, fibroblast growth factor 7; Ang-1, angiopoetin-1; Il-1ra, interleukin 1 receptor a; TSG-6, TNF-stimulated gene 6; LL-37, antimicrobial peptide. Adapted from [245].

e) MSC paracrine support via extracellular vesicles (EVs)

A relatively new discovery is that the beneficial effect of MSC is mediated via the release of various particles, such as extracellular vesicles. Extracellular vesicles (EVs) are generally referred as ectosomes or microparticles, and include apoptotic bodies (50 – 5000nm), microvesicles (MV) (100 – 1000nm) and exosomes. Exosomes have received much attention being a subclass of (nano) vesicles sized 30-100nm. Their membranes are enriched with

cholesterol, sphingomyelin, ceramide and lipid rafts. These EV contain proteins, lipids, nucleic acids and mRNAs and miRNAs [246-252] (Figure 1-11). Exosomes are derived from the late endosomes or multi-vesicular bodies (MVB). Once secreted, exosomes can either be endocytosed after binding to recipient cell or stay in biological fluids [250]. These nano vesicles were shown to be released by various cell types [253-258]. Most exosomes have an evolutionary conserved set of surface proteins like tetraspanins (CD63, CD81, and CD9), Alix or Tsg101, but also a specific set of proteins reflecting their cellular source (Figure 9). The internal EV membrane is enriched in lipids [259]. The lipid composition of exosomes is distinct from that of the cell origin, but is characteristic to a specific cell type.

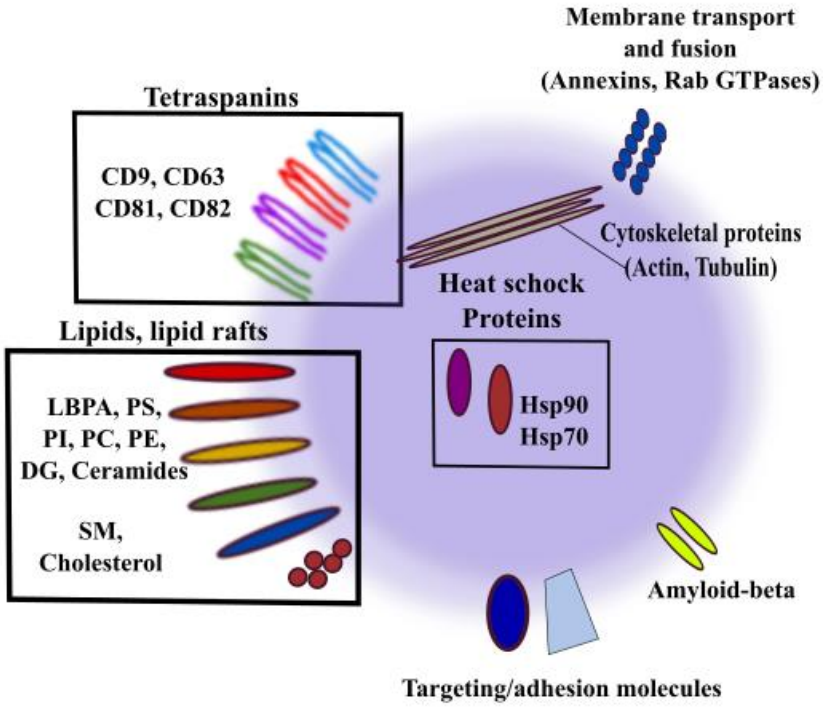

Figure 1-11. Schematic picture of exosome and some proteins and lipids present in it. Tetraspanins (CD9, CD63, CD81, CD82) and heat schock proteins (Hsp) such as Hsp90 and Hsc70 are enriched in exosomes. Phospholipidases are activated by GTPases (Rab, Rap, Ran, RhoA, Arf) and are regulated by aldolase, casein kinase II, and Hsp/Hsc70. The major phospholipids are present in exosomes but in distinct proportions as compared to parent cells, as well as lipid rafts. LBPA, lysobiphosphatidic acid; PS, phosphatidylserine; PI, phosphatidylinositol; PC, phoshatidylcholine; PE, phosphatidylethanolamine; DG, diacylalkylglycerols; SM, sphyngomyelin; Rab, a member of Ras superfamily of monomeric G proteins; Hsp, heat schock protein. Adapted from [260].

The MSC microvesicle genome analysis revealed 239 unique transcripts for genes that were involved in cell differentiation, transcription, proliferation and immune regulation [261].

Moreover, 730 proteins for cell proliferation, adhesion and migration were identified in a proteomic analysis of MV derived from human MSC [262]. Consequently, recent studies showed exosome contribution to immune response [263], exosome function as mediators of cell-cell communication [264], exosomes‘ beneficial effect in cardiac repair [252, 265, 266] and neurological recovery potential [252, 267]. An intra-tracheal MSC MV application in endotoxin-mediated lung injury displayed a potential benefit equal to the cell administration and reduced lung inflammation and prevented edema formation [228]. Another study demonstrated that MSC treated LPS-injured mice transferred mitochondria-containing MV to AECs via the gap junctions [172]. These data supported the hypothesis, that MSC derived exosomes could contribute to lung repair.

2. Aims of this work

IAV induced ARDS is associated with 60% lethality and has been frequently observed upon H5N1 and pandemic H1N1 IV infections [54, 87, 268]. Antiviral therapies are only effective in the very beginning of IV infection, and specific treatment methods for IV-induced ARDS are still lacking. Recently, MSC, multi-potent stromal cells with anti-inflammatory and regenerative potential [210, 269, 270], were attributed a beneficial role in acute and chronic lung injury [212, 221, 225, 230, 235, 271], suggesting MSC delivery to be a promising treatment strategy in IV-induced ARDS.

The first aim of the presented work was to isolate and characterize primary bone marrow derived MSC from healthy wild type (*wt)* mice. As the putative beneficial role of MSC in IAV-induced lung injury has not been studied so far, the second aim of presented thesis was to address their potential and mode of action in *in vitro* co-culture models with IAV-infected primary alveolar epithelial cells (AECs). Further, the impact of their intra-tracheal application was analysed in *in vivo* IAV induced lung injury in mice.

:

3. Materials and methods

3.1 Mice strains

Wildtype C57BL/6N mice (*wt*) were purchased from Charles River Laboratories (Germany). Gt(ROSA)26Sor $^{tm4(ACTB-tdTomato,-EGFP)Luo}$/J (*mT/mG*) [272] mice expressing a red fluorochrome (tdtomato) on all cells were purchased from Jackson Laboratory (USA), *ifnar*-/- [273] were provided by U. Kalinke (Paul-Ehrlich Institute, Langen, Germany). Mice were housed and bread under specific pathogen-free conditions (SPF) at the Justus-Liebig University of Giessen. For *in vivo* experiments 8 to 12 weeks old *wt* and *ifnar*-/- mice were monitored 1 to 2 times per day.

3.2 IAV strain

A/Puerto Rico/8/1934 H1N1 (PR/8) mouse adapted influenza A virus was used for all experiments, propagated on MDCK (Madin Darby Canine Kidney) cells and virus titres were regularly checked by plaque assay.

3.3 Primary cells and cell lines

3.3.1 Cell lines

Mesenchymal stem cells (MSC, Cyagen) and 3T3 (NIH) cells were cultured in cell culture flasks in adequate media (see table below) at 37°C and 5% CO_2. For passaging, cells were washed with PBS (PAN-BIOTECH) and then detached and singularized with Stem-Pro®Accutase® (TermoFischer Scientific). For freezing, MSCs were kept in NCR Protein-Free Cryopreservation Medium (Cyagen Biosciences) and 3T3 in 10% DMSO in FCS (Fetal Calf Serum, Life Technologies).

Cells	**Origin**	**Culture medium**
MSC, Cyagen	C57Bl/6N Mouse Bone Marrow Mesenchymal Stem Cells	Strain–OriCell™ Mouse Mesenchymal Stem cells Growth Medium (Cyagen Biosciences)

NIH/3T3	Mouse embryonic fibroblasts	DMEM (Life Technologies), 10%FCS + 1%Penicillin/Streptomycin (P/S, Sigma)) + 1%L-Glutamine (Sigma)

3.3.2 Primary Murine Alveolar Epithelial Cells (AECs)

AEC were isolated as described by Corti et al [274]. Briefly, mice were sacrificed; lungs were perfused with sterile HBSS (Gibco) via a 26-gauge cannula inserted into the right ventricle. Then sterile dispase was instilled into the lung. Lungs and trachea were removed and incubated in dispase for 40min at room temperature (RT). After incubation, heart, trachea and large bronchi were removed. Remaining lung tissue was processed in DMEM/2.5%HEPES (Biochrom) plus 0.01%DNAse (Serva) for homogenisation using gentleMACS Dissociator (Milteny Biotec). Lung tissue was then incubated for 5min at RT by gentle rotation. After incubation, cells were filtered, washed, resuspended in DMEM/2.5% HEPES and counted. Next, cells were incubated with biotinylated anti-mouse CD45, CD16/32, CD31 antibodies (BD Pharmingen) for 30min at 37°C to exclude remaining endothelial cells and leukocytes. The amounts of antibodies were calculated as following:

$$\boldsymbol{CD45}(\mu l) = \frac{number\ of\ cells}{1.000.000} \times 0.9 \qquad \boldsymbol{CD16/32}\ (\mu l) = \frac{number\ of\ cells}{1.000.000} \times 0.675 \qquad \boldsymbol{CD31}(\mu l) = \frac{number\ of\ cells}{1.000.000} \times 0.4$$

After incubation, cells were washed and mixed with streptavidin-linked magnetic beads (Invitrogen) prewashed thrice with PBS. The mixture was incubated for 30min RT with gentle rocking. The amount of magnetic beads was calculated as follows:

$$\frac{\frac{number\ of\ cells}{1.000.000}}{3} \times 50 = magnetic\ beads\ (\mu l)$$

Magnetic separation was performed at RT. The remaining suspension was washed and cells were resuspended in mAEC (murine alveolar epithelial cell) medium. Freshly isolated mAECs were stained for EpCAM (epithelial cell adhesion molecule) and pro-surfactant protein C (pro-SPC) and purity was analysed by flow cytometry (see *Flow cytometry section*). Only cell suspensions with a purity ≥90% were used for further experiments as described elsewhere. Cell viability was tested by trypan blue (Gibco) staining and was ≥95%.

3.3.3 Primary Murine Bone Marrow Mesenchymal Stem cells (BM-MSC)

Wt and *mTmG* mice were used for BM-MSC isolation. BM-MSC were isolated following a protocol adapted from Houlihan et al [131]. 8-12-week-old mice were sacrificed by cervical dislocation and isoflurane inhalation. Mice were disinfected with 70% (vol/vol) ethanol and limbs (tibias, femurs, hips and humeri) were freed from skin and hair covering. Bones were dissected from adherent muscle by blunt dissection. Dissected bones were carefully cleaned using gauze swabs to remove remaining muscle tissue. Cleaned bones were stored in 30ml ice-cold PBS. Next, they were washed in fresh ice-cold PBS thrice by vigorous shaking. Then, bones were gently crushed using sterile pestle and mortar avoiding multiple crushes per bone. The crushed bones' fragments were cut into tiny pieces with sterile scissors. The paste like mass was stored in 1-2ml HBSS+ and then three times washed with 10ml HBSS+ (see table below) per wash. Bone mass was then collected into a 50ml conical tube with 20ml preheated MSCs Medium+0.2% (wt/vol) collagenase A (Roche Diagnostics, DE) and incubated for 90min at 37°C by gentle shaking. After incubation cell suspension was filtered through a 70µm cell strainer in a conical tube and it was placed on ice to quench collagenase activity. The remaining bone fragments were placed in the mortar and crushed by gentle tapping to avoid too much damage to the BM-MSC pool. The bone mass was several times washed with HBSS+ (see table below) and cells were washed out into solution by gentle pipetting. The liquid was then filtered and centrifuged at 500g for 10min at 4°C. The pellet was erylysed with 1-2ml sterile ice-cold water for 6s. The reaction was quenched immediately after the lysis adding 1-2ml PBS2x. The suspension was again filtered through the 70µm cell strainer and then centrifuged in a precooled centrifuge at 500g for 5min. After the second centrifugation step, cell pellet was resuspended in HBSS+ and counted. Count and viability was assessed by trypan blue staining. Succeedingly, cells were prepared for FACS analysis (See *Flow cytometry and cell sorting*). Samples were stained with an antibody mix (CD45, TER119, Sca-1, PDGFRα/CD140α). Cell purity was measured after each sort, and was between 90-95%. Sorted cells were then seeded for further expansion and incubated in 37° and 5%CO2. Medium was first changed after 3-4 days and then every 2-3 days. For passaging, cells were twice washed with PBS and then detached and singularized with Stem-Pro®Accutase®. Passages 8-12 were used for further experiments.

Reagents	Composition
HBSS+	Hank`s Balanced salt solution + 2%(vol/vol) FCS + 1%(vol/vol)P/S + 10mM Hepes
MSCs Medium	DMEM low Glucose+Glutamax (Gibco) + 10%(vol/vol) FCS + 1%(vol/vol)P/S
PBS2x	Double-strength Phosphate buffered solution (PBS) + 4% (vol/vol) FCS

3.4 BM-MSC Characterization and differentiation

BM-MSCs were characterized at passage 5 to 18 following the Consensus Protocol proposed by the International Society for Cellular Therapy [149].

To examine MSC surface antigen expression, BM-MSC were stained with anti-mouse antibodies against CD105, CD73, CD90.2, PDGRFα, Sca-1, CD44, CD29, CD117, CD45, CD19, CD11b, CD31, CD34, TER119 and appropriate isotype controls (see the table in *Flow cytometry and cell sorting*).

For differentiation experiments cells were seeded in 8-well chamber slides (Thermo Scientific). Adipogenic differentiation was performed following manufacturer's instructions. Confluent culture was incubated in adipogenic induction medium (Adipogenic Induction SingleQuots®, Lonza) for 4 days and then replaced with adipogenic maintenance medium (Adipogenic Maintenance SingleQuots®, Lonza) for 3 days. After two cycles, cells were washed and then fixed. Thereafter, fixed cells were stained with Oil-red O and then slides were analysed by light microscopy.

For osteogenic differentiation, a sub-confluent BM-MSC culture was used. Samples were cultured in osteogenic medium (Osteogenic SingleQuots®, Lonza) for 14 days. Next, they were washed and fixed. After fixation, cells were stained with Alizarin Red Staining Solution (Sigma Aldrich) and then analysed by light microscopy.

For chondrogenic differentiation, confluent cells were cultured in chondrogenic maintenance medium (Chondrogenic SingleQuots®, Lonza) supplemented with TGF-β3 (10ng/ml; Lonza)

and BMP-6 (500ng/ml; R&D Systems) for at least 21 days. Thereafter, cells were washed and fixed. Samples were stained with 1% (wt/vol) Alcian Blue Staining solution and incubated over night at 37°C. The next day destaining solution consisting of 98-100% Ethanol and 98-100% Acetic Acid (ratio 3:2) was added, followed by several washing steps in PBS. Then, slides were submitted to light microscopy analysis.

3.5 BM-MSC derived exosomes

3.5.1 Isolation

The BM-MSC conditioned medium (CM) was collected daily and frozen in -20°C. Dynabeads® Biotin Binder (Invitrogen) were washed 3 times with PBS. Washed beads were incubated with CD9 and CD81 biotinylated antibodies (Biolegend) for 45min at RT in PBS + 0.1% exosome free FCS (SBI) with gentle tilting and rotation. The tubes were placed on a magnet for 1min and the supernatant was discarded. The antibody-coated beads were then 3-5 times washed with PBS+0.1% exosome free FCS. The fresh CM or unfrozen samples were filtered through 0.2µm filters and mixed with pre-coated beads. Next, the mix was incubated for 24h at 4°C by gentle rotation. After incubation, beads were collected with a magnet for ≤15min RT (Figure 3-1). Collected beads were washed thrice with PBS+0.1% of exosome free FCS, discarding the supernatant each time.

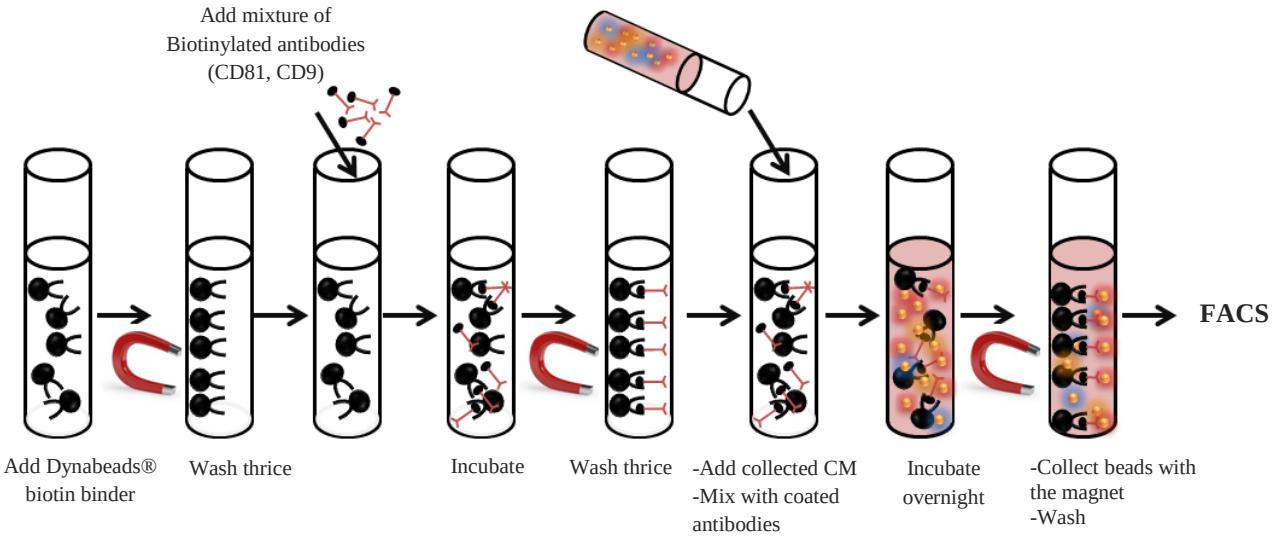

Figure 3-1. Exosome isolation protocole.

3.5.2 Exosome characterization

Coupled beads were resuspended in PBS+ 0.1% exosome free FCS and centrifuged for 5min at 3000rpm at 4°C. Probes were then stained for different surface markers and their isotypes (see table in section *Flow cytometry and cell sorting*) and analysed by FACS. Exosome count was determined by FACS analysis using the following formula:

$$\textbf{Count of exosomes} = \frac{\text{No of events in region containing exo}}{\text{No of events in absolute count bead reagion}} \times \frac{\text{No of beads per test}}{\text{Test volume (µl)}}$$

Bead saturation was defined by serial dilutions.

3.6 *In vivo* experiments and sample processing

3.6.1 Intra-tracheal IAV infection and cell application

For in vivo IAV infection or cell application after infection, animals were inoculated with Atropine sulphate (concentration of 0.05mg/kg) subcutaneously to prevent bradycardia and reduce the production of salivary and bronchial secretion to minimise the risk of airway obstruction. Mice were subjected to an intraperitoneal Xylazine hydrochloride (concentration of 16mg/kg) and Ketamine hydrochloride (100mg/kg) anaesthesia in 0.1ml/10g of body weight; or they were sedated via isoflurane inhalation. During the anaesthesia, all animals were kept warm on a heating plate to maintain a stable body temperature. The depth of anaesthesia was monitored testing pedal withdrawal reflex. After sufficient depth of anaesthesia was reached, mice were placed supine on the intubation stand. The upper incisors were secured with a fixed rounded rubber loop following fixation of the lower extremities. The stand was rotated to a 45° angle and, using a cotton swab, the tongue was rolled out. An intubation guide wire with endotracheal tube was introduced from the side of the mouth and advanced through the vocal chords into the trachea. The endotracheal tube was then advanced over the guide wire, which was immediately withdrawn. Intubation was confirmed by brief occlusion of the tube while observing the change in thoracic respiratory movements. Using a Hamilton syringe, mice were inoculated with 500pfu (plaque forming units) of PR/8 diluted in 40µl sterile PBS. In cell application experiments, PBS or 250 000 3T3 or primary *wt* BM-MSC diluted in 40µl sterile PBS or *mTmG* BM-MSC for MSC trafficking/engraftment studies were applied intra-tracheally. After the installation, mice were monitored on the

heating plate until complete recovery. Mice were then monitored 1-2 times per day until the end of the experiment.

3.6.2 Collection of Bronchoalveolar Lavage Fluid (BALF)

Mice were sacrificed as mentioned before. A small tracheal incision was made and it was cannulated by a 21-gauge cannula. Consecutive instillations and collection of 300, 400 and 500µl of ice-cold 2mM EDTA/PBS were performed. Subsequently, BAL collection was completed performing installation-collection cycles of 500µl 2nM EDTA/PBS until the final volume of 4ml was reached. Both BAL fractions were then centrifuged at 1400rpm 10min at 4°C. The supernatant of the first BAL fraction was divided into collection tubes for further cytokine quantification or alveolar leakage determination. The supernatant of the second BAL fraction was discarded and cells from both fractions were pooled and further analysed by FACS or microscopy.

3.6.3 Preparation of Lung Cell Homogenate (LH)

LH was prepared following the procedure steps as described in the section *Primary Murine Alveolar Epithelial Cells (AEC).* After filtration and washing steps, cells were resuspended in MACS buffer (1x Phosphate buffered solution + 7.5% (vol/vol) EDTA (Biochrom) + 2% (vol/vol) FCS) and submitted for flow cytometric analysis or further isolated via FACS-based cell sorting.

3.6.4 Lung permeability assay

To determine alveolar albumin leakage as determinant of lung barrier function loss, FITC-labelled albumin (1mg) diluted in 100µl of sterile NaCl 0.9% was injected intravenously into the tail vein. After 45min, mice were sacrificed with an overdose of isoflurane and the abdominal cavity was opened. Blood was drawn from the inferior vena cava with a 23-gauge cannula connected to a 1ml syringe, and immediately transferred into a 1.5ml collection tube. The BALF was collected as described before (see section *Collection of Bronchoalveolar Lavage Fluid*). Blood samples were incubated for 3h at RT until coagulation occurred and then centrifugated at 4000rpm 15min RT. Serum supernatant was collected thereafter. BALF

and serum (the latter 1:100 diluted in PBS) were tested for FITC fluorescence and compared with standard samples (serial dilutions 1:10 in PBS). These measurements were performed using a fluorescence spectrophotometer (FL 880 microplate fluorescence reader, Bio-Tek Instruments, France) operating at 488nm absorbance and 525±20nm emission wavelengths. Fluorescence signals of concentrated BALF samples to fluorescence signals of 1:100 diluted serum samples are defined as lung permeability index (LPI) and expressed as arbitrary units (AU).

3.6.5 Histological assessment of the lung

Mice were sacrificed as mentioned before. Lungs were perfused via the right ventricle with sterile HBSS. The trachea was cannulated, 1.5ml of 4% of paraformaldehyde (PFA) was slowly instilled and the trachea was fixed with a ligature after removing the cannula. The lungs were transferred into 4% PFA solution where they were incubated for 24h at 4°C. Then, lungs were embedded in paraffin (Leica ASP200S). Thereafter, 3-5µm thick tissue sections were cut, put on slides and kept at RT until staining. Tissue cuts were first deparaffinised by the following procedure: Xylene 5min (twice), 100% Ethanol (EtOH) 30sec (twice), 96%, EtOH 30s, 96% EtOH 30s, 70% EtOH 30s and 70% EtOH 30s. Then, slides were stained with haematoxylin and eosin as follows: Haematoxylin 3min, 0.1% HCl 2sec, H_2O 5min, Eosin G solution 3min, H_2O 30s, 70% EtOH 30s, 90% EtOH 30s, 100% EtOH 30s (twice), Xylene 5min (twice).

For preparation of cryo-slices, murine lungs were perfused with PBS and intra-tracheally filled with 1.5ml TissueTek (Sakura) diluted in PBS (ratio 1:1). The trachea was then fixed with a ligature and the cannula was removed. Lungs were embedded in TissueTek diluted in PBS (ratio 1:1) and snap-frozen in liquid nitrogen. Cryo-slices of 4-5 µm thickness were prepared using a Leica CM1850 UV cryotome. Cryo-slices were stored at -80°C. Thereafter, they were air-dried and fixed in Methanol and Acetone (ratio 1:1) for 3min RT. Then, fixed cryo-slices were twice washed with distilled water (dH2O). After washing, they were stained with DAPI (Sigma-Aldrich) for 5min RT and subsequently washed with dH2O. After mounting procedure (Fluoromount™, Sigma-Aldrich), slides were submitted for microscopic analysis.

All slides were analysed with Leica DM 200 microscope and ImageJ software.

3.7 *In vitro* IAV infection and cell culture assays

3.7.1 AEC culture and infection

Isolated primary cells or cell lines were cultured on transwells (12-well, Costar) for five days. To achieve the indicated MOI (multiplicity of infection) of the virus inoculum, virus stock solution (PR/8) was diluted in PBS supplemented with 0.2% of BSA (bovine serum albumin).

Prior to the infection, cells were washed with PBS, virus dilution was applied and then samples were incubated for 1h at 37°C at 5% CO2. Cells were then washed and placed into infection medium containing 0.2% BSA, 100U penicillin/ml, 0.1mg streptomycin/ml and 2 µg/ml trypsin TPCK (PAA). Infected cells were kept at 37°C 5%CO2 for the indicated time periods.

3.7.2 AEC co-culture with BM-MSC, 3T3 cells or BM-MSC-derived conditioned medium (CM)

For co-culture experiments, 60000 primary mBM-MSC or 3T3 cells were seeded at the bottom of transwells two days prior to AEC infection. After 24h inoculation with PR/8, bottom seeded cells were combined with AECs seeded on transwells (Figure 3-2).

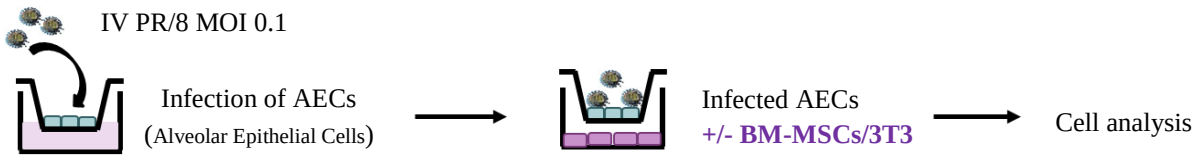

Figure 3-2. AEC co-culture model with BM-MSC or 3T3 control fibroblasts. AEC, alveolar epithelial cells; BM-MSC, bone marrow derived mesenchymal stem cells; 3T3, embryonic fibroblasts; IV, influenza virus; MOI, multiplicity of infection.

BM-MSC derived CM was collected one day after the BM-MSC had been co-incubated with PR/8-infected AEC and then incubated with PR/8-infected AEC in transwells (Figure 3-3). Cells were collected at indicated time points and used for further experiments.

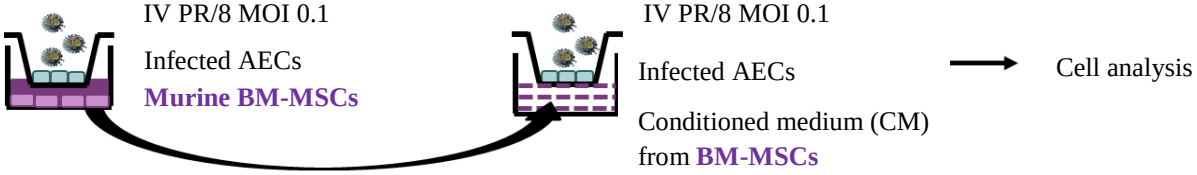

Figure 3-3. AEC co-culture model with conditioned medium (CM) of BM-MSC. AEC, alveolar epithelial cells; BM-MSC, bone marrow derived mesenchymal stem cells; IV, influenza virus; MOI, multiplicity of infection.

3.7.3 BM-MSC priming

For priming experiments, BM-MSCs were seeded two days before AEC infection with PR/8. One day before infection, cells were washed twice with PBS and incubated for indicated time points with stimuli (TLR3, 7/8 and RIG-I ligands; cytokines; see table below) diluted in MSC medium. After incubation, supernatant was discarded and cells were thoroughly washed thrice with PBS and co-cultured with mock or PR/8-infected AEC for 24h at 37°C 5%CO2. AECs were detached and submitted to FACS analysis, and culture supernatants were used for protein analysis.

Chemical	**Function**	**Concentration**	**Company**
Poly (I:C)	TLR (Toll like receptor) 3 agonist	0.5-100 µg/ml	Tocris
R848	TLR 7/8 agonist	10-100 ng/ml	InvivoGen
5′ppp-dsRNA	RIG-I agonist	0.5-1 µg/ml	InvivoGen
Recombinant protein		**Concentration**	**Company**
TNFα, mouse		10-200 ng/ml	R&D systems
IFNβ, mouse		0.1, 05 ng/ml	R&D systems

3.8 Analysis of gene expression

3.8.1 RNA isolation and cDNA synthesis

RNA isolation was performed following manufacturer's instructions (RNeasy Kit, Qiagen). Briefly, cells were washed with PBS and then lysed with 350µl RLT buffer. Thereafter, 350µl of ethanol was added and RNA was precipitated, bound to a silica membrane, washed and eluted in small volumes. RNA concentration was measured with Nanovue Plus (GE Healthcare). cDNA synthesis was performed using recombinant Taq DNA polymerase (Invitrogen) and a thermocycler (PeqSTAR thermocycler (Peqlab, Erlangern (DE)) following manufacturer's instructions (Applied Bioscience). Briefly, 250ng of isolated RNA with dH2O in a total volume of 13.5µl were heated up to 70°C for 5min and then samples were put on ice

for 3-5min. Thereafter, 11.5µl of PCR Master Mix (with reverse transcriptase) was added and samples were kept at 37°C for 1h. Reverse transcriptase was inactivated by heating up to 95°C for 5min.

3.8.2 Quantitative Real-Time Polymerase Chain Reaction (qRT-PCR)

qRT-PCR was performed with Power SYBR Green® (ThermoFisher) following the manufacturer's instructions. RPS18 (40S ribosomal protein S18) expression served as normalization control. Data are presented as fold change of gene expression over control and the formula is the following:

$$Fold\ change = 2^{-\Delta/(\Delta Ct)}$$

Where ΔCt=ΔCt target – ΔCt reference (RPS18), and Δ(ΔCt)=ΔCt condition – ΔCt control

The primers used in qRT-PCR are represented in the table below.

Primer	**Sequence**	
	Forward 5'→3'	**Reverse 5'→3'**
RPS18	CCGCCATGTCTCTAGTGATCC	TTGGTGAGGTCGATGTCTGC
VEGF	CACCATGCCAAGTGGTCCC	GTCCACCAGGGTCTCAATCG
HGF	GGGCTGAAAAGATTGGATCA	TCGAACAAAAATACCAGGACG
FGF10	CCATGAACAAGAAGGGGAAA	CCATTGTGCTGCCAGTTAAA
FGF7	TCGCACCCAGTGGTACCTG	ACTGCCACGGTCCTGATTTC
IFNβ	GTTACACTGCCTTTGCCA	GTGGAGTTCATCCAGGAGACG
IFNa1	GCATCTACAAGACCCACAATGGC	TGTCAAGGCCCTCTTGTTCCC
GM-CSF	GAAGCATGTAGAGGCCATCA	GAATATCTTCAGGCGGGTCT
STC	GCCTGATGGAGAAGATCGGG	GTGCGTTTGATGTGTGAGGG
Wnt5a	GCAGGACCTGGTCTACAT	ACTTGCAATGACAGCGTT

Melting curve analysis was performed to confirm the exclusive amplification of the expected PCR product.

3.8.3 Microarray experiments

For microarray experiments, AEC were lysed in lysis buffer (Qiagen kit). The further procedure and analysis was performed by J. Wilhem and S. Ziegler (AG Dr. Jochen Wilhelm, Giessen) using the Ovation PicoSL WTA System V2 (NuGEN) for cDNA amplification, the

QIAquick PCR Purification Kit (Qiagen) for cDNA purification and SureTag DNA Labeling Kit (Agilent) for cDNA labeling. After the purification and labeling, cDNA concentration was measured with the NanoDrop. Labeled targets were hybridized to Agilent Dual-mode Gene expression arrays. Microarray processing was continued according the manufactures instructions (NuGEN).

Gene Ontology (GO) enrichment analysis was performed and provided by Dr. J. Wilhelm. Next, each probe set was statistically tested using ANOVA, and the resultant p values were adjusted for multiple testing. Hierarchical clustering and heatmap visualization of *Z* score normalized data for complete data or select genes were performed. Further, gene expressions were ranked by average fold change and t-statistic, and subsequently summarized using volcano plots. Volcano plots represent the negative $\log_{10}$-transformed *p*-values from the gene-specific *t* test against the $\log_2$ fold change. Pathway annotation was taken from Kyoto Encyclopaedia of Genes and Genomes (KEGG) database package. Only pathways with >3 genes were considered. The tests were performed based on the *t*-statistics including both up- and downregulated genes.

3.9 Flow cytometry and cell sorting

Multicolor flow cytometry analysis was performed with a 4 laser-equipped LSR Fortessa FACS analyser using DIVA software (BD Bioscience). Cell sorting was performed with a 4 laser-equipped FACS ARIA III (BD Bioscience).

For flow cytometry analysis 1-5x10^5 cells were resuspended in FACS buffer (PBS, 7.4% EDTA, 0.5% FCS pH 7.2, 0.01% Na^+Azide (Merck)). Cells were then pelleted by centrifugation at 1200rpm 3min at 4°C. Unspecific antibody binding was blocked with 10µl Sandoglobulin® (Novartis). For intracellular staining, permeabilization was performed using 0.2% saponin in FACS buffer. For antibody staining, cells were incubated for 15min at 4°C in the dark with the fluorochrome-labelled antibodies or isotype controls at the adequate concentration (see table below), followed by secondary antibody staining where required. Between staining steps, cells were washed with FACS buffer. For cell sorting, MACS buffer (PBS, 7.4% EDTA, 0.5% FCS) was used instead of FACS buffer.

Apoptosis was measured using Annexin-V staining following manufacturer's instructions (Invitrogen). Briefly, fresh 1X Annexin-binding buffer was prepared (1:10 diluted in dH2O) and kept on ice. Then, cells were washed in ice cold PBS. Next, washed cells were

centrifuged at 1200rpm 3min at 4°C, supernatant was discarded and samples were resuspended in 1X Annexin-binding buffer 100µl/probe. Appropriate amount of Annexin-V was added and samples were incubated 15min at 4°C. After the incubation, 400µl of 1X Annexin-binding buffer was added, gently mixed, kept on ice and immediately analysed via FACS.

FlowJo software (Illumina) was used for all data analysis.

Marker	Fluorochrome	Clone	Dilution	Isotypes	Company
LH analysis					
CD45	FITC	30-F11	1:50		biolegend
CD31	488	MEC13.3	1:50		biolegend
Epcam	APC-Cy7	G8.8	1:100		biolegend
CD49f	PE	GOH3	1:50		biolegend
CD24	PE-Cy7	M1/69	1:200		biolegend
BM-MSC and BM-MSC derived exosome characterization					
CD105	APC	MJ7/18	1:50	Rat IgG2a,κ	biolegend
CD73	PB	TY/11.8	1:50	Rat IgG1,κ	biolegend
CD90.2 (Ty-1.2)	APC	53-2.1	1:100	Rat IgG2a,κ	biolegend
PDGRFα (CD140α)	APC	APA5	1:50	Rat IgG2a,κ	biolegend
Sca-1 (Ly-6A/E)	PB	D7	1:50	Rat IgG2a,κ	biolegend
CD44	PE/Cy5	IM7	1:10	Rat IgG2b,κ	eBioscience
CD29	PerCP-eFluor®710	HMβ1-1	1:100	Armenian Hamster IgG	eBioscience
CD117 (c-kit)	PE/Cy7	104D2	1:50	Rat IgG2a,κ	biolegend
CD45	FITC	30-F11	1:50	Rat IgG2b,κ	biolegend
CD19	PE	6D5	1:100	Rat IgG2a,κ	biolegend
CD11b	FITC	M1/70	1:200	Rat IgG2b,κ	biolegend
CD31	PB	390	1:500	Rat IgG2a,κ	biolegend
CD34	FITC	RAM34	1:50	Rat IgG2a,κ	BD Pharmingen
TER119	FITC	TER-119	1:20	Rat IgG2b,κ	Biolegend
CD63	PE	NVG-2	1:100	Rat IgG2a,κ	biolegend
Proliferation					
Mouse Anti Ki67 Set	FITC	B56	20µl	Mouse IgG1, κ	BD Pharmingen
Virus replication					
HA, goat		Polyclonal	1:75		abcam
NP	FITC	431	1:50		abcam

IgG, donkey anti-goat	Alex Fluor 647	Polyclonal	1:500		Invitrogen
Cell sorting (MSC)					
CD45	FITC	30-F11	1:50		biolegend
TER119	FITC	TER-119	1:20		biolegend
PDGRFα/CD140	APC	APA5	1:50		biolegend
Sca-1/Ly-6A/E	PB	D7	1:50		biolegend

3.10 Statistics

All data are given as mean ±SD. Statistical significance of two groups was analysed by unpaired Student's *t* test. One-way ANOVA and post-hoc Tukey's test were used when analysing statistical difference of three groups. All statistical analysis was performed with GraphPad Prism 5. Significance was assumed when p value was less than 0.05, and indicated as *$p<0.05$, **$p<0.01$ and ***$p<0.005$, accordingly.

4. Results

4.1 BM-MSC isolation and characterization

BM-MSCs were isolated by cell sorting from freshly prepared bone marrow cell suspension. First, hematopoietic cells defined as CD45 and TER119 positive cells were gated out and then the population of interest, the BM-MSC, was selected upon high expression of Sca-1 and PDGFRα (Figure 4-1). BM-MSC constitute a tiny population within the whole bone marrow cell pool (0.05 – 0.1%). Sorted $CD45^{-}Ter119^{-}Sca1^{+}PDGFR\alpha^{+}$ cells displayed a purity >90%.

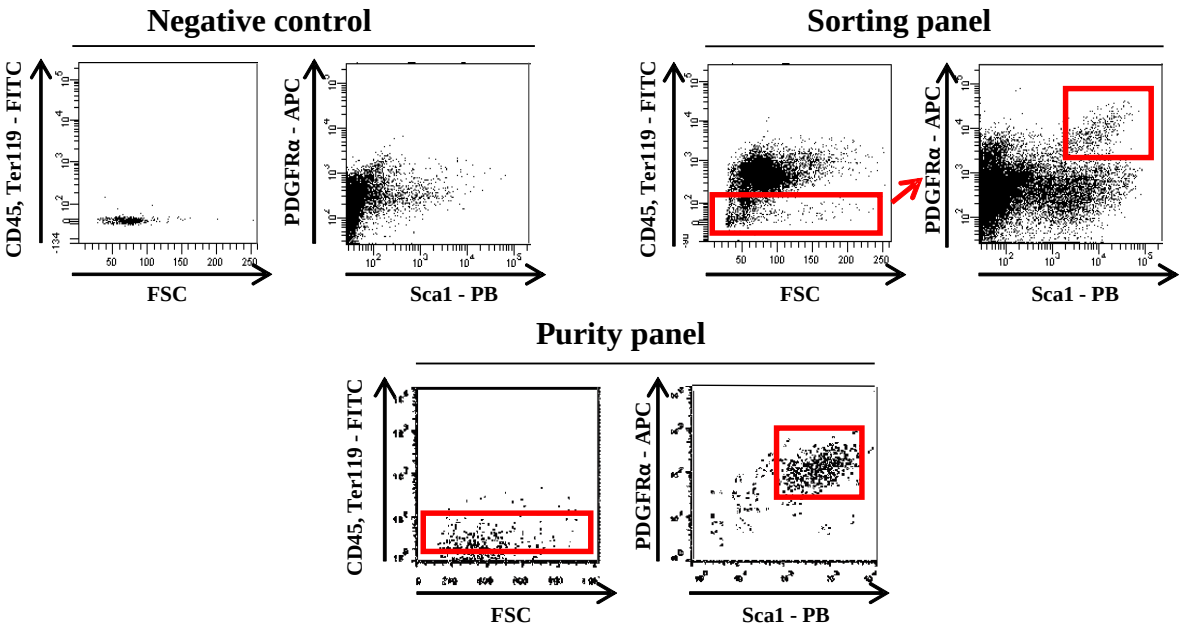

Figure 4-1. Gating strategy for BM-MSC separation by FACS. The target population is phenotyped as $CD45^{-}Ter119^{-}Sca1^{+}PDGFR\alpha^{+}$.

Sorted BM-MSCs were seeded on plastic plates and rapidly showed adherence as well as a fibroblast like shape (Figure 4-2A). BM-MSC were kept in culture (until passage 20) and their typical phenotype was preserved at least until passage 18. Figure 4-2B shows a representative image of their phenotype in culture at passage 8.

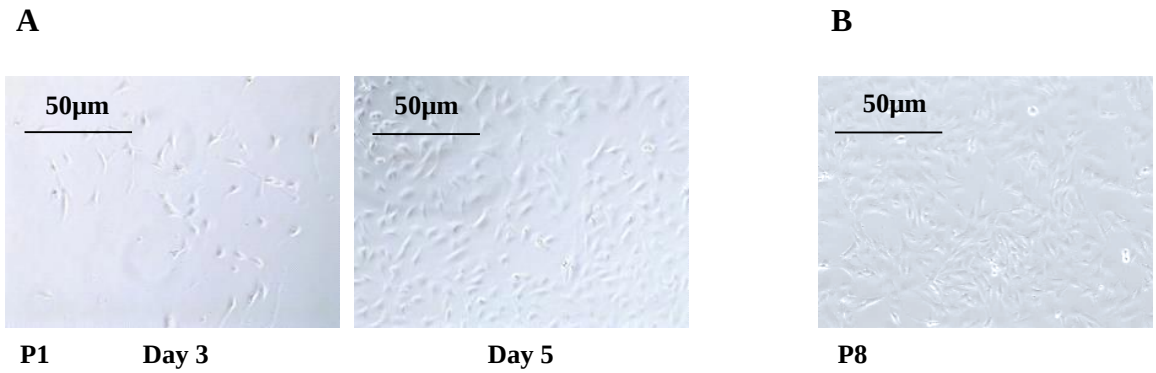

Figure 4-2. Microscopy images of BM-MSC at 3 and 5 days post-sort (*A*), and at passage 8 (*B*).

Sorted BM-MSC were analysed at passage 5 by flow cytometry for surface marker expression. The analysis confirmed their MSC identity as they uniformly expressed the typical mesenchymal stem cell markers CD29 (Integrin β1), CD44 and CD105 (Endoglin), as well as CD90 (Thy-1) and Sca-1 (Ly-6A/E). These cells were negative for hematopoietic markers as CD45 (pan-leukocyte marker), CD19 (B-cell marker), CD11b (Integrin-α-M – monocyte, macrophage marker), CD117 (c-Kit – hematopoietic stem cell marker), and CD31 (PECAM-1 – expressed on endothelial cells, monocytes, neutrophils, platelets) (Figure 4-3). They were positive for CD34, usually described as a hematopoietic progenitor and endothelial cell marker, and negative for CD73 (ecto 5' nucleotidase), another mesenchymal stem cell marker).

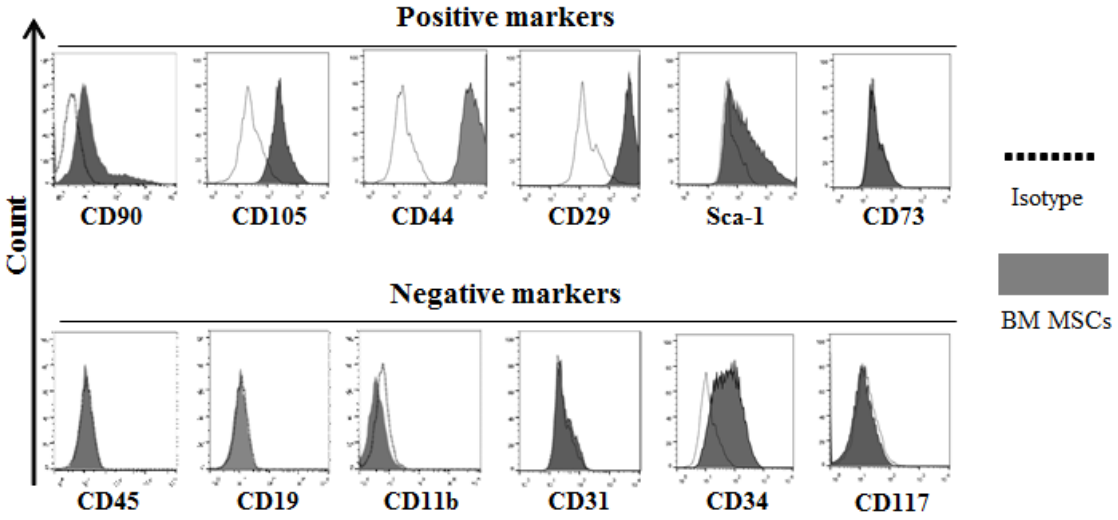

Figure 4-3. Representative histograms of flow cytometry analysis of BM-MSC of passage 5, confirming the BM-MSC phenotype according to consensus definitions.

Moreover, the potential of differentiation of passage 5 BM-MSC was also tested. Under specific consensus conditions, BM-MSC were able to enter adipogenesis, osteogenesis and chondrogenesis differentiation processes and to give rise to adipocytes, osteocytes and chondrocytes as defined by light microscopy with positive staining for Oil-Red, Alizarin-red and Alcian-blue respectively (Figure 4-4).

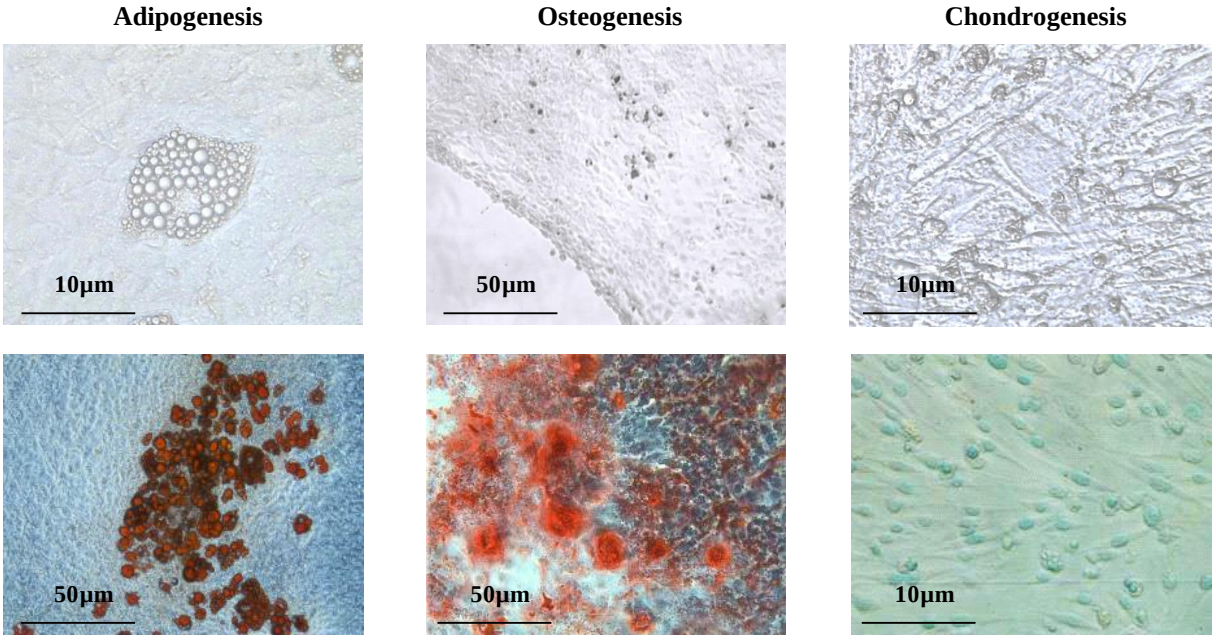

Figure 4-4. Microscopy images of differentiated BM-MSC. Top panel: unstained samples and bottom panel: stained samples with Oil-Red (adipocytes), Alizarin-red (osteocytes), Alcian-blue (chondrocytes).

Taking together, isolated BM-MSCs fulfil the consensus criteria for the definition of multipotent mesenchymal stromal (stem) cells (typical MSC phenotype after many passages, positivity for MSC expression markers and negativity for markers of hematopoietic cell origin, as well as differentiation capacity to three lineages [149]).

4.2 BM-MSC exert a protective role on infected AEC *in vitro* by stimulating alveolar proliferation and anti-viral programs

To test the protective effect of BM-MSC, a co-culture model was established of primary alveolar epithelial cells (AEC) with primary BM-MSC to determine if BM-MSC can improve AEC survival to influenza challenge. AECs were infected with PR/8 and co-cultured with or without primary murine BM-MSC. A genome array was performed comparing the profiles of infected AEC alone (iAEC) and of infected AEC in presence of BM-MSC (iAEC-M) (Figure 4-5A). Microarray analysis revealed upregulation of 457 genes (green) and downregulation of

234 genes (red) in iAEC-M in comparison to iAEC ($p<0.05$) as demonstrated by a volcano plot (Figure 4-5B). Presence of BM-MSC activates a proliferation and survival program in infected AEC as shown by significant increase of genes involved in cell division, mitosis and cell cycle GO pathways. Importantly, BM-MSC strongly induce genes associated with type I interferon signaling and antiviral response genes in infected epithelial cells (Figure 4-5C); for example, the virus resistance genes Mx2, Tetherin (Bst2) and viperin (Rsad2) are up-regulated in iAECs-M compared to iAEC (not shown).

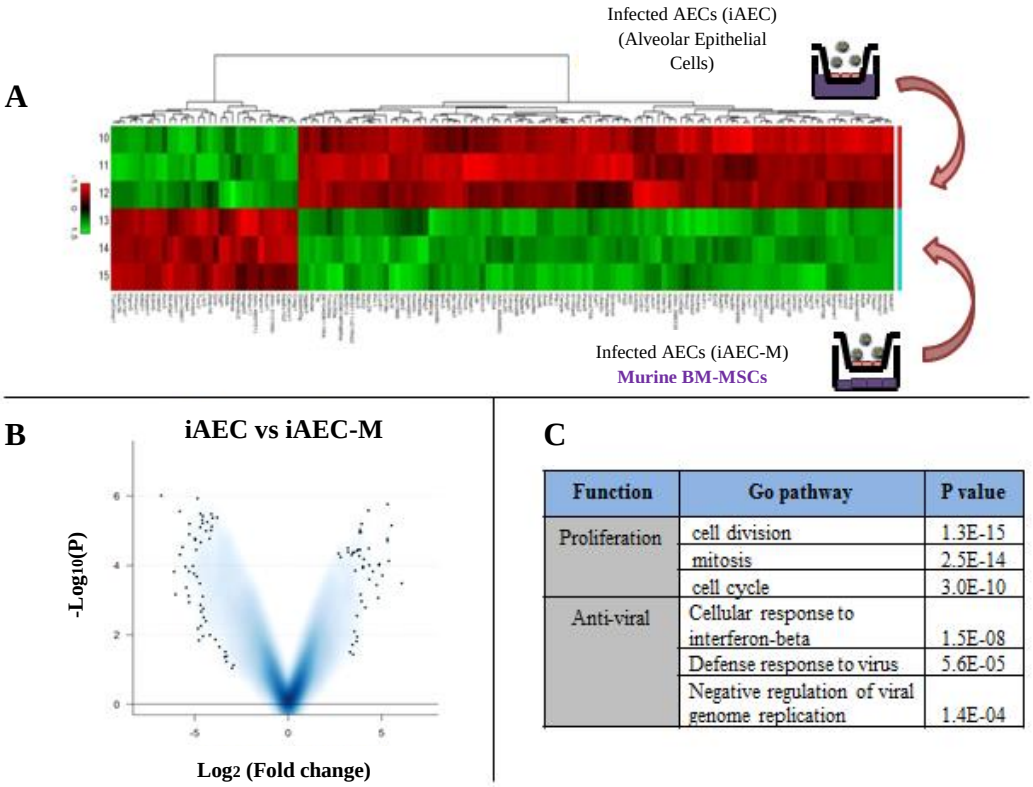

Function	Go pathway	P value
Proliferation	cell division	1.3E-15
	mitosis	2.5E-14
	cell cycle	3.0E-10
Anti-viral	Cellular response to interferon-beta	1.5E-08
	Defense response to virus	5.6E-05
	Negative regulation of viral genome replication	1.4E-04

Figure 4-5. (*A*) Hierarchical clustering and heat map analysis of individual gene expression profiles of iAEC-M versus iAEC at 24h post IV infection. Red bars indicate lower expression levels; green bars represent high expression levels. (*B*) Volcano plot comparing genes expression in iAEC-M versus iAEC 24h post IV infection. Probes identified as significant are labelled on the plot ($p<0.05$). (*C*) Top GO pathways identified in iAEC-M compared with iAEC using microarray analysis.

These data suggest that BM-MSC reprogram infected AEC to activate proliferative/survival signatures, but also induce antiviral programs. To confirm this at a phenotypic level, analysis of AEC proliferation and extent of viral infection was performed by flow cytometry. During IV infection, BM-MSC presence drastically increases the proportion of proliferating AEC as defined by Ki67 positive cells (Figure 4-6A, B). Of note, BM-MSCs foster epithelial proliferation at all analysed time points to a level highly exceeding proliferation of non-

infected AEC. Moreover, virus spread was significantly abolished in infected AECs in co-culture with BM-MSC, as the number of infected cells defined as hemagglutinin (HA) positive was 4 times and 7 times lower at 24 and 48h pi, respectively, compared with infected AECs alone (Figure 4-6 C, D). As PR/8 infection of AEC had been started without BM-MSC in the iAEC-M group, the initial infection rate was similar in all conditions, and as expected, no difference in virus-positive cells was observed after 6h which corresponds to one PR/8 replication cycle.

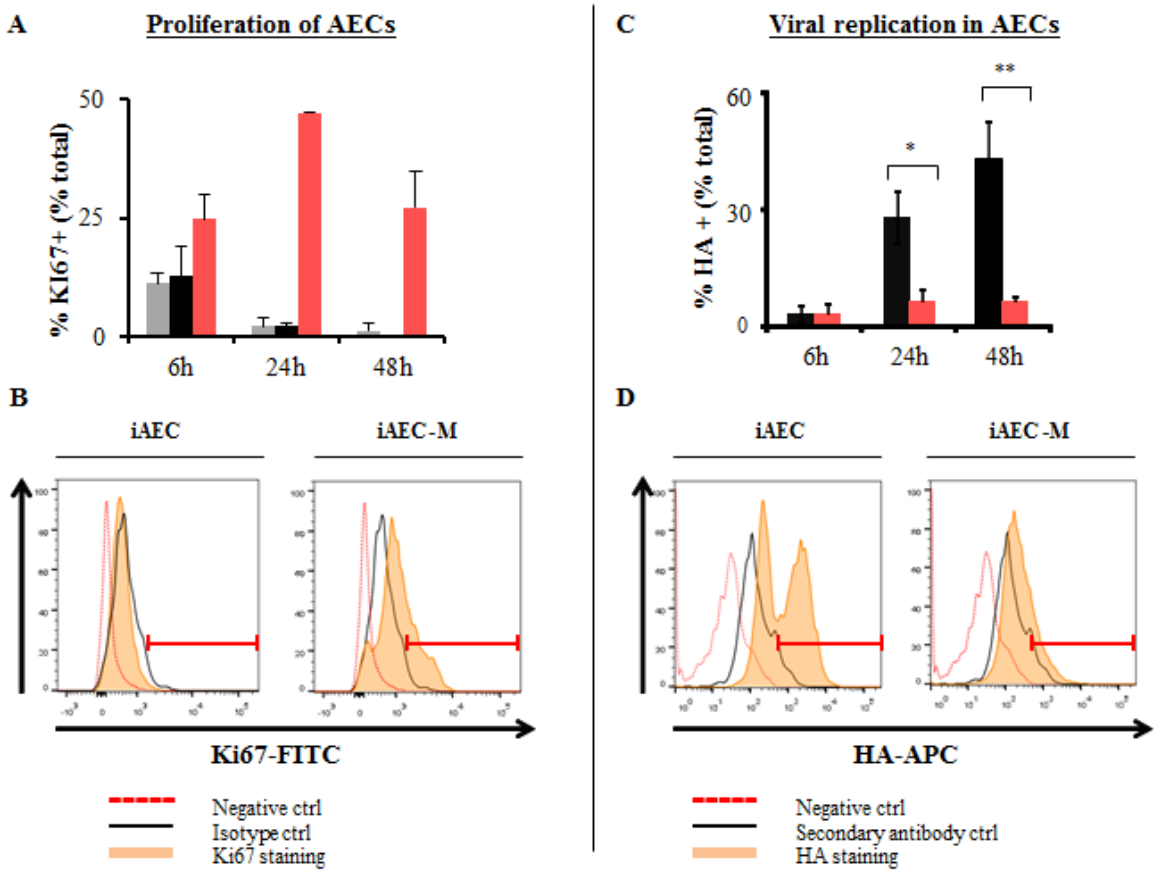

Figure 4-6. (*A*) Quantification of Ki-67 positive AECs. (*B*) Representative histograms of Ki67 staining of AEC. (*C*) Quantification of virus presence in AECs as determined by hemagglutinin (HA) surface staining. (*D*) Representative histogram of HA staining of AECs. Grey pattern, non-infected AECs alone; black pattern, infected AECs alone; red pattern, infected AECs co-cultured with BM-MSCs. iAEC – infected AECs, iAEC-M – infected AECs in co-culture with BM-MSCs. Error bars represent SD (n=3). Significance was assumed when p value was less than 0.05, *p<0.05, **p<0.01 and ***p<0.005 accordingly.

As high IV infection rates in the alveolar epithelium *in vivo* together with inflammatory injury results in severe apoptotic alveolar epithelial damage, AEC apoptosis levels were measured in co-culture system. A significant reduction of Annexin V positive AEC in the

presence of BM-MSC at 24 and 48h pi was observed, what is comparable to levels of non-infected AEC (Figure 4-7A, B).

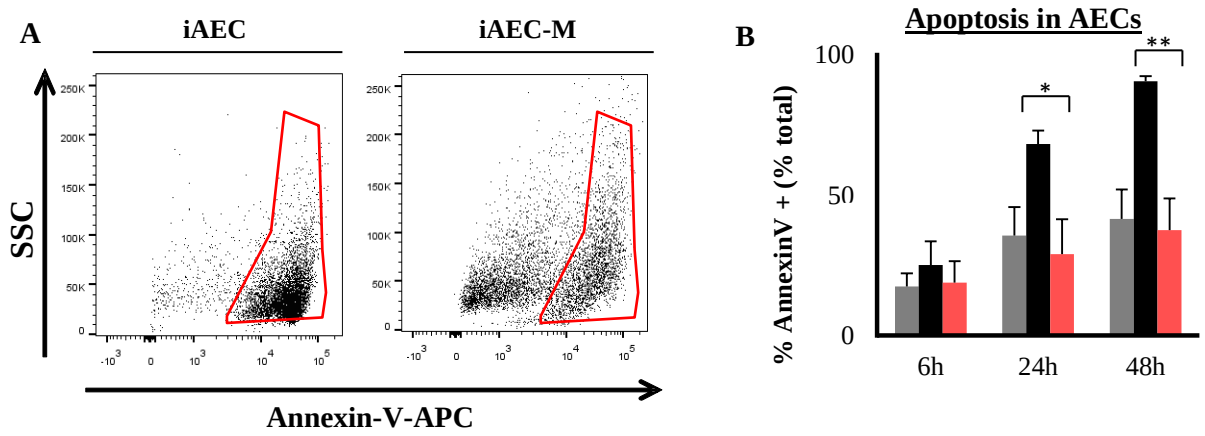

Figure 4-7. (*A*) Annexin-V representative dot plots after 48h pi. (*B*) Quantification of Annexin-V positive AECs at 6, 24 and 48h pi. Grey pattern, non -infected AECs; black pattern, infected AECs alone; red pattern, infected AECs co-cultured with BM-MSCs. iAEC – infected AECs, iAEC-M – infected AECs in co-culture with BM-MSCs. Error bars represent SD (n=3). Significance was assumed when p value was less than 0.05, *p<0.05, **p<0.01 and ***p<0.005 accordingly.

Of note, to exclude that BM-MSC themselves represented a source of viral replication, it was analysed whether BM-MSC got infected by PR/8. BM-MSC did neither get infected when incubated directly with 0.1 MOI of PR/8 for 24h (Figure 4-8), nor in co-culture with infected AECs (not shown).

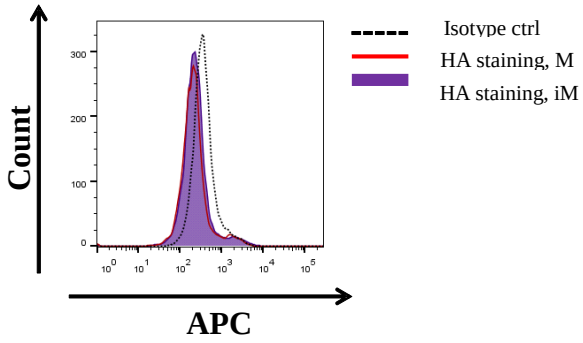

Figure 4-8. Representative histogram of HA staining of MSCs 24h pi. M – BM-MSCs, iM – infected BM-MSCs, ctrl – control.

Taken together, these results demonstrate a highly protective effect of BM-MSC in an *in vitro* co-culture model with IV-infected AECs, as they induce an antiviral program in AECs associated with reduced viral spread, and as they drive anti-apoptotic and pro-proliferative signaling in these cells. These experimental data suggest that application of BM-MSC in IV-

infected mice would be highly protective through limitation of viral spread and preserving the AEC barrier necessary for barrier function and gas exchange.

4.3 The protective role of BM-MSC on infected AEC is mediated by paracrine factors

Considering the evidence that MSC exert their beneficial properties in a paracrine manner by releasing factors such as cytokines, growth factors and antimicrobial peptides in lung injury models [193, 211, 226], I investigated the potential to reproduce their effects observed in the experiments presented above by use of BM-MSC conditioned medium (CM) instead of direct co-culture. BM-MSC derived CM was generated collecting CM one day after the BM-MSC had been co-incubated with PR/8-infected AEC. Similar to direct co-culture of BM-MSC with AEC, BM-MSC-derived CM enhanced AEC proliferation and reduced virus spread in PR/8-infected AEC at 24h pi; AEC apoptosis was also strongly reduced in presence of BM-MSC CM (Figure 4-9A-C).

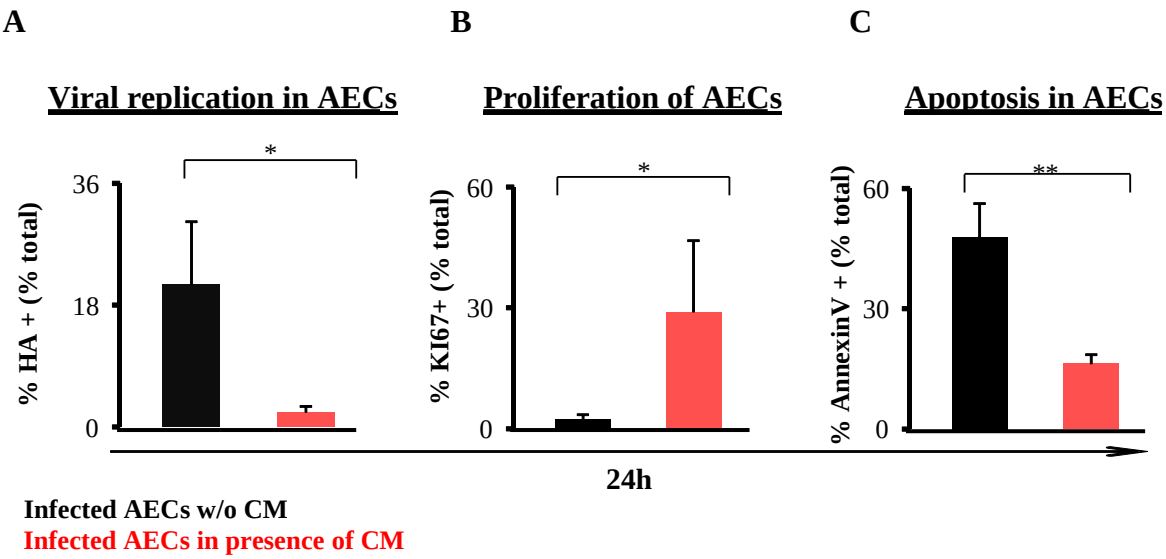

Figure 4-9. Quantitative analysis of virus-infected AEC (*A*), proliferation (*B*) and apoptosis (*C*) in AEC analysed by flow cytometry. HA, hemagglutinin. Error bars represent SD (n=3). Significance was assumed when p value was less than 0.05, *p<0.05, **p<0.01 and ***p<0.005 accordingly.

Since the paracrine action of BM-MSC had been previously related to content released by extracellular vesicles and especially exosomes [228, 256, 261], BM-MSC derived exosomes were analysed and quantified by specific magnetic beads staining after quantification of the optimal amount of Dynabeads to capture exosomes from a defined volume of BM-MSC

culture supernatant, followed by flow cytometric analysis to specify the source of exosomes by BM-MSC surface marker expression on exosomes [332]. First, exosomes were captured with the specific conserved "exosome" markers CD81 and CD9, which are tetraspanins. Flow cytometry analysis revealed that most exosomes are positive for another tetraspanin, namely CD63 (Figure 4-10).

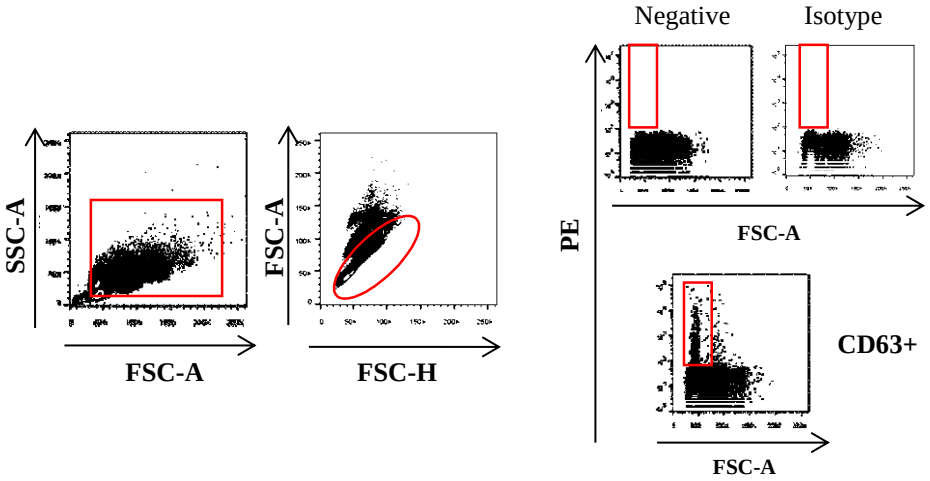

Figure 4-10. Representative dot-plots for dynabead-exosome complex detection by flow cytometry. From all dynabead-exosome complexes excluding electronic noise (red square), only singlet events are included (middle plot, oval pattern), from which CD63 PE positive events are counted as exosomes (left down, red square – the target population; representative controls – left up).

In addition, exosomes expressed CD29, CD140α and CD34, and were highly positive for CD105 and CD44 reflecting their cellular BM-MSC origin. As expected, isolated exosomes were negative for CD45 and CD11b. Sca-1, CD73 and CD90 expression could not be detected (Figure 4-11).

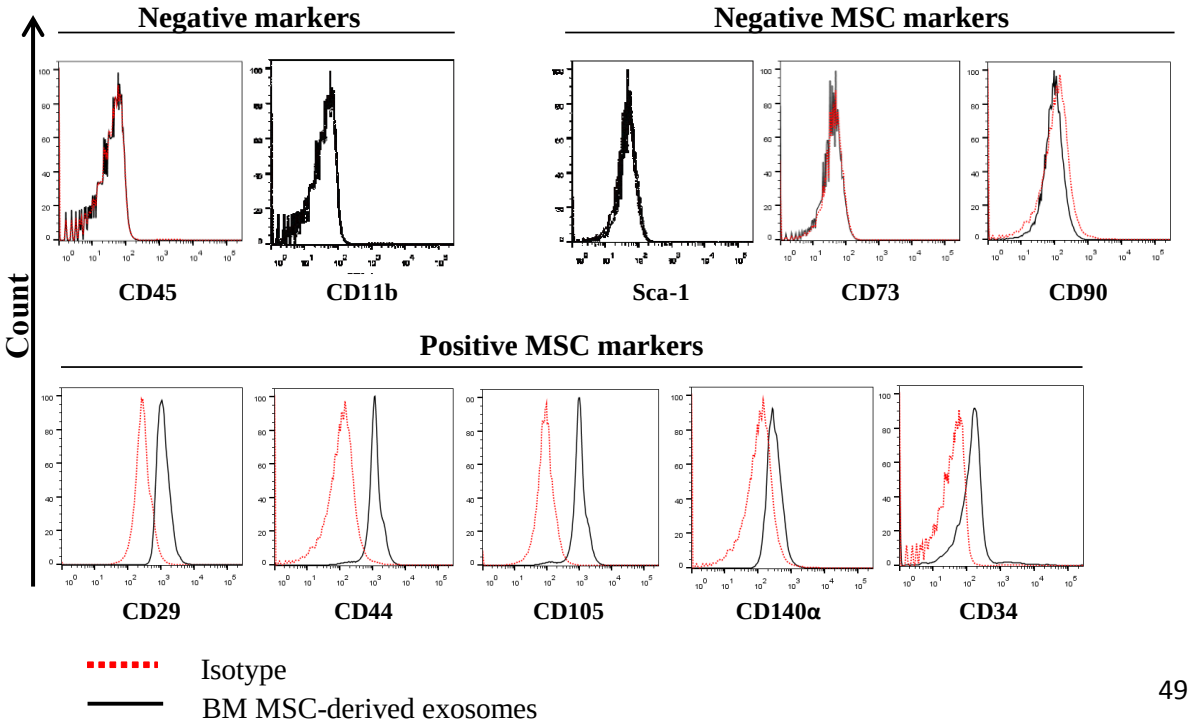

Figure 4-11. Representative histograms of flow cytometry analysis for surface markers of BM-MSC derived exosomes.

In conclusion, BM-MSCs are a substantial source of exosomes contained in the CM, and exosomal content might mediate the effects of BM-MSC as previously described [265, 275, 276].

To investigate the signaling pathways activated in MSC in the presence of AEC, we compared mRNA expression levels of putative MSC cytokines in co-culture with AECs (AEC-M) or with infected AECs (iAEC-M) (Figure 4-12). The epithelial growth factors FGF10 (fibroblast growth factor 10) and FGF7, and the anti-apoptotic factor Sta-1 (stanniocalcin 1) were found out to be upregulated in MSC in co-culture with iAECs as early as 6h pi. Expression levels of the anti-viral cytokine IFNβ and the AEC growth factor/anti-apoptotic mediator GM-CSF (granulocyte-macrophage colony-stimulating factor) [277] were upregulated in MSC in co-culture with iAECs at 48h pi. Interestingly, VEGF (vascular endothelial growth factor) was highly expressed at a baseline and expression of this gene was increasing in a time dependent manner during co-culture with iAEC (Figure 4-12). These results show that specific growth factors, anti-apoptotic and anti-viral genes are induced in BM-MSC by co-culture with infected versus non-infected AEC, suggesting that they may perceive defined signals released from the virally infected, apoptotic AEC by a yet unknown mechanism, and provide factors to counteract viral infection and AEC death, and induce AEC repair.

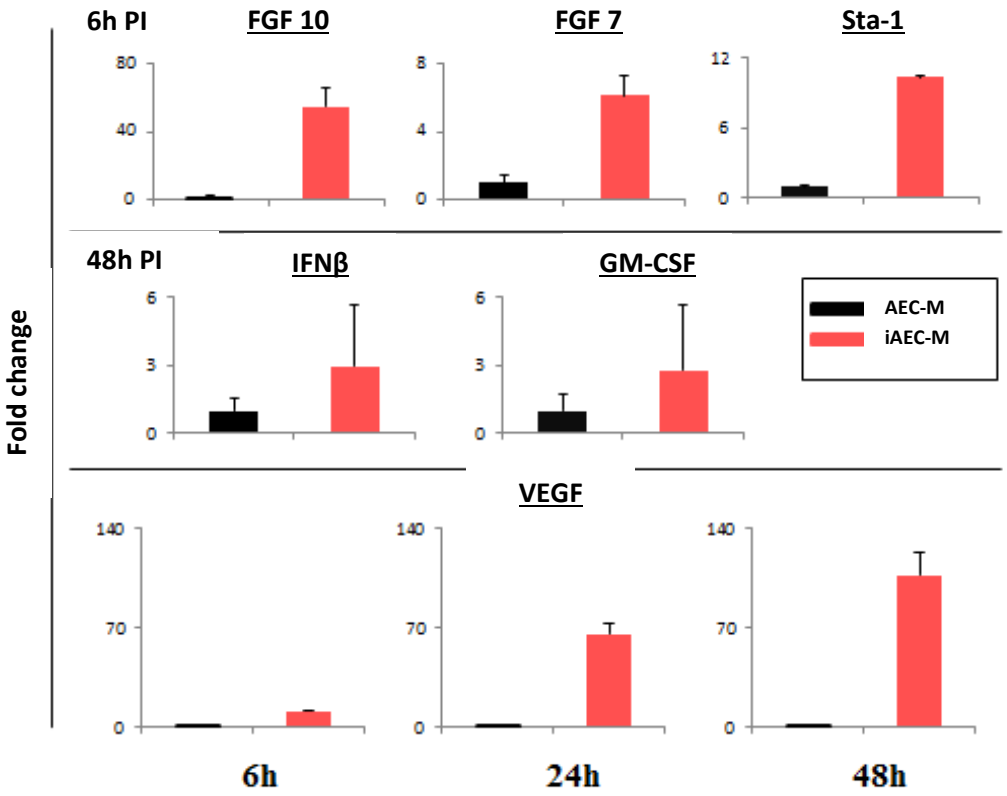

Figure 4-12. Potential candidates involved in BM-MSC therapeutic effect. Error bars represent SD (n=3). FGF10, fibroblast growth factor 10; FGF7, fibroblast growth factor 7; Sta-1, Stanniocalcin 1; IFNβ, Interferon beta; GM-CSF, Granulocyte macrophage colony stimulating factor; VEGF, Vascular endothelial growth factor; AEC-M/iAEC-M, uninfected/ infected alveolar epithelial cells in co-culture with BM-MSC; PI, post infection.

4.4 Intra-tracheal BM-MSC application improves survival and decreases ALI severity in mice challenged with influenza

MSC application after IV infection has been performed intravenously and described inefficient to reduced IV-induced ALI by Gotts et al and Darwish et al [233, 278]. As shown in this thesis previously, BM-MSC have a beneficial paracrine effect on infected AEC *in vitro*, thus has been tested their potential *in vivo* after direct intrapulmonary deposition by the intra-tracheal route of application in PR/8-infected mice.

To establish BM-MSC treatment as a therapeutic and not as a prophylactic approach, BM-MSC were applied during the course of infection, when viral replication reached its peak, as previously determined by our research group [42]. Mice were first infected intra-tracheally

with 500pfu (Plaque forming unites) of PR/8 and treated with either primary BM-MSCs or control solution (PBS) or control cells (3T3 cells) at day 3 pi (Figure 4-13).

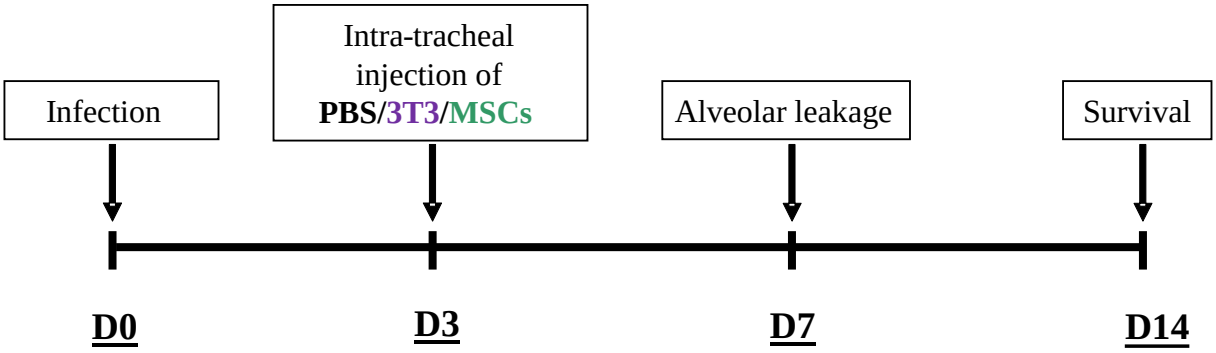

Figure 4-13. Schematic representation of the in vivo BM-MSC treatment and time points for analyses. All C57BL/6 mice were infected with 500pfu PR/8, treated at day 3 pi with PBS/3T3/BM-MSC and monitored for 7 or 14 days.

Strikingly, all BM-MSC treated mice survived PR/8 infection until 14d pi and presented a reduced weight loss compared to control mice. All PR/8-infected mice started losing weight by 4d pi, but differently from PBS and 3T3 treatment groups, BM-MSC mice lost less weight and regained it from day 8 to 9 pi (Figure 4-14B). Of note, most PBS and 3T3 treated mice had to be euthanatized before 8d pi as they displayed serious IV-induced symptoms, according to a daily applied morbidity scoring system established and approved for this infection model (Figure 4-14A).

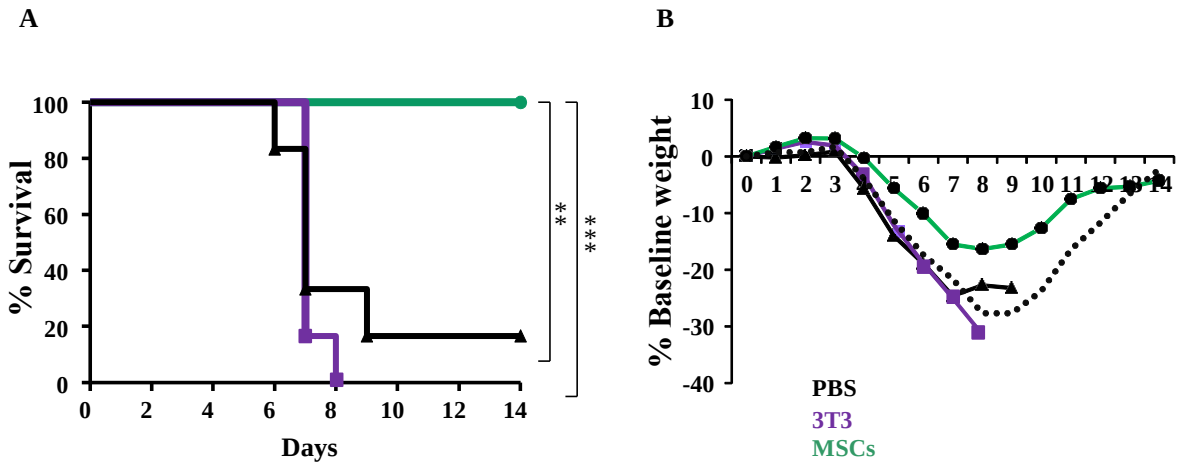

Figure 4-14. (*A*) Kaplan-Maier curves of PR/8 infected mice treated with BM-MSC or 3T3 cells or PBS 3d pi. (*B*) Mean weight loss curve of PR/8 infected mice treated with BM-MSC or 3T3 cells or PBS (black, black dotted represents the only one survivor from the PBS treatment group) 3d pi of n=6 mice each. Significance was assumed when p value was less than 0.05, *p<0.05, **p<0.01 and ***p<0.005 accordingly.

As most PR/8-infected mice survived until day 7 but already displayed substantial morbidity at this time, it was assumed that this time point is suitable to assess alveolar-capillary barrier dysfunction by alveolar FITC-albumin leakage measurement.

BM-MSC treatment of PR8 infected mice significantly reduced alveolar-capillary protein leakage compared with the mice treated with 3T3 cells or PBS (Figure 4-15).

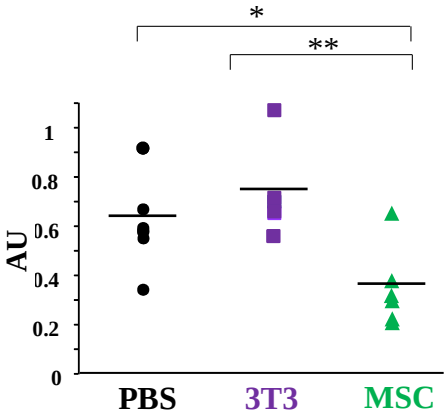

Figure 4-15. Alveolar leakage in PR/8-infected differently treated C57BL/6 mice at 7d pi. Data are given as the ratio between FITC fluorescence in BALF and serum (arbitrary units, AU). PBS, volume control; 3T3, control fibroblasts; MSC, mesenchymal stem cells. Data are presented as means ± SD from n=5 mice. Significance was assumed when p value was less than 0.05, *p<0.05 and **p<0.01 accordingly.

Additionally to alveolar leakage measurement, lung histology revealed edema (*) and accumulation of inflammatory cells (**) in mice treated with PBS or 3T3 cells on day 7 and day 14 (one mouse survived in PBS group, meanwhile in the 3T3 group no mouse survived until day 14) as expected after PR/8 challenge, whereas very subtle histological abnormalities were observed at day 7 or 14 in the BM-MSC treatment group (Figure 4-16).

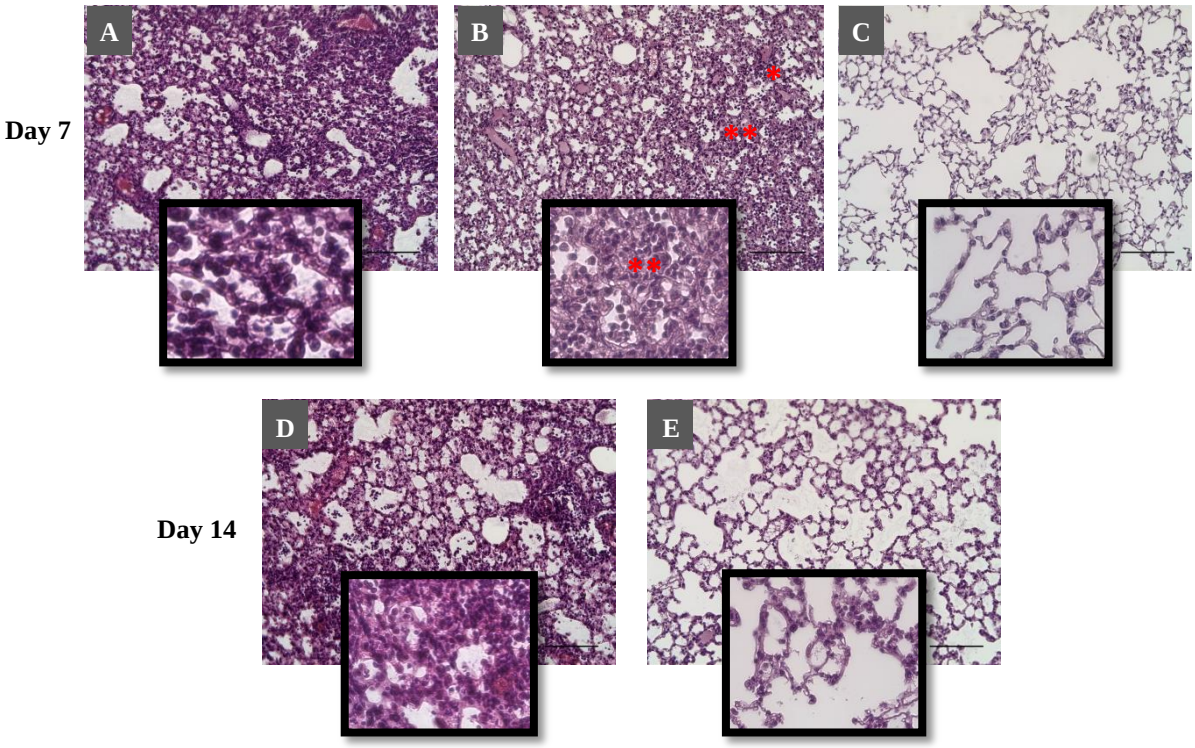

Figure 4-16. (*A-F*) Representative lung histology of PR/8 infected mice treated with PBS (*A, D*); 3T3 cells (*B)*; BM-MSC (*C, E*) at day 7 (*A-C*) or day 14 (*D-E*) pi. One mouse survived from PBS group, however, no 3T3 cell treated mouse survived until the day 14. Scale bar – 100μm. Mouse lungs were stained with haematoxylin and eosin. * - edema, ** - accumulation of inflammatory cells.

Quantification of the leukocyte numbers and composition in the BALF by Pappenheim-stained cytospin differential counts revealed that BM-MSC treatment strongly reduced the inflammatory response, particularly recruitment of neutrophils, and to lesser extent, of lymphocytes. Of note, BM-MSC also prevented alveolar haemorrhage as demonstrated by quantification of erythrocytes in the BALF (Figure 4-17).

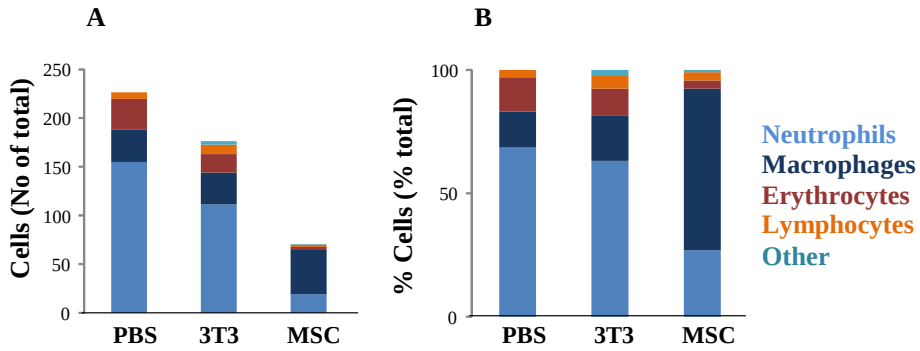

Figure 4-17. (A) Total cell number and (B) % of total BALF cells in 3T3 cell, BM-MSC or PBS-treated PR/8 infected mice at 5dpi as quantified by microscopy of cytospin preparations (n=3). "Other" refers to 3T3 cells or BM-MSC regained by BAL. 3T3, control fibroblasts; MSC, mesenchymal stem cells.

4.5 BM-MSC application *in vivo* enhances proliferation of epithelial cells and protects the AEC pool against influenza induced apoptosis

During IV infection of the distal respiratory tract, the alveolar epithelial cells are the first targets of the virus which leads to epithelial barrier disruption. Previous work done in our lab [105] demonstrated the importance of the Epithelial Stem Progenitor cell (EpiSPC) pool, phenotyped as highly positive for EpCam and CD49f and CD24 intermedium, in stem cell-mediated lung repair after PR/8 infection.

To address whether BM-MSC would enhance stem cell-mediated lung regeneration, similarly to our in vitro measurements, the impact of BM-MSC administration on the AEC pool as well

on the EpiSPC pool with respect to proliferation after lung injury was analysed by FACS. The gating strategy of AEC and EpiSPC is shown in Figure 4-18.

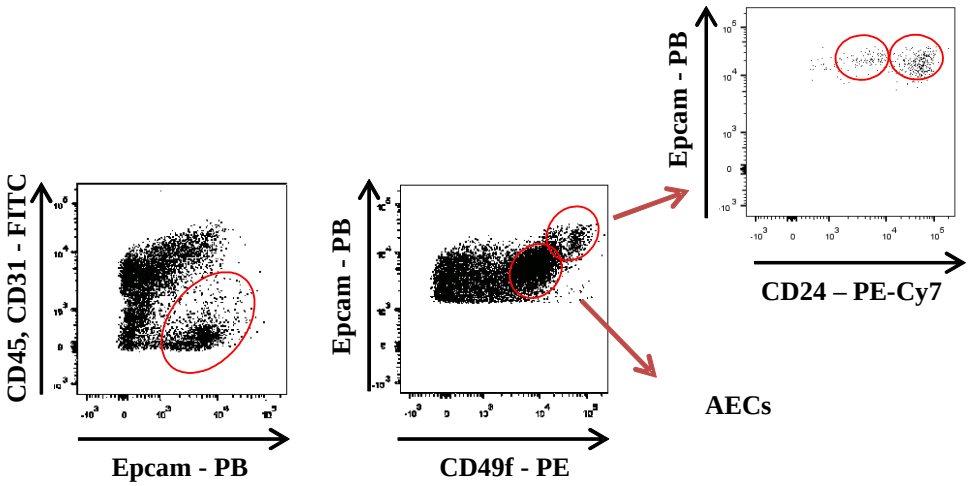

Figure 4-18. Representative dot-plots for AEC and EpiSPC (Epithelial stem progenitor cells) identification by FACS. First, CD45 and CD31 cells are gated out and the Epcam high population is selected (left). The target population of AECs is highly positive for Epcam and expresses CD49f only at moderate level (middle). The EpiSPC population highly expresses Epcam as well as CD49f and moderate levels of CD24 (right). AEC, alveolar epithelial cells.

Proliferation of the AEC pool, assessed by Ki67 staining, was increased by a factor of 2 in the BM-MSC group compared to control mice. A statistical enhancement of the EpiSPC pool proliferation was as well observed after BM-MSC administration (Figure 4-19).

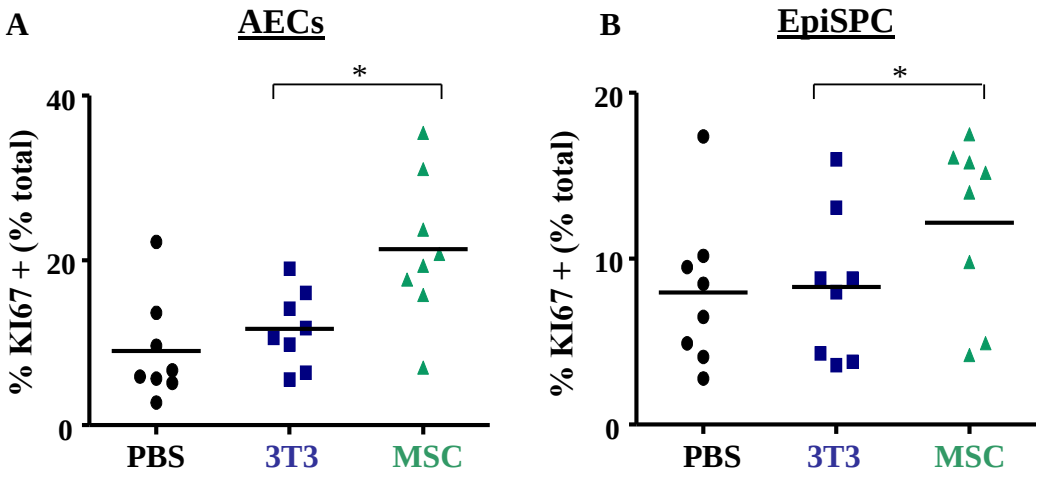

Figure 4-19. Quantification of Ki-67 positive cells in AECs (*A*) and in EpiSPC (*B*) pools from lungs of PR/8 infected mice treated as indicated at 3d pi. Lines represent means of n=8 mice. Significance was assumed when p value was less than 0.05, *p<0.05.

Of note, similar to *in vitro* data, viral replication in AECs (defined by the percentage of viral hemagglutinin positive cells by FACS) was strongly reduced in BM-MSC treated mice compared to PBS and 3T3 cell controls (Figure 4-20). Of note, the quantification of infected AEC was done at 5d pi when PR/8 replication usually reaches its peak *in vivo*.

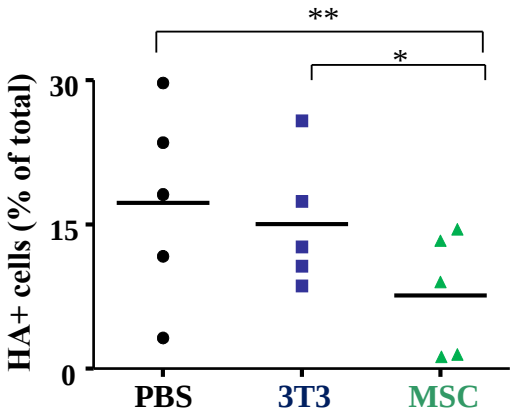

Figure 4-20. Quantification of HA (hemagglutinin) positive in AECs from lungs of PR/8 infected mice (treated at d3 as indicated) at 5d pi. Lines represent means (n=5). Significance was assumed when p value was less than 0.05, *p<0.05, **p<0.01 accordingly.

As BM-MSC application *in vivo* increased epithelial (stem) cell proliferation and reduced AEC infection rates, further AEC apoptosis levels were analysed by Annexin-V staining. A clear difference between the three groups was observed. Apoptosis in AECs (Figure 4-21) was reduced by factor 2 in presence of BM-MSC.

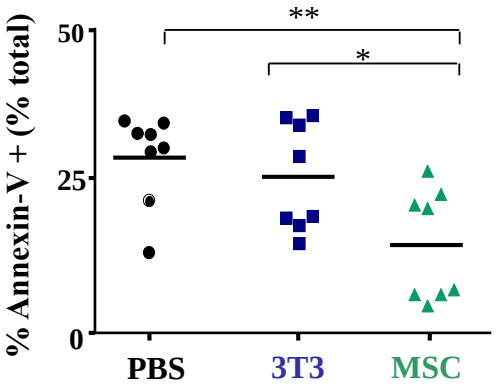

Figure 4-21. Quantification of Annexin-V positive AECs from lungs of mice analysed by FACS at 7d pi. All mice were infected with 500pfu PR/8 and treated as indicated at 3d pi. Lines represent means (n=8). Significance was assumed when p value was less than 0.05, *p<0.05, **p<0.01 accordingly.

Taken together, these findings show that intrapulmonary BM-MSC application at 3d post IAV infection strongly reduces inflammatory lung injury and loss of barrier function, protects the alveolar epithelium and induces epithelial repair processes, resulting in highly improved survival. BM-MSC application into virus-infected lungs may therefore constitute a therapeutic approach in humans with severe virus-induced lung injury.

4.6 Type I Interferon pathway is engaged to mediate the BM-MSC anti-viral potential *in vivo*

BM-MSC effects have been shown in the literature to be anti-inflammatory, immuno-modulating or tissue repair stimulating in various other lung injury models [214, 230, 232, 279]. Yet, it is not known if BM-MSC can exert pathogen-related or -specific effects. With respect to the *in vitro* and *in vivo* results and especially the genome array analysis showing upregulation of genes involved in interferon signaling, the hypothesis was raised that BM-MSC exert a specific antiviral effect through induction or enhancement of interferon signaling in AEC. To test this PR/8 infected mice lacking the type I IFN receptor (*ifnar-/-* mice) were treated with wildtype (*wt)* BM-MSC or PBS control (Figure 4-22).

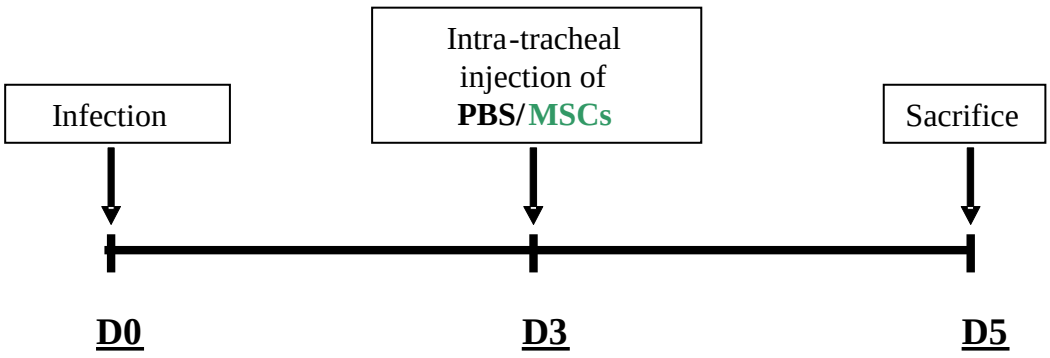

Figure 4-22. Schematic picture showing interventions and sacrifice time point. All *ifnar-/-* mice were infected with 500pfu PR/8, treated at day 3pi with PBS or *wt* BM-MSC and sacrificed 5d pi.

BM-MSC application increased AEC proliferation (Figure 4-23B) but, interestingly, did not reduce epithelial viral infection rates as quantified by detection of either HA on the AEC surface or detection of NP in the AEC cytoplasm (Figure 4-23A), in mice deficient for the type 1 interferon receptor. In addition, treatment with BM-MSC did not reduce AEC apoptosis in *ifnar*-/- mice (Figure 4-23C).

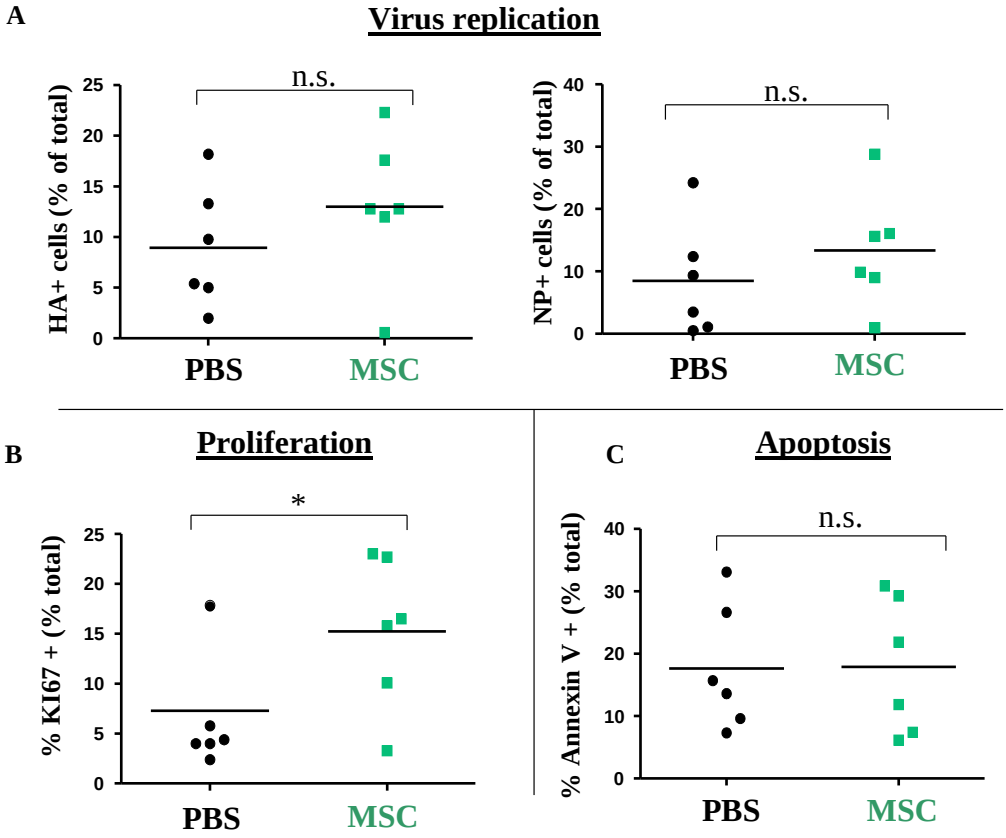

Figure 4-23. Quantification of HA and NP positive (*A*), and Ki67 (*B*) and Annexin V (*C*) positive AECs from lungs of mice analysed by FACS at 5d pi. *Ifnar*-/- mice were infected with 500pfu PR/8 and treated at 3d pi as indicated. Lines represent means of n=6 *Ifnar*-/- mice. Significance was assumed when p value was less than 0.05, *p<0.05.

Taken together, these results demonstrate that BM-MSC exert a type I IFN-independent pro-proliferative effect on the epithelium, and a type I IFN-dependent antiviral effect on AEC. Loss of the anti-apoptotic effect on AEC by BM-MSC in *ifnar*-/- mice is very likely a consequence of reduction of viral spread within the alveolar epithelial compartment.

4.7 BM-MSC anti-viral potential can be amplified through poly I:C stimulation *in vitro*

The data presented reveal that BM-MSC act – either directly or indirectly – via type I IFN and suggest that BM-MSC are capable of sensing IAV infection within the alveolar compartment. This raises the question whether BM-MSC can be primed or pre-conditioned *ex vivo* to improve their antiviral potential. Therefore, BM-MSC were stimulated with several viral PAMPs (pathogen-associated molecular patterns)/TLR agonists or cytokines, and their

antiviral potential in co-culture with iAEC was evaluated. For BM-MSC conditioning poly I:C (TLR3 agonist), R848 (TLR7 agonist), 5'ppp-dsRNA (RIG-I agonist), as well as TNFα and IFNβ were applied [166, 167, 169, 170, 280, 281]. HA FACS analysis of iAECs in co-culture with pre-conditioned or unconditioned BM-MSC revealed no changes of the amount of HA positive (infected) AEC after stimulation with R848, 5'ppp-dsRNA, TNFα or IFNβ. However, „sterile" priming of BM-MSC with 1µg/ml of TLR3 agonist poly I:C further improved their anti-viral potential after 24h pi (Figure 4-24).

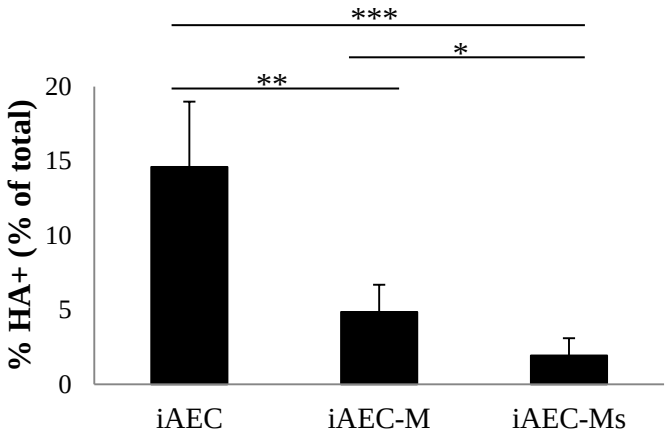

Figure 4-24. Quantification of HA positive AECs by FACS at 24h pi. Bars represent means and SD (n=5). Significance was assumed when p value was less than 0.05, *p<0.05, **p<0.01 and ***p<0.001 accordingly. iAEC, infected AECs; iAEC-M, infected AECs in co-culture with BM-MSCs; iAEC-Ms, infected AECs in co-culture with BM-MSC stimulated with 1µg/ml poly I:C.

These results show that the anti-viral potential of BM-MSC can be enhanced by pre-conditioning with TLR3 signaling activators, suggesting that BM-MSC pre-conditioning or priming can be taken into account to enhance particular beneficial properties (in this case, antiviral effects) prior to their application in vivo.

5. Discussion

Acute lung injury and ARDS due to pneumonia are severe conditions with no specific treatment available. Despite active research in understanding their pathology, ALI/ARDS remains a major cause of death in critical ill patients with a high mortality rate of roughly 40% [89, 282].

The main focus of this study was BM-MSC application as therapeutic approach, which has been attributed beneficial effects in different inflammation-injury conditions of the lung including those induced by LPS, bleomycin or live bacteria [158, 160, 164, 172, 192, 193, 196-239].

The efficacy of BM-MSC therapy will depend on the phenotype of MSC preparations. Isolation and purification of murine MSC is more challenging than from humans due to low amount in bone marrow and also frequent contamination with non-mesenchymal cells during the isolation process and cultures. In this study, to isolate primary MSC from murine bone marrow, a BM-MSC isolation protocol established by Houlihan et al. [131] was adapted. As BM-MSC are found to be localised in the perivascular zone of bone marrow [134, 135], a collagenase A digestion was applied. Next, the cells were FACS sorted. Thus, a BM-MSC population with purity of >95% representing 0.05-0.1% cells from the whole bone marrow nuclear cell pool was achieved. The purified fibroblast-like cells expressed high levels of the typical consensus markers CD29, CD44 and CD105, as well as CD90 and Sca-1. Moreover, the results indicated that these cells are negative for CD45, CD19, CD11b, CD117 and CD31. Interestingly, using the before mentioned isolation protocol BM-MSC expressed CD34, a non-typical MSC marker, and did not express CD73 – a standard MSC marker. Expression of CD34 on MSC is still debated [283], as it is commonly used as a specific marker for muscle stem cells [284, 285] or vascular progenitor cells [286, 287]. However, several studies demonstrated that adipose tissue derived MSC [124, 288] or freshly isolated BM-MSC [289, 290] express CD34. Little is known why and if the isolated MSC can lack CD73 expression [291]. After all, surface marker expression in murine MSC is not yet established completely [134, 289, 290, 292, 293]. In addition, the primary BM-MSC preserved a typical fibroblast like shape and the before mentioned marker characteristics, displayed high proliferation rates and differentiation potential into mesenchymal lineages (adipocytes, osteoblasts and chondrocytes) until passage 18 and therefore fulfilled the consensus paper of the International Society for Cellular Therapy (ISCT) MSC definition criteria [149]. Variation in marker

expression can be explained by isolation protocol specificities as well as by the multiple passages and cultivation conditions [131, 289, 290, 292-296].

The versatile features of BM-MSCs have been widely discussed and examined in different injury models. Many studies focused on their potential to stimulate regeneration of different tissues [190, 199, 204], their anti-bacterial, anti-inflammatory effects [169, 209, 210] as well as anti-apoptotic properties [185, 261]. In the *in vitro* experiments it was observed, that primary BM-MSC protected AEC from IAV induced injury via the following mechanisms. First, the increased proliferation of iAECs was noted. Moreover, the reduction of viral presence in AEC by BM-MSC suggests a specific viral sensing mechanism resulting in anti-viral properties, and not only a non-specific tissue protection effect. As a consequence, the iAEC underwent less apoptosis. To a large extent, the therapeutic efficacy of MSC is associated to their capacity to secrete multiple soluble factors in response to environmental stimuli [182, 188, 189, 245, 269, 297, 298]. The paracrine action of BM-MSC was tested using BM-MSC CM. BM-MSC CM showed a beneficial effect towards IAV induced AEC damage via reduced viral replication, increased AEC proliferation and consequently, decreased apoptosis. However, the increase in proliferation rate was twice less with CM compared to when BM-MSC were present, suggesting that the factors involved in AEC proliferation might be short-acting and need constant release by BM-MSC, or repeated application of BM-MSC derived CM. Moreover, recent studies show that the MSC secretome as opposed to whole cell application may be not sufficient to repair the organ damage [227, 279]. Certainly, MSC can exert their paracrine actions in different ways – by release of mediators or cytokines, via exosomes or microparticles [299], and even via mitochondrial transfer to AEC in vivo [172] suggesting that also direct cell-cell interactions may play a role and BM-MSC mechanisms of action is more complex. The presented qPCR data revealed that expression of different genes in BM-MSC (growth factors, as FGF7, FGF10, VEGF; anti-apoptotic molecules as Sta-1; anti-viral IFN-β) is initiated with different kinetics, suggesting that BM-MSC may be capable of sensing the particular "need" of the infected/injured epithelium and may respond accordingly in the different phases of damage.

Further, the potential of BM-MSC application *in vivo* was investigated in a mouse model of severe IV induced pneumonia. Considering MSC homing to injured lungs, several studies demonstrated pulmonary engraftment after intravenous application [205, 300-303], and some of them showed that MSC can differentiate into alveolar epithelium or endothelial cells [147, 303-306], suggesting that MSC could be used to regenerate lung tissue. Yet, these data

remain questioned by other investigations, showing that systemically installed MSC engraftment rates in lung are lower than 1% [230, 307, 308]. Moreover, as intravenous MSC application has been described as inefficient or low-efficient in the context of IV-induced *ALI/ARDS* [233, 278], the intrapulmonary application of BM-MSC was tested by the intra-tracheal route. Local application at an early time point (3d pi) resulted in a significant histological improvement in the extent of lung injury. Additionally, significant reduction in inflammation with ameliorated neutrophil influx into alveoli, edema and haemorrhage was observed in mice treated with BM-MSC. Moreover, as demonstrated in this thesis, a significant survival advantage was observed when the BM-MSCs were applied 3d pi. BM-MSC stimulated AEC proliferation and increased their survival and induced EpiSPC-mediated repair responses, which is shown to be important in lung regeneration [78]. The mice treated with BM-MSC at 3d pi furthermore showed increased virus clearance, highlighting the multiple beneficial effects of these cells *in vivo* and demonstrating that local application directly to the site of infection as opposed to systemic application (where MSC accumulate in the lung vasculature but rarely reach the alveoli) may be required to engage their full anti-viral, anti-inflammatory and regenerative potential. These findings imply that BM-MSC need to sense pathogen PAMPs or injury-induced, cell-specific DAMPs (danger-associated molecular patterns) at the site of infection/damage to deploy their full spectrum of beneficial action at the right time. This concept is further supported by the finding that pre-conditioning of BM-MSC by a TLR3 ligand improves their anti-viral properties.

In line, genome array analysis demonstrated that several virus resistance (Mx2, Bst2/Tetherin, Rsad2/Viperin, and Oas3) and numerous interferon signaling related genes (Ifna1, Ifi genes, GTPases, Trim56 etc.) were upregulated in iAEC in co-culture with BM-MSC compared to mono-cultured iAEC. Moreover, expression of the IFNβ gene was increased in MSC in co-culture with iAECs. Given that virus clearance and apoptosis, contrary to AEC proliferation, were unchanged in AEC after BM-MSC application in PR/8 infected *ifnar*-deficient mice, these data suggest that BM-MSC might sense viral presence, e.g. via PAMPS such as double-stranded RNA, and upregulate anti-viral factors such as type I IFNs which induce the mentioned anti-viral programs in AEC. Type I IFNs are critical effectors of the innate immune response to IAV infection and highly relevant to clear viral infections including IV [36, 42]. Of note, direct infection of BM-MSC (at least in the in vitro assays) was not observed, suggesting that anti-viral "priming" of these cells was not dependent on viral replication in BM-MSC. Noteworthy, the regenerative (e.g. pro-

proliferative) effects of BM-MSC in vivo, likely mediated by release of growth factors [182-186, 188-191] were still observed in *ifnar*-deficient mice and therefore occurred independently of type I IFN.

There are several limitations in using BM-MSC for therapeutic applications. One major issue in stem cell research as well as cellular therapy is the immunogenicity of the cells meaning that transplantation can be "rejected" by the host [103]. Also, senescence due to chromosomal instability of isolated MSC or MSC isolated from elder murine donors [309, 310] and potential of malignant transformation has to be considered. Additionally, gradual loss of their stemness during *ex vivo* expansion [311] must be taken into account. For *in vitro* as well as *in vivo* approaches described in this thesis were used 8-12 passage cryopreserved BM-MSC from healthy 10-12-week mice donors. Cryopreservation has been described to have no influence on MSC replication and growth as well [312]. However, few studies observed that this procedure can affect immunomodulatory properties of MSC *in vitro* [313, 314]. For all studies, BM-MSC were cultivated 1-2 days before application. No visible tumor outgrowth in the lung sections have been noticed, however, the time course of 14 days is likely to be too short to rule out this phenomenon and a longitudinal study with repeated MSC application would be necessary to better determine the risk of tumor formation as described in few studies [315, 316].

Another issue to consider is that MSC display very strong anti-inflammatory properties, and the susceptibility to bacterial superinfection after viral pneumonia, very commonly observed in humans [55, 317], after MSC application need to be tested [5, 55, 317] if repeated BM-MSC applications are used as therapeutics. However, we did not observe any signs of bacterial superinfection in BM-MSC treated animals during 14d observation period, and previous reports demonstrated potent specific anti-bacterial effects of MSC apart from anti-inflammatory properties [209]. An additional point to discuss is their dosage. There is no defined protocol for intra-tracheal application of BM-MSC and the dosage varies from 1-10^5 to 5x10^6 in mice [209, 212, 239, 318]. For each experiment, I delivered 2.5x10^5 cells per 24-26g mouse and a dosage of more than 5x10^5 in 40µl volume was not well tolerated. It will have to be addressed whether the number of cells applied into the lung can be reduced to further increase safety of application, particularly when *in vitro* pre-conditioning approaches will be applied to enhance their efficacy prior to application.

Further questions to be answered relate to BM-MSC application in ALI induced by different IAV strains. To date, there is one study showing their beneficial effect ameliorating H5N1 induced lung injury and modestly improving mouse survival [319]. However, this study focuses on intravenous application and addresses particularly MSC anti-inflammatory properties. Another question is how the anti-viral MSC effects could be amplified *in vitro* to increase beneficial therapeutic potential for applications *in vivo*. Several investigations focused on enhancing MSC anti-apoptotic, anti-inflammatory or immunomodulatory potential [167, 320, 321], yet studies focusing on "virus-specific" priming of MSC are lacking. In this thesis described *in vitro* BM-MSC stimulation experiment showed promising results and suggested targeting them via TLR3 activation could be one such strategy. Moreover, there is an ongoing debate if and how BM-MSC could be directly attracted from bone marrow to the site of injury, or how homing of intravenously applied MSC into injured organs could be improved by endowing them with certain chemokine receptors or adhesion molecules (for example, CXCR4 [322, 323] or CXCL9 [324], Vascular cell adhesion molecule (VCAM)-1/CD106, endoglin/CD105 or intercellular adhesion molecule ICAM-1/3 (CD54 and CD50 respectively) [325]) to avoid the intrapulmonary application route, which is challenging in ARDS patients. Strategies of direct recruitment from the bone marrow to the injured organ excludes pre-conditioning, but could be beneficial, as changes in cultivation conditions can easily stimulate BM-MSC differentiation *in vitro* leading to phenotype changes and possibly reduced beneficial potential [326, 327].

Concluding, as the interest regarding their therapeutic potential grows and more and more clinical trials use BM-MSC in phase I and II studies [328-330], the current thesis demonstrates that early local treatment with BM-MSC in IAV induced ALI provides a significant survival advantage due to multifactorial mechanisms. First, it decreased lung edema and inflammation. Second, it improves lung repair-promoting AEC and EpiSPC proliferation. And most important, it has anti-viral effects with consequently decreased AEC apoptosis/lung injury levels. Moreover, the upregulation of type I IFN-associated signaling pathways suggests that these cells engage innate anti-viral strategies to enhance their therapeutic potential. Given that, current BM-MSC applications in ALI/ARDS in humans show promising results. This study demonstrates for the first time that MSC act in an anti-viral way, provides important knowledge on the molecular mechanisms underlying these effects, and demonstrates that local application might be more effective compared to systemic application.

6.Summary

Influenza virus (IV) infects the upper respiratory tract and occasionally spreads to the alveolar compartment causing primary IV pneumonia. This frequently progresses to acute respiratory distress syndrome (ARDS) with severe alveolar damage, lung edema and hypoxemia, requiring mechanical ventilation or extracorporeal membrane oxygenation (ECMO) procedures. Antiviral therapies are only effective in the very beginning of infection and specific treatment strategies for IV-induced ARDS are still lacking. Mesenchymal stem cells (MSC) are multi-potent stromal cells with anti-inflammatory and regenerative potential: recently they were attributed a beneficial role in acute and chronic lung injury. This study investigated MSC delivery into the lung as a promising treatment strategy in IV-induced ARDS.

In this study MSC were isolated from bone marrow (mBM-MSC) of C57Bl6. These MSC had fibroblast-like shape and expressed stem cell-specific markers and demonstrated de-differentiation potential upon defined culture conditions. No phenotypic changes were observed until passage 18. Genome array analysis revealed a strong up-regulation of the genes involved in cell proliferation (cell division, cyclins), in interferon signaling (ISGs) and virus resistance (Mx2, Bst2/Tetherin) in infected alveolar epithelial cells (iAECs) co-cultured with BM-MSC compared to iAECs in monoculture. In *ex vivo* infection experiments, BM-MSC as well as their conditioned medium (CM) strongly diminished IV replication, increased AEC regeneration and consequently decreased IV-induced AEC apoptosis.

In vivo, intra-tracheal instillation of BM-MSC into C57BL/6 mice after 3 days post IV challenge strongly increased IV clearance, decreased alveolar injury and was associated with better outcome. Of note, BM-MSCs also increased the regenerative response of the epithelial stem/progenitor cell pool of the distal lung *in vivo*. Interferon alpha and beta receptor knockout (*ifnar*-/-) mice after IV infection could not clear the virus even under BM-MSCs treatment, demonstrating that the type I IFN pathway is responsible for the BM-MSC anti-viral (and concomitantly, anti-apoptotic) potential *in vivo*.

In conclusion, our *ex vivo* as well as *in vivo* experiments show a beneficial role of BM-MSCs in IV pneumonia and demonstrate the therapeutic potential of these cells in IV-induced lung injury. Furthermore, the upregulation of type I IFN signaling-related pathways suggests that

these cells are activated in a pathogen-specific way in presence of virus, which enhances their beneficial properties.

7. Zusammenfassung

Influenza Virus (IV) infiziert die oberen Atemwege, kann sich aber auch bis in die Alveolen ausbreiten und eine primäre virale Pneumonie verursachen. In schweren Fällen kommt es zum akuten Lungenversagen (Acute Lung Injury(ALI)/ Acute Respiratory Distress Syndrome (ARDS)). ARDS ist gekennzeichnet durch eine schwere Schädigung des alveolären Epithels, die Ausbildung einer refraktären Hypoxämie und die Bildung von Lungenödemen. Eine antivirale Therapie ist nur in den ersten Stunden nach der Infektion wirksam, weitere Therapiemöglichkeiten für IV-induziertes ALI/ARDS sind noch nicht vorhanden. Mesenchymale Stammzellen (MSC) sind multipotente Zellen, denen seit kurzem eine positive Wirkung auf die Entzündungsauflösung und Regenerierung des Lungenepithels bei akuter oder chronischer Verletzung zugeschrieben wird. In der vorliegenden Arbeit wurde die intratracheale Applikation von MSC als vielversprechende Behandlungsmöglichkeit bei IV-induziertem ARDS untersucht.

In Rahmen dieser Studie wurden MSC aus dem Knochenmark (murine bone marrow MSC (BM-MSC)) von C57BL/6 Mäusen gewonnen. BM-MSC haben eine fibroblastenartige Form, exprimieren stammzellspezifische Marker und besitzen das Potential unter bestimmten Kulturbedingungen in andere Zelltypen zu differenzieren. Bis Passage 18 konnten keine phänotypischen Veränderungen in isolierten BM-MSC beobachtet werden. Der Einfluss von BM-MSC auf IV-infizierte primäre alveoläre Epithelzellen (infected alveolar epithelial cells (iAEC)) wurde in einem *in vitro* Ko-Kulturmodell untersucht und mit iAEC in Monokultur verglichen. Die Expressionsanalyse von ko-kultivierten iAEC zeigte eine deutliche Hochregulation von Genen, beteiligt an Prozessen der Zellproliferation (Zellteilung, Cycline), Interferon-Signalwegen (ISGs), sowie von Virusresistenzgenen (Mx2, Bst2/Tetherin). Des Weiteren wiesen iAEC in Ko-Kultur oder durch Zugabe von MSC-konditioniertem Medium eine stark verminderte Apoptose- und IV Replikationsrate, sowie eine erhöhte Regenerationsfähigkeit auf.

In *in vivo* Versuchen konnte durch die intratracheale Applikation von BM-MSC die Viruslast sowie die Schädigung des Alveolarepithels in IV-infizierten Mäusen deutlich verringert werden. Darüber hinaus konnte auch eine erhöhte Proliferationsrate der epithelialen Stamm/Progenitorzellen in der distalen Lunge detektiert werden. Insgesamt zeigt dies eine Verbesserung der Regenerationsfähigkeit des Lungenepithels durch die Gabe von BM-MSC. In weiteren *in vivo* Infektionsversuchen mit Interferon-α/β-Rezeptor-Knockout-Mäusen

(*ifnar-/-*) konnte gezeigt werden, dass Typ I Interferon-induzierte Signalwege an den beobachteten antiviralen Effekten der BM-MSC-Gabe beteiligt sind. Infizierte *ifnar-/-* -Mäuse waren, auch nach BM-MSC-Applikation, nicht in der Lage die Viruslast in der Lunge zu verringern.

Zusammenfassend ist zu sagen, dass die positive Rolle von BM-MSC in der IV-induzierten Pneumonie und dem damit verbunden therapeutischen Potential in *in vitro* und *in vivo* Versuchen klar dargelegt werden konnte. Des Weiteren lässt die Hochregulation der durch Typ I Interferon induzierten Signalwege vermuten, dass BM-MSC in der Gegenwart von IV spezifisch aktiviert werden, wodurch sich ihre vorteilhaften anti-viralen Eigenschaften noch erhöhen.

8. References

1. Taubenberger, J.K. and D.M. Morens, *The pathology of influenza virus infections.* Annu Rev Pathol, 2008. **3**: p. 499-522.
2. WHO, *Fact sheet N°211, Influenza (seasonal).* 2016.
3. Centers for Disease, C. and Prevention, *Estimates of deaths associated with seasonal influenza --- United States, 1976-2007.* MMWR Morb Mortal Wkly Rep, 2010. **59**(33): p. 1057-62.
4. Yoon, S.W., R.J. Webby, and R.G. Webster, *Evolution and ecology of influenza A viruses.* Curr Top Microbiol Immunol, 2014. **385**: p. 359-75.
5. Kuiken, T. and J.K. Taubenberger, *Pathology of human influenza revisited.* Vaccine, 2008. **26 Suppl 4**: p. D59-66.
6. Taubenberger, J.K. and J.C. Kash, *Influenza virus evolution, host adaptation, and pandemic formation.* Cell Host Microbe, 2010. **7**(6): p. 440-51.
7. Medina, R.A. and A. Garcia-Sastre, *Influenza A viruses: new research developments.* Nat Rev Microbiol, 2011. **9**(8): p. 590-603.
8. Centers for Disease, C.a.P., *Influenza Type A Viruses.*
9. Wise, H.M., et al., *A complicated message: Identification of a novel PB1-related protein translated from influenza A virus segment 2 mRNA.* J Virol, 2009. **83**(16): p. 8021-31.
10. Chen, R. and E.C. Holmes, *Avian influenza virus exhibits rapid evolutionary dynamics.* Mol Biol Evol, 2006. **23**(12): p. 2336-41.
11. Thompson, W.W., L. Comanor, and D.K. Shay, *Epidemiology of seasonal influenza: use of surveillance data and statistical models to estimate the burden of disease.* J Infect Dis, 2006. **194 Suppl 2**: p. S82-91.
12. Johnson, N.P. and J. Mueller, *Updating the accounts: global mortality of the 1918-1920 "Spanish" influenza pandemic.* Bull Hist Med, 2002. **76**(1): p. 105-15.
13. Perez-Padilla, R., et al., *Pneumonia and respiratory failure from swine-origin influenza A (H1N1) in Mexico.* N Engl J Med, 2009. **361**(7): p. 680-9.
14. Novel Swine-Origin Influenza, A.V.I.T., et al., *Emergence of a novel swine-origin influenza A (H1N1) virus in humans.* N Engl J Med, 2009. **360**(25): p. 2605-15.
15. Hendrickson, C.M. and M.A. Matthay, *Viral pathogens and acute lung injury: investigations inspired by the SARS epidemic and the 2009 H1N1 influenza pandemic.* Semin Respir Crit Care Med, 2013. **34**(4): p. 475-86.

16. Maines, T.R., et al., *Transmission and pathogenesis of swine-origin 2009 A(H1N1) influenza viruses in ferrets and mice.* Science, 2009. **325**(5939): p. 484-7.
17. Takayama, I., et al., *Novel Reassortant Avian Influenza A(H5N1) Virus in Human, Southern Vietnam, 2014.* Emerg Infect Dis, 2016. **22**(3).
18. Wang, T.T., M.K. Parides, and P. Palese, *Seroevidence for H5N1 influenza infections in humans: meta-analysis.* Science, 2012. **335**(6075): p. 1463.
19. Puzelli, S., et al., *Human infection with highly pathogenic A(H7N7) avian influenza virus, Italy, 2013.* Emerg Infect Dis, 2014. **20**(10): p. 1745-9.
20. Koopmans, M., et al., *Transmission of H7N7 avian influenza A virus to human beings during a large outbreak in commercial poultry farms in the Netherlands.* Lancet, 2004. **363**(9409): p. 587-93.
21. Wang, Z., et al., *Avian Influenza Viruses, Inflammation, and CD8(+) T Cell Immunity.* Front Immunol, 2016. **7**: p. 60.
22. Lin, Y.P., et al., *Avian-to-human transmission of H9N2 subtype influenza A viruses: relationship between H9N2 and H5N1 human isolates.* Proc Natl Acad Sci U S A, 2000. **97**(17): p. 9654-8.
23. Peiris, M., et al., *Human infection with influenza H9N2.* Lancet, 1999. **354**(9182): p. 916-7.
24. Herold, S., et al., *Influenza virus-induced lung injury: pathogenesis and implications for treatment.* Eur Respir J, 2015. **45**(5): p. 1463-78.
25. Pichlmair, A., et al., *RIG-I-mediated antiviral responses to single-stranded RNA bearing 5'-phosphates.* Science, 2006. **314**(5801): p. 997-1001.
26. Vercammen, E., J. Staal, and R. Beyaert, *Sensing of viral infection and activation of innate immunity by toll-like receptor 3.* Clin Microbiol Rev, 2008. **21**(1): p. 13-25.
27. Diebold, S.S., et al., *Innate antiviral responses by means of TLR7-mediated recognition of single-stranded RNA.* Science, 2004. **303**(5663): p. 1529-31.
28. Jensen, S. and A.R. Thomsen, *Sensing of RNA viruses: a review of innate immune receptors involved in recognizing RNA virus invasion.* J Virol, 2012. **86**(6): p. 2900-10.
29. Iwasaki, A. and P.S. Pillai, *Innate immunity to influenza virus infection.* Nat Rev Immunol, 2014. **14**(5): p. 315-28.
30. Loo, Y.M. and M. Gale, Jr., *Immune signaling by RIG-I-like receptors.* Immunity, 2011. **34**(5): p. 680-92.

31. Uematsu, S. and S. Akira, *Toll-like receptors and Type I interferons.* J Biol Chem, 2007. **282**(21): p. 15319-23.
32. Randall, R.E. and S. Goodbourn, *Interferons and viruses: an interplay between induction, signalling, antiviral responses and virus countermeasures.* J Gen Virol, 2008. **89**(Pt 1): p. 1-47.
33. Yoneyama, M. and T. Fujita, *Function of RIG-I-like receptors in antiviral innate immunity.* J Biol Chem, 2007. **282**(21): p. 15315-8.
34. Horisberger, M.A., *Interferons, Mx genes, and resistance to influenza virus.* Am J Respir Crit Care Med, 1995. **152**(4 Pt 2): p. S67-71.
35. Xiao, H., et al., *The human interferon-induced MxA protein inhibits early stages of influenza A virus infection by retaining the incoming viral genome in the cytoplasm.* J Virol. **87**(23): p. 13053-8.
36. Perry, A.K., et al., *The host type I interferon response to viral and bacterial infections.* Cell Res, 2005. **15**(6): p. 407-22.
37. Ivashkiv, L.B. and L.T. Donlin, *Regulation of type I interferon responses.* Nat Rev Immunol, 2014. **14**(1): p. 36-49.
38. Arimori, Y., et al., *Type I interferon limits influenza virus-induced acute lung injury by regulation of excessive inflammation in mice.* Antiviral Res, 2013. **99**(3): p. 230-7.
39. Peteranderl, C., et al., *Macrophage-epithelial paracrine crosstalk inhibits lung edema clearance during influenza infection.* J Clin Invest, 2016. **126**(4): p. 1566-80.
40. Herold, S., et al., *Alveolar epithelial cells direct monocyte transepithelial migration upon influenza virus infection: impact of chemokines and adhesion molecules.* J Immunol, 2006. **177**(3): p. 1817-24.
41. Peper, R.L. and H. Van Campen, *Tumor necrosis factor as a mediator of inflammation in influenza A viral pneumonia.* Microb Pathog, 1995. **19**(3): p. 175-83.
42. Herold, S., et al., *Lung epithelial apoptosis in influenza virus pneumonia: the role of macrophage-expressed TNF-related apoptosis-inducing ligand.* J Exp Med, 2008. **205**(13): p. 3065-77.
43. van de Sandt, C.E., J.H. Kreijtz, and G.F. Rimmelzwaan, *Evasion of influenza A viruses from innate and adaptive immune responses.* Viruses, 2012. **4**(9): p. 1438-76.
44. Goraya, M.U., et al., *Induction of innate immunity and its perturbation by influenza viruses.* Protein Cell, 2015. **6**(10): p. 712-21.
45. Ludwig, S., et al., *Ringing the alarm bells: signalling and apoptosis in influenza virus infected cells.* Cell Microbiol, 2006. **8**(3): p. 375-86.

46. Stephenson, I. and M. Zambon, *The epidemiology of influenza.* Occup Med (Lond), 2002. **52**(5): p. 241-7.
47. Carcione, D., et al., *Comparison of pandemic (H1N1) 2009 and seasonal influenza, Western Australia, 2009.* Emerg Infect Dis, 2010. **16**(9): p. 1388-95.
48. Shiley, K.T., et al., *Differences in the epidemiological characteristics and clinical outcomes of pandemic (H1N1) 2009 influenza, compared with seasonal influenza.* Infect Control Hosp Epidemiol, 2010. **31**(7): p. 676-82.
49. Warren-Gash, C., *Comparing complications of pandemic and seasonal influenza is complicated.* Clin Infect Dis, 2014. **59**(2): p. 175-6.
50. Reed, C., et al., *Complications among adults hospitalized with influenza: a comparison of seasonal influenza and the 2009 H1N1 pandemic.* Clin Infect Dis, 2014. **59**(2): p. 166-74.
51. Perez-Padilla, R., et al., *Pneumonia and respiratory failure from swine-origin influenza A (H1N1) in Mexico.* N Engl J Med, 2009. **361**(7): p. 680-9.
52. Carlson, A., S.F. Thung, and E.R. Norwitz, *H1N1 Influenza in Pregnancy: What All Obstetric Care Providers Ought to Know.* Rev Obstet Gynecol, 2009. **2**(3): p. 139-45.
53. Jamieson, D.J., et al., *H1N1 2009 influenza virus infection during pregnancy in the USA.* Lancet, 2009. **374**(9688): p. 451-8.
54. Louie, J.K., et al., *Factors associated with death or hospitalization due to pandemic 2009 influenza A(H1N1) infection in California.* JAMA, 2009. **302**(17): p. 1896-902.
55. Joseph, C., Y. Togawa, and N. Shindo, *Bacterial and viral infections associated with influenza.* Influenza Other Respir Viruses, 2013. **7 Suppl 2**: p. 105-13.
56. Force, A.D.T., et al., *Acute respiratory distress syndrome: the Berlin Definition.* JAMA, 2012. **307**(23): p. 2526-33.
57. Matthay, M.A. and R.L. Zemans, *The acute respiratory distress syndrome: pathogenesis and treatment.* Annu Rev Pathol, 2011. **6**: p. 147-63.
58. Matthay, M.A., L.B. Ware, and G.A. Zimmerman, *The acute respiratory distress syndrome.* J Clin Invest. **122**(8): p. 2731-40.
59. Matthay, M.A. and J.P. Wiener-Kronish, *Intact epithelial barrier function is critical for the resolution of alveolar edema in humans.* Am Rev Respir Dis, 1990. **142**(6 Pt 1): p. 1250-7.
60. Cepkova, M. and M.A. Matthay, *Pharmacotherapy of acute lung injury and the acute respiratory distress syndrome.* J Intensive Care Med, 2006. **21**(3): p. 119-43.

61. Cross, L.J. and M.A. Matthay, *Biomarkers in acute lung injury: insights into the pathogenesis of acute lung injury.* Crit Care Clin, 2011. **27**(2): p. 355-77.
62. Martin, T.R., et al., *Apoptosis and epithelial injury in the lungs.* Proc Am Thorac Soc, 2005. **2**(3): p. 214-20.
63. Herold, S., et al., *Apoptosis signaling in influenza virus propagation, innate host defense, and lung injury.* J Leukoc Biol. **92**(1): p. 75-82.
64. Hogner, K., et al., *Macrophage-expressed IFN-beta contributes to apoptotic alveolar epithelial cell injury in severe influenza virus pneumonia.* PLoS Pathog, 2013. **9**(2): p. e1003188.
65. Gotts, J.E. and M.A. Matthay, *Endogenous and exogenous cell-based pathways for recovery from acute respiratory distress syndrome.* Clin Chest Med, 2014. **35**(4): p. 797-809.
66. Bannenberg, G.L., et al., *Molecular circuits of resolution: formation and actions of resolvins and protectins.* J Immunol, 2005. **174**(7): p. 4345-55.
67. Levy, B.D. and C.N. Serhan, *Resolution of acute inflammation in the lung.* Annu Rev Physiol, 2014. **76**: p. 467-92.
68. Herold, S., K. Mayer, and J. Lohmeyer, *Acute lung injury: how macrophages orchestrate resolution of inflammation and tissue repair.* Front Immunol. **2**: p. 65.
69. Michelson, P.H., et al., *Keratinocyte growth factor stimulates bronchial epithelial cell proliferation in vitro and in vivo.* Am J Physiol, 1999. **277**(4 Pt 1): p. L737-42.
70. Ulich, T.R., et al., *Keratinocyte growth factor is a growth factor for type II pneumocytes in vivo.* J Clin Invest, 1994. **93**(3): p. 1298-306.
71. Chandel, N.S., et al., *Keratinocyte growth factor expression is suppressed in early acute lung injury/acute respiratory distress syndrome by smad and c-Abl pathways.* Crit Care Med, 2009. **37**(5): p. 1678-84.
72. Baba, Y., et al., *Keratinocyte growth factor gene transduction ameliorates acute lung injury and mortality in mice.* Hum Gene Ther, 2007. **18**(2): p. 130-41.
73. Tong, L., et al., *Keratinocyte growth factor-2 is protective in lipopolysaccharide-induced acute lung injury in rats.* Respir Physiol Neurobiol. **201**: p. 7-14.
74. Lindsay, C.D., *Novel therapeutic strategies for acute lung injury induced by lung damaging agents: the potential role of growth factors as treatment options.* Hum Exp Toxicol, 2011. **30**(7): p. 701-24.

75. Mura, M., et al., *The early responses of VEGF and its receptors during acute lung injury: implication of VEGF in alveolar epithelial cell survival.* Crit Care, 2006. **10**(5): p. R130.
76. Medford, A.R. and A.B. Millar, *Vascular endothelial growth factor (VEGF) in acute lung injury (ALI) and acute respiratory distress syndrome (ARDS): paradox or paradigm?* Thorax, 2006. **61**(7): p. 621-6.
77. Medford, A.R., et al., *Vascular Endothelial Growth Factor (VEGF) isoform expression and activity in human and murine lung injury.* Respir Res, 2009. **10**: p. 27.
78. Giangreco, A., et al., *Stem cells are dispensable for lung homeostasis but restore airways after injury.* Proc Natl Acad Sci U S A, 2009. **106**(23): p. 9286-91.
79. Kim, C.F., et al., *Identification of bronchioalveolar stem cells in normal lung and lung cancer.* Cell, 2005. **121**(6): p. 823-35.
80. Reynolds, S.D. and A.M. Malkinson, *Clara cell: progenitor for the bronchiolar epithelium.* Int J Biochem Cell Biol, 2010. **42**(1): p. 1-4.
81. Hayden, F.G. and M.D. de Jong, *Emerging influenza antiviral resistance threats.* J Infect Dis, 2011. **203**(1): p. 6-10.
82. Hayden, F.G., et al., *Emergence and apparent transmission of rimantadine-resistant influenza A virus in families.* N Engl J Med, 1989. **321**(25): p. 1696-702.
83. Schaduangrat, N., et al., *The significance of naturally occurring neuraminidase quasispecies of H5N1 avian influenza virus on resistance to oseltamivir: a point of concern.* J Gen Virol, 2016.
84. Ruangrung, K., et al., *Neuraminidase Activity and The Resistance of 2009 Pandemic H1N1 Influenza Virus to Antiviral Activity in Bronchoalveolar Fluid.* J Virol, 2016.
85. Storms, A.D., et al., *Oseltamivir-resistant pandemic (H1N1) 2009 virus infections, United States, 2010-11.* Emerg Infect Dis, 2012. **18**(2): p. 308-11.
86. Moscona, A., *Global transmission of oseltamivir-resistant influenza.* N Engl J Med, 2009. **360**(10): p. 953-6.
87. Jhung, M.A., et al., *Epidemiology of 2009 pandemic influenza A (H1N1) in the United States.* Clin Infect Dis, 2011. **52 Suppl 1**: p. S13-26.
88. Zambon, M. and J.L. Vincent, *Mortality rates for patients with acute lung injury/ARDS have decreased over time.* Chest, 2008. **133**(5): p. 1120-7.
89. Rubenfeld, G.D., et al., *Incidence and outcomes of acute lung injury.* N Engl J Med, 2005. **353**(16): p. 1685-93.

90. Diaz, J.V., et al., *Therapeutic strategies for severe acute lung injury.* Crit Care Med, 2010. **38**(8): p. 1644-50.
91. Oba, Y. and G.A. Salzman, *Ventilation with lower tidal volumes as compared with traditional tidal volumes for acute lung injury.* N Engl J Med, 2000. **343**(11): p. 813; author reply 813-4.
92. Levitt, J.E. and M.A. Matthay, *Clinical review: Early treatment of acute lung injury--paradigm shift toward prevention and treatment prior to respiratory failure.* Crit Care, 2012. **16**(3): p. 223.
93. Venkategowda, P.M., et al., *Prone position and pressure control inverse ratio ventilation in H1N1 patients with severe acute respiratory distress syndrome.* Indian J Crit Care Med, 2016. **20**(1): p. 44-9.
94. Sud, S., et al., *Effect of prone positioning during mechanical ventilation on mortality among patients with acute respiratory distress syndrome: a systematic review and meta-analysis.* CMAJ, 2014. **186**(10): p. E381-90.
95. Peek, G.J., et al., *Efficacy and economic assessment of conventional ventilatory support versus extracorporeal membrane oxygenation for severe adult respiratory failure (CESAR): a multicentre randomised controlled trial.* Lancet, 2009. **374**(9698): p. 1351-63.
96. Hemmila, M.R., et al., *Extracorporeal life support for severe acute respiratory distress syndrome in adults.* Ann Surg, 2004. **240**(4): p. 595-605; discussion 605-7.
97. Brun-Buisson, C., et al., *Early corticosteroids in severe influenza A/H1N1 pneumonia and acute respiratory distress syndrome.* Am J Respir Crit Care Med, 2011. **183**(9): p. 1200-6.
98. Kim, S.H., et al., *Corticosteroid treatment in critically ill patients with pandemic influenza A/H1N1 2009 infection: analytic strategy using propensity scores.* Am J Respir Crit Care Med, 2011. **183**(9): p. 1207-14.
99. Louie, J.K., et al., *Treatment with neuraminidase inhibitors for critically ill patients with influenza A (H1N1)pdm09.* Clin Infect Dis, 2012. **55**(9): p. 1198-204.
100. WHO, *WHO Guidelines for Pharmacological Management of Pandemic Influenza A(H1N1) 2009 and Other Influenza Viruses*, in *WHO Guidelines for Pharmacological Management of Pandemic Influenza A(H1N1) 2009 and Other Influenza Viruses*. 2010: Geneva.
101. Lensch, M.W., et al., *Teratoma formation assays with human embryonic stem cells: a rationale for one type of human-animal chimera.* Cell Stem Cell, 2007. **1**(3): p. 253-8.

102. Blum, B. and N. Benvenisty, *The tumorigenicity of human embryonic stem cells.* Adv Cancer Res, 2008. **100**: p. 133-58.
103. Wobus, A.M. and K.R. Boheler, *Embryonic stem cells: prospects for developmental biology and cell therapy.* Physiol Rev, 2005. **85**(2): p. 635-78.
104. Hayes, M., et al., *Clinical review: Stem cell therapies for acute lung injury/acute respiratory distress syndrome - hope or hype?* Crit Care. **16**(2): p. 205.
105. Quantius, J., et al., *Influenza Virus Infects Epithelial Stem/Progenitor Cells of the Distal Lung: Impact on Fgfr2b-Driven Epithelial Repair.* PLoS Pathog, 2016. **12**(6): p. e1005544.
106. Vaughan, A.E., et al., *Lineage-negative progenitors mobilize to regenerate lung epithelium after major injury.* Nature, 2015. **517**(7536): p. 621-5.
107. Yang, C., et al., *Stem/progenitor cells in endogenous repairing responses: new toolbox for the treatment of acute lung injury.* J Transl Med, 2016. **14**(1): p. 47.
108. Akram, K.M., et al., *Lung Regeneration: Endogenous and Exogenous Stem Cell Mediated Therapeutic Approaches.* Int J Mol Sci, 2016. **17**(1).
109. Friedenstein, A.J., et al., *Stromal cells responsible for transferring the microenvironment of the hemopoietic tissues. Cloning in vitro and retransplantation in vivo.* Transplantation, 1974. **17**(4): p. 331-40.
110. Friedenstein, A.J., J.F. Gorskaja, and N.N. Kulagina, *Fibroblast precursors in normal and irradiated mouse hematopoietic organs.* Exp Hematol, 1976. **4**(5): p. 267-74.
111. Ribeiro, A., et al., *Mesenchymal stem cells from umbilical cord matrix, adipose tissue and bone marrow exhibit different capability to suppress peripheral blood B, natural killer and T cells.* Stem Cell Res Ther, 2013. **4**(5): p. 125.
112. Moretti, P., et al., *Mesenchymal stromal cells derived from human umbilical cord tissues: primitive cells with potential for clinical and tissue engineering applications.* Adv Biochem Eng Biotechnol, 2010. **123**: p. 29-54.
113. Bieback, K. and H. Kluter, *Mesenchymal stromal cells from umbilical cord blood.* Curr Stem Cell Res Ther, 2007. **2**(4): p. 310-23.
114. Barry, F.P. and J.M. Murphy, *Mesenchymal stem cells: clinical applications and biological characterization.* Int J Biochem Cell Biol, 2004. **36**(4): p. 568-84.
115. Zhang, X., et al., *Isolation and characterization of mesenchymal stem cells from human umbilical cord blood: reevaluation of critical factors for successful isolation and high ability to proliferate and differentiate to chondrocytes as compared to*

mesenchymal stem cells from bone marrow and adipose tissue. J Cell Biochem, 2011. **112**(4): p. 1206-18.

116. Anzalone, R., et al., *New emerging potentials for human Wharton's jelly mesenchymal stem cells: immunological features and hepatocyte-like differentiative capacity.* Stem Cells Dev, 2010. **19**(4): p. 423-38.
117. Anzalone, R., et al., *Wharton's jelly mesenchymal stem cells as candidates for beta cells regeneration: extending the differentiative and immunomodulatory benefits of adult mesenchymal stem cells for the treatment of type 1 diabetes.* Stem Cell Rev, 2011. **7**(2): p. 342-63.
118. Heo, J.S., et al., *Comparison of molecular profiles of human mesenchymal stem cells derived from bone marrow, umbilical cord blood, placenta and adipose tissue.* Int J Mol Med, 2016. **37**(1): p. 115-25.
119. Hass, R., et al., *Different populations and sources of human mesenchymal stem cells (MSC): A comparison of adult and neonatal tissue-derived MSC.* Cell Commun Signal. **9**: p. 12.
120. Rossi, D., et al., *Characterization of the conditioned medium from amniotic membrane cells: prostaglandins as key effectors of its immunomodulatory activity.* PLoS One. **7**(10): p. e46956.
121. Ren, H., et al., *Comparative Analysis of Human Mesenchymal Stem Cells from Umbilical Cord, Dental Pulp, and Menstrual Blood as Sources for Cell Therapy.* Stem Cells Int, 2016. **2016**: p. 3516574.
122. Gargett, C.E., et al., *Isolation and culture of epithelial progenitors and mesenchymal stem cells from human endometrium.* Biol Reprod, 2009. **80**(6): p. 1136-45.
123. Spitzer, T.L., et al., *Perivascular human endometrial mesenchymal stem cells express pathways relevant to self-renewal, lineage specification, and functional phenotype.* Biol Reprod, 2012. **86**(2): p. 58.
124. Baer, P.C., *Adipose-derived mesenchymal stromal/stem cells: An update on their phenotype in vivo and in vitro.* World J Stem Cells. **6**(3): p. 256-65.
125. Strioga, M., et al., *Same or not the same? Comparison of adipose tissue-derived versus bone marrow-derived mesenchymal stem and stromal cells.* Stem Cells Dev, 2012. **21**(14): p. 2724-52.
126. Fournier, B.P., H. Larjava, and L. Hakkinen, *Gingiva as a source of stem cells with therapeutic potential.* Stem Cells Dev, 2013. **22**(24): p. 3157-77.

127. Gao, Y., et al., *Isolation and multiple differentiation potential assessment of human gingival mesenchymal stem cells.* Int J Mol Sci, 2014. **15**(11): p. 20982-96.
128. Yang, H., et al., *Comparison of mesenchymal stem cells derived from gingival tissue and periodontal ligament in different incubation conditions.* Biomaterials, 2013. **34**(29): p. 7033-47.
129. Ozeki, N., et al., *Synovial mesenchymal stem cells promote meniscus regeneration augmented by an autologous Achilles tendon graft in a rat partial meniscus defect model.* Stem Cells, 2015. **33**(6): p. 1927-38.
130. Suzuki, S., et al., *Properties and usefulness of aggregates of synovial mesenchymal stem cells as a source for cartilage regeneration.* Arthritis Res Ther, 2012. **14**(3): p. R136.
131. Houlihan, D.D., et al., *Isolation of mouse mesenchymal stem cells on the basis of expression of Sca-1 and PDGFR-alpha.* Nat Protoc. **7**(12): p. 2103-11.
132. Calio, M.L., et al., *Transplantation of bone marrow mesenchymal stem cells decreases oxidative stress, apoptosis, and hippocampal damage in brain of a spontaneous stroke model.* Free Radic Biol Med, 2014. **70**: p. 141-54.
133. Sacchetti, B., et al., *Self-renewing osteoprogenitors in bone marrow sinusoids can organize a hematopoietic microenvironment.* Cell, 2007. **131**(2): p. 324-36.
134. da Silva Meirelles, L., A.I. Caplan, and N.B. Nardi, *In search of the in vivo identity of mesenchymal stem cells.* Stem Cells, 2008. **26**(9): p. 2287-99.
135. Murray, I.R. and B. Peault, *Q&A: Mesenchymal stem cells - where do they come from and is it important?* BMC Biol, 2015. **13**(1): p. 99.
136. Bianco, P., et al., *The meaning, the sense and the significance: translating the science of mesenchymal stem cells into medicine.* Nat Med, 2013. **19**(1): p. 35-42.
137. Uccelli, A., L. Moretta, and V. Pistoia, *Mesenchymal stem cells in health and disease.* Nat Rev Immunol, 2008. **8**(9): p. 726-36.
138. Galli, D., M. Vitale, and M. Vaccarezza, *Bone marrow-derived mesenchymal cell differentiation toward myogenic lineages: facts and perspectives.* Biomed Res Int, 2014. **2014**: p. 762695.
139. Dezawa, M., et al., *Potential of bone marrow stromal cells in applications for neuro-degenerative, neuro-traumatic and muscle degenerative diseases.* Curr Neuropharmacol, 2005. **3**(4): p. 257-66.
140. Kopen, G.C., D.J. Prockop, and D.G. Phinney, *Marrow stromal cells migrate throughout forebrain and cerebellum, and they differentiate into astrocytes after*

injection into neonatal mouse brains. Proc Natl Acad Sci U S A, 1999. **96**(19): p. 10711-6.

141. Phinney, D.G. and D.J. Prockop, *Concise review: mesenchymal stem/multipotent stromal cells: the state of transdifferentiation and modes of tissue repair--current views.* Stem Cells, 2007. **25**(11): p. 2896-902.
142. Makino, S., et al., *Cardiomyocytes can be generated from marrow stromal cells in vitro.* J Clin Invest, 1999. **103**(5): p. 697-705.
143. Hattan, N., et al., *Purified cardiomyocytes from bone marrow mesenchymal stem cells produce stable intracardiac grafts in mice.* Cardiovasc Res, 2005. **65**(2): p. 334-44.
144. Williams, A.R. and J.M. Hare, *Mesenchymal stem cells: biology, pathophysiology, translational findings, and therapeutic implications for cardiac disease.* Circ Res, 2011. **109**(8): p. 923-40.
145. Christ, B. and P. Stock, *Mesenchymal stem cell-derived hepatocytes for functional liver replacement.* Front Immunol, 2012. **3**: p. 168.
146. Ye, J.S., et al., *Signalling pathways involved in the process of mesenchymal stem cells differentiating into hepatocytes.* Cell Prolif, 2015. **48**(2): p. 157-65.
147. Liu, A.R., et al., *Activation of canonical wnt pathway promotes differentiation of mouse bone marrow-derived MSCs into type II alveolar epithelial cells, confers resistance to oxidative stress, and promotes their migration to injured lung tissue in vitro.* J Cell Physiol. **228**(6): p. 1270-83.
148. Gao, P., et al., *Salvianolic acid B improves bone marrow-derived mesenchymal stem cell differentiation into alveolar epithelial cells type I via Wnt signaling.* Mol Med Rep, 2015. **12**(2): p. 1971-6.
149. M Dominici, K.L.B., I Mueller, I Slaper-Cortenbach, FC Marini, and R.D. DS Krause, A Keating, DJ Prockop and EM Horwitz, *Minimal criteria for defining multipotent mesenchymal stromal cells. The International Society for Cellular Therapy position statement.* Cytotherapy, 2006. **Vol8**(4): p. 3.
150. Le Blanc, K., et al., *HLA expression and immunologic properties of differentiated and undifferentiated mesenchymal stem cells.* Exp Hematol, 2003. **31**(10): p. 890-6.
151. Le Blanc, K., *Immunomodulatory effects of fetal and adult mesenchymal stem cells.* Cytotherapy, 2003. **5**(6): p. 485-9.
152. Tse, W.T., et al., *Suppression of allogeneic T-cell proliferation by human marrow stromal cells: implications in transplantation.* Transplantation, 2003. **75**(3): p. 389-97.

153. Di Nicola, M., et al., *Human bone marrow stromal cells suppress T-lymphocyte proliferation induced by cellular or nonspecific mitogenic stimuli.* Blood, 2002. **99**(10): p. 3838-43.
154. Klyushnenkova, E., et al., *T cell responses to allogeneic human mesenchymal stem cells: immunogenicity, tolerance, and suppression.* J Biomed Sci, 2005. **12**(1): p. 47-57.
155. Rasmusson, I., et al., *Mesenchymal stem cells inhibit the formation of cytotoxic T lymphocytes, but not activated cytotoxic T lymphocytes or natural killer cells.* Transplantation, 2003. **76**(8): p. 1208-13.
156. Beyth, S., et al., *Human mesenchymal stem cells alter antigen-presenting cell maturation and induce T-cell unresponsiveness.* Blood, 2005. **105**(5): p. 2214-9.
157. Yang, S.H., et al., *Soluble mediators from mesenchymal stem cells suppress T cell proliferation by inducing IL-10.* Exp Mol Med, 2009. **41**(5): p. 315-24.
158. Figueroa, F.E., et al., *Mesenchymal stem cell treatment for autoimmune diseases: a critical review.* Biol Res. **45**(3): p. 269-77.
159. Battiwalla, M. and P. Hematti, *Mesenchymal stem cells in hematopoietic stem cell transplantation.* Cytotherapy, 2009. **11**(5): p. 503-15.
160. Tyndall, A. and A. Uccelli, *Multipotent mesenchymal stromal cells for autoimmune diseases: teaching new dogs old tricks.* Bone Marrow Transplant, 2009. **43**(11): p. 821-8.
161. Stagg, J., *Immune regulation by mesenchymal stem cells: two sides to the coin.* Tissue Antigens, 2007. **69**(1): p. 1-9.
162. Salem, H.K. and C. Thiemermann, *Mesenchymal stromal cells: current understanding and clinical status.* Stem Cells, 2010. **28**(3): p. 585-96.
163. Bernardo, M.E. and W.E. Fibbe, *Mesenchymal stromal cells: sensors and switchers of inflammation.* Cell Stem Cell. **13**(4): p. 392-402.
164. Mei, S.H., et al., *Prevention of LPS-induced acute lung injury in mice by mesenchymal stem cells overexpressing angiopoietin 1.* PLoS Med, 2007. **4**(9): p. e269.
165. Tai, W.L., et al., *Therapeutic effect of intravenous bone marrow-derived mesenchymal stem cell transplantation on early-stage LPS-induced acute lung injury in mice.* Nan Fang Yi Ke Da Xue Xue Bao, 2012. **32**(3): p. 283-90.

166. Romieu-Mourez, R., et al., *Cytokine modulation of TLR expression and activation in mesenchymal stromal cells leads to a proinflammatory phenotype.* J Immunol, 2009. **182**(12): p. 7963-73.
167. Mastri, M., et al., *Activation of Toll-like receptor 3 amplifies mesenchymal stem cell trophic factors and enhances therapeutic potency.* Am J Physiol Cell Physiol. **303**(10): p. C1021-33.
168. Lei, J., et al., *Ligation of TLR2 and TLR4 on murine bone marrow-derived mesenchymal stem cells triggers differential effects on their immunosuppressive activity.* Cell Immunol, 2011. **271**(1): p. 147-56.
169. Zhao, X., et al., *The toll-like receptor 3 ligand, poly(I:C), improves immunosuppressive function and therapeutic effect of mesenchymal stem cells on sepsis via inhibiting MiR-143.* Stem cells. **32**(2): p. 521-33.
170. Hwang, S.H., et al., *Toll like receptor 3 & 4 responses of human turbinate derived mesenchymal stem cells: stimulation by double stranded RNA and lipopolysaccharide.* PLoS One. **9**(7): p. e101558.
171. Auletta, J.J., R.J. Deans, and A.M. Bartholomew, *Emerging roles for multipotent, bone marrow-derived stromal cells in host defense.* Blood, 2012. **119**(8): p. 1801-9.
172. Islam, M.N., et al., *Mitochondrial transfer from bone-marrow-derived stromal cells to pulmonary alveoli protects against acute lung injury.* Nat Med. **18**(5): p. 759-65.
173. Plotnikov, E.Y., et al., *Cell-to-cell cross-talk between mesenchymal stem cells and cardiomyocytes in co-culture.* J Cell Mol Med, 2008. **12**(5A): p. 1622-31.
174. Ren, G., et al., *Mesenchymal stem cell-mediated immunosuppression occurs via concerted action of chemokines and nitric oxide.* Cell Stem Cell, 2008. **2**(2): p. 141-50.
175. Ryan, J.M., et al., *Interferon-gamma does not break, but promotes the immunosuppressive capacity of adult human mesenchymal stem cells.* Clin Exp Immunol, 2007. **149**(2): p. 353-63.
176. Sheng, H., et al., *A critical role of IFNgamma in priming MSC-mediated suppression of T cell proliferation through up-regulation of B7-H1.* Cell Res, 2008. **18**(8): p. 846-57.
177. Lee, R.H., et al., *Intravenous hMSCs improve myocardial infarction in mice because cells embolized in lung are activated to secrete the anti-inflammatory protein TSG-6.* Cell Stem Cell, 2009. **5**(1): p. 54-63.

178. Liotta, F., et al., *Toll-like receptors 3 and 4 are expressed by human bone marrow-derived mesenchymal stem cells and can inhibit their T-cell modulatory activity by impairing Notch signaling.* Stem Cells, 2008. **26**(1): p. 279-89.
179. Maumus, M., C. Jorgensen, and D. Noel, *Mesenchymal stem cells in regenerative medicine applied to rheumatic diseases: role of secretome and exosomes.* Biochimie, 2013. **95**(12): p. 2229-34.
180. Emmons, R., et al., *Acute exercise mobilizes hematopoietic stem and progenitor cells and alters the mesenchymal stromal cell secretome.* J Appl Physiol (1985), 2016. **120**(6): p. 624-32.
181. Meirelles Lda, S., et al., *Mechanisms involved in the therapeutic properties of mesenchymal stem cells.* Cytokine Growth Factor Rev, 2009. **20**(5-6): p. 419-27.
182. Boomsma, R.A. and D.L. Geenen, *Mesenchymal stem cells secrete multiple cytokines that promote angiogenesis and have contrasting effects on chemotaxis and apoptosis.* PLoS One. **7**(4): p. e35685.
183. de Almeida, D.C., et al., *In search of mechanisms associated with mesenchymal stem cell-based therapies for acute kidney injury.* Clin Biochem Rev. **34**(3): p. 131-44.
184. Haider, H., et al., *IGF-1-overexpressing mesenchymal stem cells accelerate bone marrow stem cell mobilization via paracrine activation of SDF-1alpha/CXCR4 signaling to promote myocardial repair.* Circ Res, 2008. **103**(11): p. 1300-8.
185. Togel, F., et al., *Vasculotropic, paracrine actions of infused mesenchymal stem cells are important to the recovery from acute kidney injury.* Am J Physiol Renal Physiol, 2007. **292**(5): p. F1626-35.
186. Block, G.J., et al., *Multipotent stromal cells are activated to reduce apoptosis in part by upregulation and secretion of stanniocalcin-1.* Stem Cells, 2009. **27**(3): p. 670-81.
187. Suga, H., et al., *IFATS collection: Fibroblast growth factor-2-induced hepatocyte growth factor secretion by adipose-derived stromal cells inhibits postinjury fibrogenesis through a c-Jun N-terminal kinase-dependent mechanism.* Stem Cells, 2009. **27**(1): p. 238-49.
188. Chen, L., et al., *Paracrine factors of mesenchymal stem cells recruit macrophages and endothelial lineage cells and enhance wound healing.* PLoS One, 2008. **3**(4): p. e1886.
189. Lee, J.W., et al., *Concise review: Mesenchymal stem cells for acute lung injury: role of paracrine soluble factors.* Stem cells. **29**(6): p. 913-9.

190. Zisa, D., et al., *Vascular endothelial growth factor (VEGF) as a key therapeutic trophic factor in bone marrow mesenchymal stem cell-mediated cardiac repair.* Biochem Biophys Res Commun, 2009. **390**(3): p. 834-8.
191. Lee, J.W., et al., *Therapeutic effects of human mesenchymal stem cells in ex vivo human lungs injured with live bacteria.* Am J Respir Crit Care Med. **187**(7): p. 751-60.
192. Wen, Z., et al., *Repair mechanisms of bone marrow mesenchymal stem cells in myocardial infarction.* J Cell Mol Med. **15**(5): p. 1032-43.
193. Ortiz, L.A., et al., *Interleukin 1 receptor antagonist mediates the antiinflammatory and antifibrotic effect of mesenchymal stem cells during lung injury.* Proc Natl Acad Sci U S A, 2007. **104**(26): p. 11002-7.
194. Gnecchi, M., et al., *Paracrine mechanisms in adult stem cell signaling and therapy.* Circ Res, 2008. **103**(11): p. 1204-19.
195. Tropea, K.A., et al., *Bronchioalveolar stem cells increase after mesenchymal stromal cell treatment in a mouse model of bronchopulmonary dysplasia.* Am J Physiol Lung Cell Mol Physiol, 2012. **302**(9): p. L829-37.
196. Jorgensen, C., *Mesenchymal stem cells in arthritis: role of bone marrow microenvironment.* Arthritis Res Ther, 2010. **12**(4): p. 135.
197. Horwitz, E.M., et al., *Transplantability and therapeutic effects of bone marrow-derived mesenchymal cells in children with osteogenesis imperfecta.* Nat Med, 1999. **5**(3): p. 309-13.
198. Togel, F., et al., *Administered mesenchymal stem cells protect against ischemic acute renal failure through differentiation-independent mechanisms.* Am J Physiol Renal Physiol, 2005. **289**(1): p. F31-42.
199. Wise, A.F., et al., *Human mesenchymal stem cells alter macrophage phenotype and promote regeneration via homing to the kidney following ischemia-reperfusion injury.* Am J Physiol Renal Physiol. **306**(10): p. F1222-35.
200. Cras, A., et al., *Update on mesenchymal stem cell-based therapy in lupus and scleroderma.* Arthritis Res Ther, 2015. **17**: p. 301.
201. Dominguez-Bendala, J., et al., *Concise review: mesenchymal stem cells for diabetes.* Stem Cells Transl Med, 2012. **1**(1): p. 59-63.
202. Fiorina, P., et al., *Immunomodulatory function of bone marrow-derived mesenchymal stem cells in experimental autoimmune type 1 diabetes.* J Immunol, 2009. **183**(2): p. 993-1004.

203. Volarevic, V., et al., *Concise review: Therapeutic potential of mesenchymal stem cells for the treatment of acute liver failure and cirrhosis.* Stem cells.
204. Berardis, S., et al., *Use of mesenchymal stem cells to treat liver fibrosis: current situation and future prospects.* World J Gastroenterol, 2015. **21**(3): p. 742-58.
205. Barbash, I.M., et al., *Systemic delivery of bone marrow-derived mesenchymal stem cells to the infarcted myocardium: feasibility, cell migration, and body distribution.* Circulation, 2003. **108**(7): p. 863-8.
206. Charwat, S., et al., *Role of adult bone marrow stem cells in the repair of ischemic myocardium: current state of the art.* Exp Hematol, 2008. **36**(6): p. 672-80.
207. Shake, J.G., et al., *Mesenchymal stem cell implantation in a swine myocardial infarct model: engraftment and functional effects.* Ann Thorac Surg, 2002. **73**(6): p. 1919-25; discussion 1926.
208. Cribbs, S.K., M.A. Matthay, and G.S. Martin, *Stem cells in sepsis and acute lung injury.* Crit Care Med, 2010. **38**(12): p. 2379-85.
209. Krasnodembskaya, A., et al., *Antibacterial effect of human mesenchymal stem cells is mediated in part from secretion of the antimicrobial peptide LL-37.* Stem cells. **28**(12): p. 2229-38.
210. Mei, S.H., et al., *Mesenchymal stem cells reduce inflammation while enhancing bacterial clearance and improving survival in sepsis.* Am J Respir Crit Care Med, 2010. **182**(8): p. 1047-57.
211. Nemeth, K., et al., *Bone marrow stromal cells attenuate sepsis via prostaglandin E(2)-dependent reprogramming of host macrophages to increase their interleukin-10 production.* Nat Med, 2009. **15**(1): p. 42-9.
212. Gupta, N., et al., *Intrapulmonary delivery of bone marrow-derived mesenchymal stem cells improves survival and attenuates endotoxin-induced acute lung injury in mice.* J Immunol, 2007. **179**(3): p. 1855-63.
213. Xu, J., et al., *Prevention of endotoxin-induced systemic response by bone marrow-derived mesenchymal stem cells in mice.* Am J Physiol Lung Cell Mol Physiol, 2007. **293**(1): p. L131-41.
214. Xu, J., et al., *Mesenchymal stem cell-based angiopoietin-1 gene therapy for acute lung injury induced by lipopolysaccharide in mice.* J Pathol, 2008. **214**(4): p. 472-81.
215. Lee, J.W., et al., *Allogeneic human mesenchymal stem cells for treatment of E. coli endotoxin-induced acute lung injury in the ex vivo perfused human lung.* Proc Natl Acad Sci U S A, 2009. **106**(38): p. 16357-62.

216. Iyer, S.S., C. Co, and M. Rojas, *Mesenchymal stem cells and inflammatory lung diseases.* Panminerva Med, 2009. **51**(1): p. 5-16.
217. Goodwin, M., et al., *Bone marrow-derived mesenchymal stromal cells inhibit Th2-mediated allergic airways inflammation in mice.* Stem Cells, 2011. **29**(7): p. 1137-48.
218. Nemeth, K., et al., *Bone marrow stromal cells use TGF-beta to suppress allergic responses in a mouse model of ragweed-induced asthma.* Proc Natl Acad Sci U S A, 2010. **107**(12): p. 5652-7.
219. Ge, X., et al., *Intratracheal transplantation of bone marrow-derived mesenchymal stem cells reduced airway inflammation and up-regulated CD4(+)CD25(+) regulatory T cells in asthmatic mouse.* Cell Biol Int, 2013. **37**(7): p. 675-86.
220. Hansmann, G., et al., *Mesenchymal stem cell-mediated reversal of bronchopulmonary dysplasia and associated pulmonary hypertension.* Pulm Circ. **2**(2): p. 170-81.
221. Conese, M., et al., *Hematopoietic and mesenchymal stem cells for the treatment of chronic respiratory diseases: role of plasticity and heterogeneity.* ScientificWorldJournal. **2014**: p. 859817.
222. Mueller, M., et al., *Mesenchymal stem/stromal cells-a key mediator for regeneration after perinatal morbidity?* Mol Cell Pediatr, 2016. **3**(1): p. 6.
223. Rejman, J., C. Colombo, and M. Conese, *Engraftment of bone marrow-derived stem cells to the lung in a model of acute respiratory infection by Pseudomonas aeruginosa.* Mol Ther, 2009. **17**(7): p. 1257-65.
224. Sutsko, R.P., et al., *Long-term reparative effects of mesenchymal stem cell therapy following neonatal hyperoxia-induced lung injury.* Pediatr Res. **73**(1): p. 46-53.
225. Toonkel, R.L., et al., *Mesenchymal stem cells and idiopathic pulmonary fibrosis. Potential for clinical testing.* Am J Respir Crit Care Med. **188**(2): p. 133-40.
226. Chen, J., et al., *Keratinocyte growth factor gene delivery via mesenchymal stem cells protects against lipopolysaccharide-induced acute lung injury in mice.* PLoS One. **8**(12): p. e83303.
227. Hayes, M., et al., *Mesenchymal stromal cells are more effective than the MSC secretome in diminishing injury and enhancing recovery following ventilator-induced lung injury.* Intensive Care Med Exp. **3**(1): p. 29.
228. Zhu, Y.G., et al., *Human mesenchymal stem cell microvesicles for treatment of Escherichia coli endotoxin-induced acute lung injury in mice.* Stem cells. **32**(1): p. 116-25.

229. Liu, Q.P., et al., *Bone marrow mesenchymal stem cells ameliorates seawater-exposure-induced acute lung injury by inhibiting autophagy in lung tissue.* Patholog Res Int. **2014**: p. 104962.
230. Ortiz, L.A., et al., *Mesenchymal stem cell engraftment in lung is enhanced in response to bleomycin exposure and ameliorates its fibrotic effects.* Proc Natl Acad Sci U S A, 2003. **100**(14): p. 8407-11.
231. Rojas, M., et al., *Infusion of freshly isolated autologous bone marrow derived mononuclear cells prevents endotoxin-induced lung injury in an ex-vivo perfused swine model.* Stem Cell Res Ther. **4**(2): p. 26.
232. Rojas, M., et al., *Bone marrow-derived mesenchymal stem cells in repair of the injured lung.* Am J Respir Cell Mol Biol, 2005. **33**(2): p. 145-52.
233. Gotts, J.E., J. Abbott, and M.A. Matthay, *Influenza causes prolonged disruption of the alveolar-capillary barrier in mice unresponsive to mesenchymal stem cell therapy.* Am J Physiol Lung Cell Mol Physiol. **307**(5): p. L395-406.
234. Gupta, N., et al., *Mesenchymal stem cells enhance survival and bacterial clearance in murine Escherichia coli pneumonia.* Thorax, 2012. **67**(6): p. 533-9.
235. Aslam, M., et al., *Bone marrow stromal cells attenuate lung injury in a murine model of neonatal chronic lung disease.* Am J Respir Crit Care Med, 2009. **180**(11): p. 1122-30.
236. Guo, Z., et al., *Mesenchymal stem cells reprogram host macrophages to attenuate obliterative bronchiolitis in murine orthotopic tracheal transplantation.* Int Immunopharmacol, 2013. **15**(4): p. 726-34.
237. Tan, R., et al., *GAPDH is critical for superior efficacy of female bone marrow-derived mesenchymal stem cells on pulmonary hypertension.* Cardiovasc Res, 2013. **100**(1): p. 19-27.
238. Skrahin, A., et al., *Autologous mesenchymal stromal cell infusion as adjunct treatment in patients with multidrug and extensively drug-resistant tuberculosis: an open-label phase 1 safety trial.* Lancet Respir Med, 2014. **2**(2): p. 108-22.
239. Baber, S.R., et al., *Intratracheal mesenchymal stem cell administration attenuates monocrotaline-induced pulmonary hypertension and endothelial dysfunction.* Am J Physiol Heart Circ Physiol, 2007. **292**(2): p. H1120-8.
240. Ware, L.B. and M.A. Matthay, *Alveolar fluid clearance is impaired in the majority of patients with acute lung injury and the acute respiratory distress syndrome.* Am J Respir Crit Care Med, 2001. **163**(6): p. 1376-83.

241. Fang, X., et al., *Allogeneic human mesenchymal stem cells restore epithelial protein permeability in cultured human alveolar type II cells by secretion of angiopoietin-1.* J Biol Chem, 2010. **285**(34): p. 26211-22.

242. Pati, S., et al., *Bone marrow derived mesenchymal stem cells inhibit inflammation and preserve vascular endothelial integrity in the lungs after hemorrhagic shock.* PLoS One, 2011. **6**(9): p. e25171.

243. Pati, S., et al., *Human mesenchymal stem cells inhibit vascular permeability by modulating vascular endothelial cadherin/beta-catenin signaling.* Stem Cells Dev, 2011. **20**(1): p. 89-101.

244. Liang, Z.X., et al., *Bone marrow-derived mesenchymal stem cells protect rats from endotoxin-induced acute lung injury.* Chin Med J (Engl), 2011. **124**(17): p. 2715-22.

245. Walter, J., L.B. Ware, and M.A. Matthay, *Mesenchymal stem cells: mechanisms of potential therapeutic benefit in ARDS and sepsis.* Lancet Respir Med. **2**(12): p. 1016-26.

246. Lai, R.C., T.S. Chen, and S.K. Lim, *Mesenchymal stem cell exosome: a novel stem cell-based therapy for cardiovascular disease.* Regen Med. **6**(4): p. 481-92.

247. Crescitelli, R., et al., *Distinct RNA profiles in subpopulations of extracellular vesicles: apoptotic bodies, microvesicles and exosomes.* J Extracell Vesicles. **2**.

248. Zomer, A., et al., *Exosomes: Fit to deliver small RNA.* Commun Integr Biol, 2010. **3**(5): p. 447-50.

249. Squadrito, M.L., et al., *Endogenous RNAs modulate microRNA sorting to exosomes and transfer to acceptor cells.* Cell Rep. **8**(5): p. 1432-46.

250. Raposo, G. and W. Stoorvogel, *Extracellular vesicles: exosomes, microvesicles, and friends.* J Cell Biol. **200**(4): p. 373-83.

251. Bellingham, S.A., et al., *Exosomes: vehicles for the transfer of toxic proteins associated with neurodegenerative diseases?* Front Physiol, 2012. **3**: p. 124.

252. Yu, B., X. Zhang, and X. Li, *Exosomes derived from mesenchymal stem cells.* Int J Mol Sci. **15**(3): p. 4142-57.

253. Kulshreshtha, A., et al., *Proinflammatory role of epithelial cell-derived exosomes in allergic airway inflammation.* J Allergy Clin Immunol. **131**(4): p. 1194-203, 1203 e1-14.

254. Tan, S.S., et al., *Therapeutic MSC exosomes are derived from lipid raft microdomains in the plasma membrane.* J Extracell Vesicles. **2**.

255. Lugini, L., et al., *Immune surveillance properties of human NK cell-derived exosomes.* J Immunol. **189**(6): p. 2833-42.
256. Zhou, Y., et al., *Exosomes released by human umbilical cord mesenchymal stem cells protect against cisplatin-induced renal oxidative stress and apoptosis in vivo and in vitro.* Stem Cell Res Ther. **4**(2): p. 34.
257. Bhatnagar, S. and J.S. Schorey, *Exosomes released from infected macrophages contain Mycobacterium avium glycopeptidolipids and are proinflammatory.* J Biol Chem, 2007. **282**(35): p. 25779-89.
258. Kosaka, N., et al., *Neutral sphingomyelinase 2 (nSMase2)-dependent exosomal transfer of angiogenic microRNAs regulate cancer cell metastasis.* J Biol Chem. **288**(15): p. 10849-59.
259. Kobayashi, T., F. Gu, and J. Gruenberg, *Lipids, lipid domains and lipid-protein interactions in endocytic membrane traffic.* Semin Cell Dev Biol, 1998. **9**(5): p. 517-26.
260. Michel Record a, b., c,d,*, CarolineSubra a,b,c,d, SandrineSilvente-Poirot a,b,c,d, MarcPoirot *Exosomes as intercellular signalosomes and pharmacological effectors.* Biochemical pharmacology, 2011.
261. Bruno, S., et al., *Mesenchymal stem cell-derived microvesicles protect against acute tubular injury.* J Am Soc Nephrol, 2009. **20**(5): p. 1053-67.
262. Kim, H.S., et al., *Proteomic analysis of microvesicles derived from human mesenchymal stem cells.* J Proteome Res, 2012. **11**(2): p. 839-49.
263. Bobrie, A., et al., *Exosome secretion: molecular mechanisms and roles in immune responses.* Traffic. **12**(12): p. 1659-68.
264. Urbanelli, L., et al., *Signaling pathways in exosomes biogenesis, secretion and fate.* Genes (Basel). **4**(2): p. 152-70.
265. Sahoo, S. and D.W. Losordo, *Exosomes and cardiac repair after myocardial infarction.* Circ Res. **114**(2): p. 333-44.
266. Gramal-Eldin Ibrahim A., *Exosomes as critical agents of cardiac regeneration triggered by cell therapy.* Stem cell reports, 2014.
267. Xin, H., et al., *Exosome-mediated transfer of miR-133b from multipotent mesenchymal stromal cells to neural cells contributes to neurite outgrowth.* Stem cells. **30**(7): p. 1556-64.
268. Yang, L., et al., *Excess mortality associated with the 2009 pandemic of influenza A(H1N1) in Hong Kong.* Epidemiol Infect, 2012. **140**(9): p. 1542-50.

269. Akram, K.M., et al., *Mesenchymal stem cells promote alveolar epithelial cell wound repair in vitro through distinct migratory and paracrine mechanisms.* Respir Res, 2013. **14**: p. 9.

270. Lau, A.N., et al., *Stem cells and regenerative medicine in lung biology and diseases.* Mol Ther. **20**(6): p. 1116-30.

271. Ge, X., et al., *Intratracheal transplantation of bone marrow-derived mesenchymal stem cells reduced airway inflammation and up-regulated CD4(+)CD25(+) regulatory T cells in asthmatic mouse.* Cell Biol Int. **37**(7): p. 675-86.

272. Muzumdar, M.D., et al., *A global double-fluorescent Cre reporter mouse.* Genesis, 2007. **45**(9): p. 593-605.

273. Muller, U., et al., *Functional role of type I and type II interferons in antiviral defense.* Science, 1994. **264**(5167): p. 1918-21.

274. Corti, M., A.R. Brody, and J.H. Harrison, *Isolation and primary culture of murine alveolar type II cells.* Am J Respir Cell Mol Biol, 1996. **14**(4): p. 309-15.

275. Nagaishi, K., et al., *Mesenchymal stem cell therapy ameliorates diabetic nephropathy via the paracrine effect of renal trophic factors including exosomes.* Sci Rep, 2016. **6**: p. 34842.

276. Rager, T.M., et al., *Exosomes secreted from bone marrow-derived mesenchymal stem cells protect the intestines from experimental necrotizing enterocolitis.* J Pediatr Surg, 2016. **51**(6): p. 942-7.

277. Cakarova, L., et al., *Macrophage tumor necrosis factor-alpha induces epithelial expression of granulocyte-macrophage colony-stimulating factor: impact on alveolar epithelial repair.* Am J Respir Crit Care Med, 2009. **180**(6): p. 521-32.

278. Darwish, I., et al., *Mesenchymal stromal (stem) cell therapy fails to improve outcomes in experimental severe influenza.* PLoS One, 2013. **8**(8): p. e71761.

279. Hayes, M., et al., *Mesenchymal stromal cells are more effective than the MSC secretome in diminishing injury and enhancing recovery following ventilator-induced lung injury.* Intensive Care Med Exp, 2015. **3**(1): p. 29.

280. Cassatella, M.A., et al., *Toll-like receptor-3-activated human mesenchymal stromal cells significantly prolong the survival and function of neutrophils.* Stem Cells, 2011. **29**(6): p. 1001-11.

281. Wang, Y., et al., *TGF-alpha increases human mesenchymal stem cell-secreted VEGF by MEK- and PI3-K- but not JNK- or ERK-dependent mechanisms.* Am J Physiol Regul Integr Comp Physiol, 2008. **295**(4): p. R1115-23.

282. Ware, L.B. and M.A. Matthay, *The acute respiratory distress syndrome.* N Engl J Med, 2000. **342**(18): p. 1334-49.
283. Lin, C.S., et al., *Is CD34 truly a negative marker for mesenchymal stromal cells?* Cytotherapy, 2012. **14**(10): p. 1159-63.
284. Lee, J.Y., et al., *Clonal isolation of muscle-derived cells capable of enhancing muscle regeneration and bone healing.* J Cell Biol, 2000. **150**(5): p. 1085-100.
285. Sinanan, A.C., N.P. Hunt, and M.P. Lewis, *Human adult craniofacial muscle-derived cells: neural-cell adhesion-molecule (NCAM; CD56)-expressing cells appear to contain multipotential stem cells.* Biotechnol Appl Biochem, 2004. **40**(Pt 1): p. 25-34.
286. Fina, L., et al., *Expression of the CD34 gene in vascular endothelial cells.* Blood, 1990. **75**(12): p. 2417-26.
287. Hristov, M. and C. Weber, *Endothelial progenitor cells in vascular repair and remodeling.* Pharmacol Res, 2008. **58**(2): p. 148-51.
288. Sidney, L.E., et al., *Concise review: evidence for CD34 as a common marker for diverse progenitors.* Stem Cells, 2014. **32**(6): p. 1380-9.
289. Peister, A., et al., *Adult stem cells from bone marrow (MSCs) isolated from different strains of inbred mice vary in surface epitopes, rates of proliferation, and differentiation potential.* Blood, 2004. **103**(5): p. 1662-8.
290. Morikawa, S., et al., *Prospective identification, isolation, and systemic transplantation of multipotent mesenchymal stem cells in murine bone marrow.* J Exp Med, 2009. **206**(11): p. 2483-96.
291. Kouris, N.A., et al., *A nondenatured, noncrosslinked collagen matrix to deliver stem cells to the heart.* Regen Med, 2011. **6**(5): p. 569-82.
292. Baddoo, M., et al., *Characterization of mesenchymal stem cells isolated from murine bone marrow by negative selection.* J Cell Biochem, 2003. **89**(6): p. 1235-49.
293. Meirelles Lda, S. and N.B. Nardi, *Murine marrow-derived mesenchymal stem cell: isolation, in vitro expansion, and characterization.* Br J Haematol, 2003. **123**(4): p. 702-11.
294. Ben Azouna, N., et al., *Phenotypical and functional characteristics of mesenchymal stem cells from bone marrow: comparison of culture using different media supplemented with human platelet lysate or fetal bovine serum.* Stem Cell Res Ther. **3**(1): p. 6.
295. Siegel, G., et al., *Phenotype, donor age and gender affect function of human bone marrow-derived mesenchymal stromal cells.* BMC Med. **11**: p. 146.

296. Sakaguchi, Y., et al., *Suspended cells from trabecular bone by collagenase digestion become virtually identical to mesenchymal stem cells obtained from marrow aspirates.* Blood, 2004. **104**(9): p. 2728-35.
297. Drago, D., et al., *The stem cell secretome and its role in brain repair.* Biochimie. **95**(12): p. 2271-85.
298. Popov, B.V., et al., *Lung epithelial cells induce endodermal differentiation in mouse mesenchymal bone marrow stem cells by paracrine mechanism.* Tissue Eng, 2007. **13**(10): p. 2441-50.
299. Baglio, S.R., D.M. Pegtel, and N. Baldini, *Mesenchymal stem cell secreted vesicles provide novel opportunities in (stem) cell-free therapy.* Front Physiol. **3**: p. 359.
300. Zhu, H., et al., *The role of the hyaluronan receptor CD44 in mesenchymal stem cell migration in the extracellular matrix.* Stem Cells, 2006. **24**(4): p. 928-35.
301. Fischer, U.M., et al., *Pulmonary passage is a major obstacle for intravenous stem cell delivery: the pulmonary first-pass effect.* Stem Cells Dev, 2009. **18**(5): p. 683-92.
302. Kraitchman, D.L., et al., *Dynamic imaging of allogeneic mesenchymal stem cells trafficking to myocardial infarction.* Circulation, 2005. **112**(10): p. 1451-61.
303. Spees, J.L., et al., *Bone marrow progenitor cells contribute to repair and remodeling of the lung and heart in a rat model of progressive pulmonary hypertension.* FASEB J, 2008. **22**(4): p. 1226-36.
304. Krause, D.S., et al., *Multi-organ, multi-lineage engraftment by a single bone marrow-derived stem cell.* Cell, 2001. **105**(3): p. 369-77.
305. Wang, G., et al., *Adult stem cells from bone marrow stroma differentiate into airway epithelial cells: potential therapy for cystic fibrosis.* Proc Natl Acad Sci U S A, 2005. **102**(1): p. 186-91.
306. Spees, J.L., et al., *Engraftment of bone marrow progenitor cells in a rat model of asbestos-induced pulmonary fibrosis.* Am J Respir Crit Care Med, 2007. **176**(4): p. 385-94.
307. Kotton, D.N., A.J. Fabian, and R.C. Mulligan, *Failure of bone marrow to reconstitute lung epithelium.* Am J Respir Cell Mol Biol, 2005. **33**(4): p. 328-34.
308. Loi, R., et al., *Limited restoration of cystic fibrosis lung epithelium in vivo with adult bone marrow-derived cells.* Am J Respir Crit Care Med, 2006. **173**(2): p. 171-9.
309. Sethe, S., A. Scutt, and A. Stolzing, *Aging of mesenchymal stem cells.* Ageing Res Rev, 2006. **5**(1): p. 91-116.

310. Rubio, D., et al., *Molecular characterization of spontaneous mesenchymal stem cell transformation.* PLoS One, 2008. **3**(1): p. e1398.
311. Fossett, E., et al., *Effect of age and gender on cell proliferation and cell surface characterization of synovial fat pad derived mesenchymal stem cells.* J Orthop Res, 2012. **30**(7): p. 1013-8.
312. Liu, G., et al., *Evaluation of the viability and osteogenic differentiation of cryopreserved human adipose-derived stem cells.* Cryobiology, 2008. **57**(1): p. 18-24.
313. Francois, M., et al., *Cryopreserved mesenchymal stromal cells display impaired immunosuppressive properties as a result of heat-shock response and impaired interferon-gamma licensing.* Cytotherapy, 2012. **14**(2): p. 147-52.
314. Moll, G., et al., *Do cryopreserved mesenchymal stromal cells display impaired immunomodulatory and therapeutic properties?* Stem Cells, 2014. **32**(9): p. 2430-42.
315. Jeong, J.O., et al., *Malignant tumor formation after transplantation of short-term cultured bone marrow mesenchymal stem cells in experimental myocardial infarction and diabetic neuropathy.* Circ Res, 2011. **108**(11): p. 1340-7.
316. Wong, R.S., *Mesenchymal stem cells: angels or demons?* J Biomed Biotechnol. **2011**: p. 459510.
317. Rice, T.W., et al., *Critical illness from 2009 pandemic influenza A virus and bacterial coinfection in the United States.* Crit Care Med, 2012. **40**(5): p. 1487-98.
318. van Haaften, T., et al., *Airway delivery of mesenchymal stem cells prevents arrested alveolar growth in neonatal lung injury in rats.* Am J Respir Crit Care Med, 2009. **180**(11): p. 1131-42.
319. Chan, M.C., et al., *Human mesenchymal stromal cells reduce influenza A H5N1-associated acute lung injury in vitro and in vivo.* Proc Natl Acad Sci U S A, 2016.
320. Giuliani, M., et al., *TLR ligands stimulation protects MSC from NK killing.* Stem cells. **32**(1): p. 290-300.
321. He, A., et al., *The antiapoptotic effect of mesenchymal stem cell transplantation on ischemic myocardium is enhanced by anoxic preconditioning.* Can J Cardiol, 2009. **25**(6): p. 353-8.
322. Eseonu, O.I. and C. De Bari, *Homing of mesenchymal stem cells: mechanistic or stochastic? Implications for targeted delivery in arthritis.* Rheumatology (Oxford), 2015. **54**(2): p. 210-8.

323. Sordi, V., et al., *Bone marrow mesenchymal stem cells express a restricted set of functionally active chemokine receptors capable of promoting migration to pancreatic islets.* Blood, 2005. **106**(2): p. 419-27.
324. Chamberlain, G., et al., *Mesenchymal stem cells exhibit firm adhesion, crawling, spreading and transmigration across aortic endothelial cells: effects of chemokines and shear.* PLoS One, 2011. **6**(9): p. e25663.
325. Fox, J.M., et al., *Recent advances into the understanding of mesenchymal stem cell trafficking.* Br J Haematol, 2007. **137**(6): p. 491-502.
326. Fink, T., et al., *Induction of adipocyte-like phenotype in human mesenchymal stem cells by hypoxia.* Stem cells, 2004. **22**(7): p. 1346-55.
327. Amiri, F., A. Jahanian-Najafabadi, and M.H. Roudkenar, *In vitro augmentation of mesenchymal stem cells viability in stressful microenvironments: In vitro augmentation of mesenchymal stem cells viability.* Cell Stress Chaperones, 2015. **20**(2): p. 237-51.
328. Wilson, J.G., et al., *Mesenchymal stem (stromal) cells for treatment of ARDS: a phase 1 clinical trial.* Lancet Respir Med, 2015. **3**(1): p. 24-32.
329. Liu, K.D., et al., *Design and implementation of the START (STem cells for ARDS Treatment) trial, a phase 1/2 trial of human mesenchymal stem/stromal cells for the treatment of moderate-severe acute respiratory distress syndrome.* Ann Intensive Care, 2014. **4**: p. 22.
330. Chang, Y.S., et al., *Mesenchymal stem cells for bronchopulmonary dysplasia: phase 1 dose-escalation clinical trial.* J Pediatr, 2014. **164**(5): p. 966-972 e6.

9.Supplement

9.1 List of Figures

Figure 1-1	Schematic picture of influenza virus structure, adapted from http://visual-science.com
Figure 1-2	IAV replication cycle in alveolar epithelial cell (AEC) [24]
Figure 1-3	Host immune response to IAV infection [24]
Figure 1-4	Chest X-ray images illustrating early ALI (A) and ARDS (B). Adapted from [58]
Figure 1-5	The schematic picture representative normal and injured alveolus during the ALI/ARDS [57]
Figure 1-6	Schematic picture representing location of MSCs in the bone marrow subendothelial region, adapted from Bianco et al [136]
Figure 1-7	Differentiation and self-renewal potential of BM-MSC [137]
Figure 1-8	Polarization of MSC into pro- and anti-inflammatory phenotype [163]
Figure 1-9	Paracrine effects of cultured MSCs [181]
Figure 1-10	The potential beneficial paracrine action of intravenously or intra-tracheally installed MSC. Adapted from [245]
Figure 1-11	Schematic picture of exosome and its markers [260]
Figure 3-1	Exosome isolation protocol
Figure 3-2	AEC co-culture with BM-MSC, 3T3
Figure 3-3	AEC co-culture with BM-MSC derived Conditioned Medium
Figure 4-1	Gating strategy for BM-MSC isolation by FACS.
Figure 4 -2	Microscopy pictures of BM-MSC at day 3 and 5 post sort (A), and passage 8 (B)
Figure 4-3	Representative histograms of flow cytometry analysis of BM-MSC marker expression
Figure 4-4	Microscopy pictures of differentiated BM-MSC
Figure 4-5	Hierarchical clustering and heat map analysis of individual gene expression profiles of iAEC-M versus iAEC at 24h post IV infection

Figure 4-6	Representative histograms and quantification graphs of Ki-67 and HA positive AECs, infected AECs or infected AECs in co-culture with BM-MSC
Figure 4-7	Representatives dot plots and quantification graphs of Annexin V positive AECs
Figure 4-8	Representative histograms comparing infected versus non-infected MSC and isotype control
Figure 4-9	Quantitative analysis of virus replication, proliferation and apoptosis in infected AEC versus infected AEC in presence of BM-MSC CM
Figure 4-10	Representative dot-plots for dynabead-exosome complex detection by flow cytometry
Figure 4-11	Representative histograms of flow cytometry analysis for surface markers of BM-MSC derived exosomes
Figure 4-12	Potential candidates involved in BM-MSC therapeutic effect
Figure 4-13	Schematic representation of interventions and sacrifice time points monitored for 7 or 14 days
Figure 4-14	Kaplan-Meier curves of PR/8 infected mice treated with BM-MSC or 3T3or PBS 3d pi
Figure 4-15	Alveolar leakage in IV infected differently treated C57BL/6 mice at 7d pi
Figure 4-16	Representative lung histological pictures of PR/8 infected mice treated with PBS, 3T3 and MSC at day 7 or day 14 pi
Figure 4-17	Representative BALF cell quantification graphs of three different treatment groups at 5d pi
Figure 4-18	Representative dot-plots for AEC and EpiSPC identification by FACS
Figure 4-19	Quantification of Ki-67 positive AECs and EpiSPC of PR/8 infected differently treated mice
Figure 4-20	Quantification of HA positive in AECs pool from LH of PR/8 infected mice treated at d3 at 5d pi
Figure 4-21	Quantification of Annexin V positive AECs from LH analysed by FACS at 7d pi
Figure 4-22	Schematic picture showing interventions and sacrifice time points of *ifnar*-/- mice
Figure 4-23	Quantification of HA and NP positive, and Ki67 and Annexin V positive

	AECs from LH (*ifnar-/-)* analysed by FACS at 5dpi
Figure 4-24	Quantification of HA positive iAECs alone or in co-culture with BM-MSC or poly I:C stimulated BM-MSC

9.2 Materials: chemicals, antibodies, kits

2-Propanol	Sigma-Aldrich, Taufkirchen (DE)
Accutase	StemPro, Gibco, BRL, Karlsruhe (DE)
Acetic acid	Merc Millipore, Darmstadt (DE)
Alcian Blue	Sigma-Aldrich, Taufkirchen (DE)
Alizarin Red	Sigma-Aldrich, Taufkirchen (DE)
Annexin binding buffer	Life Technologies, Carlsbad (USA)
Annexin V-Alex Fluor 647	Life Technologies, Carlsbad (USA)
Atropine	B.Braun, Melsungen (DE)
Biotin-binder magnetic beads	Life Technologies, Carlsbad (USA)
BSA (Bovine serum albumin)	Sigma-Aldrich, Taufkirchen (DE)
Cell culture flask 75cm2, 175 cm2	Greiner, Nürtingen (DE)
Cell culture plates, single- and multi-well	Greiner, Nürtingen (DE)
Cell nylon net filters 20µm	Merc Millipore, Darmstadt (DE)
Cell strainer filters 40, 70 and 100µm	BD Biosciences, San Jose (USA)
Collagenase A	Roche Diagnostics GmbH, Mannheim (DE)
CryoPure tubes 1.5ml	Sarstedt. Nümbrecht (DE)
DAPI	Sigma-Aldrich, Taufkirchen (DE)
dH2O	Pharmacia & Upjohn, Peapack (USA)
Dispase	Corning Life Sciences, Tewksbury (USA)
DMEM (Dulbecco's Modified Eagle Medium) (1x) low glucose GlutaMax, supplement pyruvate	Gibco, BRL, Karlsruhe (DE)
DMEM (Dulbecco's Modified Eagle Medium) high glucose	Gibco, BRL, Karlsruhe (DE)
DMSO (Dimethyl sulfoxide)	Sigma-Aldrich, Taufkirchen (DE)

Dnase	Serva, Heidelberg (DE)
dNTPáse (desoxynucleoside triphosphate)	Thermo Scientific, Watham (USA)
DPBS (Dulbecco's phosphate-buffer saline)	Life Technologies, Carlsbad (USA)
Dynabeads® Biotin Binder	Invitrogen (NO)
EDTA (Ethylenediaminetetraacetic acid)	Roth, Karlsruhe (DE)
Eosin G Solution	Merc Millipore, Darmstadt (DE)
Ethanol	Sigma-Aldrich, Taufkirchen (DE)
Exi-FBS™ Exosome-depleted FBS Medium	System Biosciences, Palo Alto (USA)
FCS (fetal calf serum)	Life Technologies, Carlsbad (USA)
FITC-Albumin	Sigma-Aldrich, Taufkirchen (DE)
Fluoromount™	Sigma-Aldrich, Taufkirchen (DE)
GentleMACS C tubes	Miltenyi Biotec, Bergisch Gladbach (DE)
GW4869 (hydrochloride hydrate)	R&D Systems, Minneapolis (USA)
Haematoxylin solution	Merc Millipore, Darmstadt (DE)
HBSS (Hank's balanced salt solution) (1x), no phenol red	Gibco, BRL, Karlsruhe (DE)
HEPES	Merc Millipore, Darmstadt (DE)
hMSC Adipogenic Induction SingleQuots®	Lonza, Walkerswill (USA)
hMSC Adipogenic Maintenance SingleQuots®	Lonza, Walkerswill (USA)
hMSC Chondrogenic SingleQuots®	Lonza, Walkerswill (USA)
hMSC Osteogenic SingleQuots®	Lonza, Walkerswill (USA)
Hydrochloridic acid	Sigma-Aldrich, Taufkirchen (DE)
Isoflurane	Abbott, Chicago (USA)
Ketaminhydrochloride (Ketavet)	Pharmacia & Upjohn, Peapack (USA)
L-Glutamine [200mM]	Gibco, BRL, Karlsruhe (DE)
Lipofectamine 2000	Life Technologies, Carlsbad (USA)
Methanol	Roth, Karlsruhe (DE)

Mouse Mesenchymal Stem Cell Growth Medium	Cyagen/OriCell™, Santa Clara (USA)
mouse recombinant interferon-β	pbl interferon source, Logan (USA)
mTNFα (Tumor necrosis factor alpha, mouse)	R&D Systems, Minneapolis (USA)
NaCl 0.9%	Pharmacia & Upjohn, Peapack (USA)
NCR Protein-Free Cryopreservation Medium	Cyagen/OriCell™, Santa Clara (USA)
Oil-Red	Merc Millipore, Darmstadt (DE)
Parafilm	American National, Greenwich (USA)
Paraformaldehyde (PFA)	Merc Millipore, Darmstadt (DE)
Paraffin	Leica biosystems, Nussloch (DE)
PBS (Dulbecco's phosphate-buffer saline) containing MgCl	PAN-Biotech, Aidenbach (DE)
Penicillin/Streptomycin [5000U/l]	Gibco, BRL, Karlsruhe (DE)
Platinum SYBR Green qPCR SuperMix	Life Technologies, Carlsbad (USA)
Poly I:C	Tocris, Bristol (UK)
Polystyrene round-bottom tubes 5ml	BD Biosciences, San Jose (USA)
Polystyrene tubes 15ml and 50ml	Greiner, Nürtingen (DE)
Propodium iodide	Sigma-Aldrich, Taufkirchen (DE)
R848 (Imidazoquinoline compound)	InvivoGen, San Diego (USA)
Reaction tubes 0.5 and 1.5ml	Eppendorf, Hamburg (DE)
rmBMP-6 (Bone morphogenetic protein 6, recombinant mouse)	R&D Systems, Minneapolis (USA)
Rneasy Micro Kit	Quiagen, Hilden (DE)
Sandoglobulin	Novartis, Basel (CH)
Saponine	Merc Millipore, Darmstadt (DE)
Sodium Azid	Merc Millipore, Darmstadt (DE)
Syringe 1, 10 and 20ml	B.Braun, Melsungen (DE)
TGF-B3 (transforming growth factor 3, mouse)	Lonza, Walkerswill (USA)
Transwell® permeable support 24 and	Cornig, Kennebunk (USA)

12mm with 0.4µm Polyester Membrane	
Trypan Blue Stain 0.4%	Gibco, BRL, Karlsruhe (DE)
Trypsin-EDTA	Merc Millipore, Darmstadt (DE)
Trypsin-TPCK	Worthington Biochemical, Lakewood (USA)
Vectashield Mounting Medium (DAPI)	Vector Laboratories, Burlingame (USA)
Xylazine hydrochloride, Rompum	Bayer AG, Leverkusen (DE)
Xylole	Merc Millipore, Darmstadt (DE)
Antibodies	
Armenian Hamster IgG-PerCP/eFluor710	Ebioscience, Frankfurt (DE)
biotinylated rat anti-mouse CD16/32	BD Biosciences, San Jose (USA)
biotinylated rat anti-mouse CD31	BD Biosciences, San Jose (USA)
biotinylated rat anti-mouse CD45	BD Biosciences, San Jose (USA)
biotinylated rat anti-mouse CD81	biolegend, San Diego (USA)
biotinylated rat anti-mouse CD9	biolegend, San Diego (USA)
CD105-APC, MJ7/18, anti-mouse	biolegend, San Diego (USA)
CD117 (c-kit)-PE7Cy7, 104D2	biolegend, San Diego (USA)
CD11b-PB, MI/70, anti-mouse	biolegend, San Diego (USA)
CD11c-FITC, N418, anti-mouse	biolegend, San Diego (USA)
CD19-PE, 6D5	biolegend, San Diego (USA)
CD206-APC, C068C2, anti-mouse	biolegend, San Diego (USA)
CD24-PE-Cy7, M1/69, anti-mouse	biolegend, San Diego (USA)
CD29-PerCP/eFluor710, HMb1-1	Ebioscience, Frankfurt (DE)
CD31-Alexa Fluor 488, MEC13.3, anti-mouse	biolegend, San Diego (USA)
CD31-PB, 390, anti-mouse	biolegend, San Diego (USA)
CD326 (Epcam)-APC/Cy7, G8.8, anti-mouse	biolegend, San Diego (USA)
CD326 (Epcam)-efluor450, G8.8, anti-mouse	Ebioscience, Frankfurt (DE)
CD34-FITC, RAM34	BD Biosciences, San Jose (USA)

CD40-PE/Cy5, 3/23, anti-mouse	biolegend, San Diego (USA)
CD44-PE/Cy5, D7	Ebioscience, Frankfurt (DE)
CD45-APC, 30-F11, anti-mouse	biolegend, San Diego (USA)
CD45-FITC, 30-F11, anti-mouse	biolegend, San Diego (USA)
CD45-V450, 30-F11, anti-mouse	BD Biosciences, San Jose (USA)
CD49f-PE, GOH3, anti-mouse	biolegend, San Diego (USA)
CD63-PE, NVG-2	biolegend, San Diego (USA)
CD73-PB, TY/11.8	biolegend, San Diego (USA)
CD90.2-APC, 53-2.1	biolegend, San Diego (USA)
Gr1 (Ly-6C)-PE/Cy7, RB6-8C5, anti-mouse	biolegend, San Diego (USA)
HA-APC, goat polyclonal	Abcam, Cambridge (UK)
NP-FITC, 431, anti-mouse	Abcam, Cambridge (UK)
PDGFRα (CD140)-APC, APA5	biolegend, San Diego (USA)
Rat IgG1, κ-PB	biolegend, San Diego (USA)
Rat IgG2a, κ-APC	biolegend, San Diego (USA)
Rat IgG2a, κ-FITC	biolegend, San Diego (USA)
Rat IgG2a, κ-PB	biolegend, San Diego (USA)
Rat IgG2a, κ-PE	biolegend, San Diego (USA)
Rat IgG2a, κ-PE/Cy5	biolegend, San Diego (USA)
Rat IgG2a, κ-PE/Cy7	biolegend, San Diego (USA)
Rat IgG2b, k-FITC	biolegend, San Diego (USA)
Rat IgG2b, κ-PE/Cy5	biolegend, San Diego (USA)
Sca-1/Ly-6A/E-PB, D7	biolegend, San Diego (USA)
secondary goat Alexa Fluor 488	Life Technologies, Carlsbad (USA)
secondary goat APC	Life Technologies, Carlsbad (USA)
secondary rabbit Alexa Fluor 488	Life Technologies, Carlsbad (USA)
SiglecF-PE, E50-2440	BD Biosciences, San Jose (USA)
Syrian Hamster IgG-APC	biolegend, San Diego (USA)
T1α-APC, 8.1.1., anti-mouse	biolegend, San Diego (USA)
TER119-FITC, TER-119	biolegend, San Diego (USA)

pro-SPC, anti-mouse	Merc Millipore, Darmstadt (DE)
Ki67-FITC, mouse anti-human	BD Biosciences, San Jose (USA)
BD Compensation Beads Plus	BD Biosciences, San Jose (USA)
ELISA	
Mouse IFNα, detection limit 12.5 pg/ml	Pbl interferon source, Logan (USA)
Mouse IFNβ, detection limit 15.6 pg/ml	Pbl interferon source, Logan (USA)
Mouse HGF, detection limit 400pg/ml	Thermo Scientific, Watham (USA)
Human KGF/FGF7 DuoSet, detection limit 31.2 pg/ml	R&D Systems, Minneapolis (USA)

9.3 Abbreviations

°C	Celsius
3T3	Mouse embryonic fibroblast cell line
AEC	Alveolar epithelial cells
AFC	Alveolar fluid clearance
ALI	Acute lung injury
AM	Alveolar macrophage
Ang-1	Angiopoietin 1
APC	Allophycocyanin
ARDS	Acute respiratory distress syndrome
AU	Arbitrary units
BALF	Bronchoalveolar lavage fluid
bFGF	Basic fibroblast growth factor
BM	Bone marrow
BM-MSC	Bone marrow derived mesenchymal stem cells
BSA	Bovine serum albumin
Bst2	Bone marrow stromal antigen 2
CARDS	Caspase activation and recruitment domains
CCL	Chemokine ligands

CD	Cluster of differentiation
cDNA	Complementary DNA.
CM	Conditioned medium
CMV	Cytomegalovirus
CMV	Cytomegalovirus
CO2	Carbone dioxide
CXCL	C-X-C motif chemokine
CXCR	Chemokine receptor
DAMPs	Danger-associated molecular patterns
DAPI	4',6-diamidino-2-phenylindole
DC	Dendritic cell
dH2O	Deionized water
DMEM	Dulbecco's modified Eagle's medium
DMSO	Dimethylsulfoxide
DNA	Deoxyribonucleic Acid
dNTP	Deoxynucleosid triphosphate
DPBS	Dulbecco's phosphate buffer saline
Dpi	Days post infection
dsDNA	Double stranded DNA
dsRNA	Double stranded RNA
ECMO	Extracorporeal membrane oxygenation
EDTA	Ethylendinitrilotetraacetic acid
EGF	Epidermal growth factor
eIF2α	Eukaryotic translation initiation factor 2α
ELISA	Enzyme Linked Immunosorbent Assay
EpCAM	Epithelial cell adhesion molecule
EPCs	Endothelial progenitors
EpiSPC	Epithelial stem progenitor cell
ESC	Embryonic pluripotent stem cell
EtOH	Ethanol
EV	Extracellular vesicles
FACS	Fluorescence activated cell sorting, flow cytometry

FCS	Fetal calf serum
FGF	Fibroblast growth factor
FiO2	Fraction of inspired oxygen
FITC	Fluorescein isothiocyanate
FSC	Forward scatter
G	Gram
GM-CSF	Granulocyte macrophage colony-stimulating factor
GO	Gene Ontology
h	Hours
HA	Hemagglutinin
HBSS	Hank's balanced salt solution
HCl	Hydrochloric acid
HGF	Hepatocyte growth factor
HLA-G5	Human leukocyte antigen G5
HSC	Hematopoietic stem cells
iAEC	Infected alveolar epithelial cells
iAEC-M	Infected alveolar epithelial cells in co-culture with mesenchymal stem cells
IAV	Influenza A virus
ICAM	Intercellular adhesion molecule
ICU	Intensive Care Unit
IDO	Indoleamine 2,3-dioxygenase
IFI	Interferon-inducible genes
IFN	Type I Interferon
IFNAR	Interferon alpha/beta receptor
IFNα	Interferon alpha
IFNβ	Interferon beta
IFNγ	Interferon gamma
Ig	Immunoglobulin
IGF-1	Insulin-like growth factor 1
IL	Interleukin
IL-1R	Interleukin 1 receptor
IL1RN	Interleukin 1 receptor antagonist

iNOS	Inducible nitric oxide synthase
iPSCs	Induced pluripotent stem cells
IRAK 1	Interleukin 1 receptor associated kinase
ISGs	IFN-stimulated genes
It	Intra-tracheal
IV	Influenza virus
JAK/STAT	Janus kinase/Signal Transducer and Activator of Transcription
KC	Keratinocyte-derived protein chemokine
KEGG	Kyoto Encyclopaedia of Genes and Genomes
Kg	Kilogram
KGF	Keratinocyte growth factor
KO	Knockout
l	Litre
LH	Lung homogenate
LIF	Leukemia inhibitory factor
LPI	Lung permeability index
LRT	Lower respiratory tract
M	Molar
m	Milli
M1	Matrix protein 1
M2	Matrix protein 2
mAEC	Murine alveolar epithelial cells
MAPKs	Mitogen-activated kinases
MAVS	Mitochondrial antiviral signalling protein
mBM-MSC	Murine bone marrow-derived mesenchymal stem cells
MCP-1	Monocyte Chemoattractant Protein-1
M-CSF	Macrophage colony-stimulating factor
MDCK	Madin Darbey Canine Kidney epithelial cell line
MHC	Histocompatibility complex
Min	Minute
MIP-2	Macrophage inflammatory protein 2
miRNA	Micro ribonucleic acid

MMP	Matrix metalloproteinases
MOI	Multiplicity of infection
Mol	Mole
mRNA	Messenger RNA
MSC	Mesenchymal stem cells
mtDNA	Mitochondrial DNA
MVB	Multi-vesicular bodies
Mx2	MX dynamin like GTPase 2
MyD88	Myeloid differentiation primary response gene 88
n	Nano
NA	Neuraminidase
NaAz	Sodium Azide
NaCl	Sodium chloride
NEP	Nuclear export protein
NF-κB	Kappa-light-chain-enhancer of activated B cells
NLRP3	NOD-like receptor family member pyrin domain-containing 3
NO	Nitric oxide
NOD	Nucleotide oligomerization domain
NOS	Nitric oxide synthase
NP	Nucleoprotein
OAS	2’5’-oligoadenylate synthetase
PaO2	Partial pressure arterial oxygen
PAMPs	Pathogen-associated molecular patterns
PB	Pacific blue
PB1	Polymerase protein basic 1
PB2	Polymerase protein basic 2
PBS	Phosphate buffer saline
PCR	Polymerase chain reaction
PDGFRα	Platelet derived growth factor receptor alpha
PE	Phycoerythrin
PFA	Paraformaldehyde
Pfu	Plaque forming units

PGE2	Prostaglandin E2
pH	Potentia hydrogenii
pi	Post infection
PI	Propidium iodide
PIGF	Placental growth factor
PKR	Protein kinase R
PR/8	Influenza virus A/Puerto Rico/8/34 (H1N1)
proSP-C	Pro-surfactant protein C
PRRs	Pattern recognition receptors
qRT-PCR	Quantitative real-time polymerase chain reaction
RANTES	Regulated on activation, normal T cell expressed and secreted
RIG-I	Retinoic acid-inducible gene 1
rmBMP-6	Bone morphogenetic protein 6, recombinant mouse
RNA	Ribonucleic acid
ROS	Reactive oxygen species
Rpm	Rounds per minute
Rsad2	Radical S-adenosyl methionine domain containing 2
RT	Room temperature
s	Second
SA	Sialic acid
Sca-1	Stem cells antigen 1
SCF	Stem cell factor
SD	Standard deviation
SDF-1	Stromal-derived factor1
SEM	Standard error of mean
SOCS	Suppressor of cytokine signalling
SPF	Specific pathogen free
SPM	Specialized pro-resolving mediators
SSC	Side scatter
ssDNA	Single stranded DNA
ssRNA	Single stranded RNA
Sta-1	Stanniocalcin-1

TER119	Glycophorin-A associated antigen
TGF-β	Tumor growth factor beta
TGF-3	Transforming growth factor 3
TLR	Toll-like receptor
TNF	Tumor necrosis factors
TRAIL	TNF-related apoptosis-induced ligand
TRAF6	Tumor necrosis factors receptor associated factor 6
TRIF	TIR-domain-containing adapter-inducing interferon-beta
TRIM25	Tripartite motif-containing protein 25
TRIM56	Tripartite motif-containing protein 56
Tsg101	Tumor susceptibility gene 101
TSG-6	Tumor necrosis stimulated gene 6
U	Units
URT	Upper respiratory tract
US	United States
VCAM	Vascular cell adhesion molecule
VEGF	Vascular endothelial growth factor
vol	Volume
vRNP	Viral ribonucleoprotein
WHO	World health organization
wt	Wildtype
wt	Weight
µ	Micro

Der Lebenslauf wurde aus der elektronischen Version der Arbeit entfernt.

The curriculum vitae was removed from the electronic version of the paper.

[redacted]

[redacted]

[redacted]

[redacted]

Publications:

1. A mediastinal mass mimicking asthma symptoms. V. Miseviciene, L. Labanauskas, R. Kiudeliene, R. Kevalas, J. Zaveckiene, L. Jankauskaite. Medicina (Kaunas), 2013:49(2):67-70
2. Mediastinal mass mimicking allergic asthma, a case report. L. Jankauskaite, V. Miseviciene, R. Kiudeliene, R. Kevalas. Pediatric Respiratory Review 2012;13S1 S51-85
3. Recurrent apnoea episodes as an onset of a primary pulmonary hypertension, a case report. L. Jankauskaite, V. Miseviciene, R. Kevalas. Pediatric Respiratory Review 2012;13S1 S51-85
4. Shaken Baby Syndrome–Condition of Concern in the Context of Consciousness. D. Grinkeviciute, L. Jankauskaite, R. Kevalas, V. Gurskis. Functional Neurology, Rehabilitation and Ergonomics; Vol 1, pp 83–90

Awards

ERS LSC (European Respiratory Society Lung Science Conference) Travel grant – 2015

KIT (Kongress fur Infektologie und Tropenmedizin) travel grant and best poster award – 2014

Lithuanian pediatric conference travel grant and best oral presentation – 2012

EAACI (European Academy for Allergy and Clinical Immunology) fellowship award – 2011

Presentations

2016

„Murine Bone Marrow-derived Mesenchymal stem cells exert Anti-viral and Barrier-protective properties in Influenza Virus Infection“. Poster A6291. Poster discussion in session: Respiratory failure: mechanistic insights from lung injury models. ATS International Conference, San Francisco, USA

„Murine bone marrow-derived mesenchymal stem cells exert Anti-viral and Barrier-protective properties in Influenza Virus Infection“. Poster presentation in ALI/ARDS section. DZL annual conference, Hannover, Germany

2015

„Murine Bone Marrow-derived Mesenchymal stem cells exert anti-viral and barrier-protective properties in influenza virus infection“. Speed talk in Pneumonia session. Joint annual meeting of the DGI and DZIF, Munich, Germany

„Murine Bone Marrow-derived Mesenchymal stem cells as therapeutic option for influenza virus induced acute lung injury“. Oral presentation. ERS international conference, Amsterdam, Netherlands

„Murine Bone Marrow-derived Mesenchymal stem cells as therapeutic option for influenza virus induced acute lung injury“. Oral presentation. International conference of GSCN, Frankfurt, Germany

„Murine Bone Marrow-derived Mesenchymal stem cells as therapeutic option for influenza virus induced acute lung injury“. Poster presentation. International ERS Lung science conference. Estoril, Portugal

„Murine bone marrow derived mesenchymal stem cells as treatment of influenza-virus induced lung injury“. Poster presentation. DZL Annual meeting, Hamburg, Germany

2014

“Therapeutic effect of murine bone marrow derived mesenchymal stem cells in influenza virus induced acute lung injury“. Poster presentation. KIT, Cologne, Germany

"Therapeutic effect of murine bone marrow derived mesenchymal stem cells in influenza virus induced acute lung injury". Poster presentation. 3rd International DZL Symposium: Lung Regeneration and Beyond – BREATH meets REBIRTH, Hannover, Germany

"Therapeutic effect of murine bone marrow derived mesenchymal stem cells in influenza virus induced acute lung injury". Poster presentation. International Influenza Meeting. Munster, Germany

"Pediatric asthma: what was hidden?". Oral presentation at Salzburg CHOP seminar in Pediatric Allergy and Immunology, Salzburg, Austria

9.5 Acknowledgements

I would like to acknowledge and extend my biggest gratitude to these persons who have made the completion of this Dissertation possible.

First of all, I would like to express my sincere gratitude to Prof. Werner Seeger for this unique opportunity to start my research carrier in Department of Internal Medicine II and for his support and help in accomplishing my PhD aims.

Sincere thanks goes for my supervisor Prof. Susanne Herold for her support, encouragement and help during my PhD time. Furthermore, I am very thankful for her helpful suggestions and wise ideas for my research topic and for giving me possibility to evolve as a clinician-scientist. My biggest thanks go to my supervisor-postdoc Dr. Carol Schmoldt, who had patience to teach me good research practice and provided me immense knowledge about basic science as well as encouraged me to never give up. Besides my supervisors, I would like to thank Prof. Juergen Lohmeyer for wise ideas and inspiration.

My sincere thanks also goes to all my lab members – Anna Ivonne Vasquez Armendariz, Monika Heiner, and Christin Peteranderln, whom I had opportunity to work with and to share all the funny moments in these four years. My cordial thanks go to our lab technical support Julia Rupp, Laetitia Rabin, Julia Bespalowa, Maria Koch and Steffani Jarmer for their assistance in the everyday lab work.

I thank Dr. Rory Morty for giving me opportunity to join the International Program "Molecular Biology and Medicine of the Lung" and for this unique possibility to evolve in the lung biology. Additionally, I want to thank Lorna Luck and all the GGL members, for having possibility to increase knowledge in different aspects of molecular biology.

My sincere thanks go to Dr. Jochen Wilhelm and Susanna Ziegler for performing genome array analysis and sharing knowledge about it.

Additional thanks goes to me choir (Cantamus Giessen) and sports friends (Clox-fitness) for all the moral support and my cultural and mental development.

Most importantly I would like to thank all my friends and beloved family for their never-ending optimism, inspiration and encouragement. I will be always thankful for their continuous love and faith in me, and spiritual and material support.

9.6 Declaration

I hereby declare that I have composed and completed this dissertation solely by myself and without the unauthorized help of a second party and only with the assistance acknowledged previously. I have appropriately acknowledged and referenced all the published or unpublished work/data of others, and all information that relates to verbal communications. I have abided by the principles of good scientific conduct laid down in the charter of Justus Liebig University of Giessen in carrying out the investigations described in the dissertation.

Lina Jankauskaite

Giessen, 17 08 2017